

UNIVERSITY OF ZAGREB
FACULTY OF SCIENCE
PHYSICS DEPARTMENT

Luka Popov

Lepton flavor violation in supersymmetric low-scale seesaw models

Doctoral Thesis submitted to the Physics Department
Faculty of Science, University of Zagreb
for the academic degree of
Doctor of Natural Sciences (Physics)

Zagreb, 2013.

This thesis was made under the mentorship of Prof Amon Ilakovac, within University doctoral study at Physics Department of Faculty of Science of University of Zagreb.

Ova disertacija izrađena je pod vodstvom prof. dr. sc. Amona Ilakovca, u sklopu Sveučilišnog doktorskog studija pri Fizičkom odsjeku Prirodoslovno-matematičkoga fakulteta Sveučilišta u Zagrebu.

A. M. D. G.

Acknowledgments

First and above all, I wish to thank my beloved wife Mirela, for illuminating our home with the warmth of her heart.

I would also like to thank my parents Danka and Bojan who never ceased to give me moral support throughout my work and studies.

My sincere gratitude goes to my colleagues Branimir, Mirko, Ivica and Sanjin for all the discussions regarding physics and beyond. I was honoured with your friendship.

I use this opportunity to say thanks to all my professors for generously sharing their knowledge with us.

Special gratitude goes to Mrs Marina Kavur from students' office, for always being on our side during the never-ending bureaucratic battles.

I also which to express my gratitude to our collaborator Prof Apostolos Pilaftsis from University of Manchester for his participation on this project.

Last but not least, I thank my mentor Prof Amon Ilakovac, without whose patient guidance and support this thesis would never see the light of day.

BASIC DOCUMENTATION CARD

University of Zagreb
Faculty of Science
Physics Department

Doctoral Thesis

Lepton flavor violation in supersymmetric low-scale seesaw models

LUKA POPOV
Faculty of Science, Zagreb

The minimal supersymmetric standard model with a low scale see-saw mechanism is presented. Within this framework, the lepton flavour violation in the charged lepton sector is thoroughly studied. Special attention is paid to the individual loop contributions due to the heavy neutrinos $N_{1,2,3}$, sneutrinos $\tilde{N}_{1,2,3}$ and soft SUSY-breaking terms. For the first time, the complete set of box diagrams is included, in addition to the photon and Z -boson mediated interactions. The complete set of chiral amplitudes and their associate form-factors related to the neutrinoless three-body charged lepton flavor violating decays of the muon and tau, such as $\mu \rightarrow eee$, $\tau \rightarrow \mu\mu\mu$, $\tau \rightarrow e\mu\mu$ and $\tau \rightarrow ee\mu$, as well as the coherent $\mu \rightarrow e$ conversion in nuclei, were derived. The obtained analytical results are general and can be applied to most of the New Physics models with charged lepton flavor violation. This systematic analysis has revealed the existence of two new box form factors, which have not been considered before in the existing literature in this area of physics.

In the same model, the systematic study of one-loop contributions to the muon anomalous magnetic dipole moment a_μ and the electron electric dipole

moment d_e is performed. Special attention is paid to the effect of the sneutrino soft SUSY-breaking parameters, B_ν and A_ν , and their universal CP phases (θ and ϕ) on a_μ and d_e .

(135 pages, 169 references, original in English)

Keywords: Lepton Flavor Violation, Supersymmetry, MSSM, Seesaw mechanism, Low-scale seesaw, Lepton Dipole Moments

Supervisor: Prof Amon Ilakovac, University of Zagreb

Committee:

1. Prof Krešimir Kumerički, University of Zagreb
2. Dr Vuko Brigljević, Senior scientist, IRB Zagreb
3. Prof Amon Ilakovac, University of Zagreb
4. Prof Apostolos Pilaftsis, University of Manchester
5. Prof Mirko Planinić, University of Zagreb

Replacements:

1. Prof Dubravko Klabučar, University of Zagreb
2. Dr Krešo Kadija, Senior scientist, IRB Zagreb

Thesis accepted: 2013

Contents

Contents	xi
Introduction	1
1 Experimental survey	3
1.1 Neutrino oscillations	4
1.2 Searching for CLFV	5
1.3 Measuring lepton dipole moments	6
2 Theoretical framework	9
2.1 Basic features of the MSSM	10
2.2 Seesaw mechanism	15
2.3 MSSM extended with right-handed neutrinos	19
3 CLFV observables	25
3.1 The Decays $l \rightarrow l'\gamma$ and $Z \rightarrow ll^C$	26
3.2 Three-Body Leptonic Decays $l \rightarrow l'l_1l_2^C$	28
3.3 Coherent $\mu \rightarrow e$ Conversion in a Nucleus	31
3.4 Numerical Results	34
4 Lepton Dipole Moments	49
4.1 Magnetic and electric dipole moments	50
4.2 Numerical results	53
4.2.1 Results for a_μ	54
4.2.2 Results for d_e	57
4.3 Technical remarks	60
5 Conclusions	63

Appendices	67
A Interaction vertices	69
B Loop functions	73
C One-loop form factors	79
C.1 Photon Form factors	79
C.2 Z-Boson Form factors	81
C.3 Leptonic Box Form factors	82
C.4 Semileptonic Box Form factors	85
D Form factor analysis	87
Prošireni sažetak	95
Pregled tekućih i budućih eksperimenata	96
Teorijski okvir	99
CLFV observable	105
Dipolni momenti leptona	111
Zaključak	114
Bibliography	119
Curriculum Vitæ	i

Introduction

In the first part of this thesis the study of charged lepton flavor violation (CLFV) is performed in low-scale seesaw model of minimal supersymmetric standard model (ν_R MSSM) within the framework of minimal supergravity (mSUGRA). There are two dominant sources of CLFV: one originating from the usual soft supersymmetry-breaking sector, and other entirely supersymmetric coming from the supersymmetric neutrino Yukawa sector. Both sources are taken into account within this framework, and number of possible lepton-flavor-violating transitions are calculated. Supersymmetric low-scale seesaw models offer distinct correlated predictions for lepton flavor violating signatures, which might be discovered in current and projected experiments.

In the second part, the same model is used to study the anomalous magnetic and electric dipole moments of charged leptons. The numerical estimates of the muon anomalous magnetic moment and the electron electric dipole moment will be given as a function of key parameters. The electron electric dipole moment is found to be naturally small in this model, and can be probed in the present and future experiments.

The thesis is organized as follows:

- The first chapter gives a brief experimental survey, the current and projected experiments regarding the detection of charged lepton flavor violation and anomalous dipole moments of charged leptons.
- The second chapter presents the theoretical framework which underlines the study of lepton flavor violation and anomalous dipole moments

given in the thesis.

- The third chapter exposes the analytic and numerical results for various lepton flavor violating transitions, as well as some important physical implications which follow.
- The fourth chapter gives the analysis of the muon anomalous magnetic moment and the electron electric dipole moment in supersymmetric low-scale seesaw models with right-handed neutrino superfields.
- Concluding remarks are given in the fifth chapter.
- The appendices contain technical details regarding the relevant interaction vertices, loop functions and formfactors.

The main results of the thesis are the following:

- The soft SUSY-breaking effects in the Z -boson-mediated graphs dominate the CLFV observables for appreciable regions of the ν_R MSSM parameter space in mSUGRA. But for $m_N \lesssim 1$ TeV the box diagrams involving heavy neutrinos in the loop can be comparable to, or even greater than the corresponding Z -boson-mediated diagrams in $\mu \rightarrow eee$ and $\mu \rightarrow e$ conversion in nuclei. Therefore, the usual paradigm with the photon dipole-moment operators dominating the CLFV observables in high-scale seesaw models have to be radically modified.
- Heavy singlet neutrino and sneutrino contributions to anomalous magnetic dipole moment of the muon are small, typically one to two orders of magnitude below the muon anomaly Δa_μ . The largest effect on Δa_μ instead comes from left-handed sneutrinos and sleptons, exactly as is the case in the MSSM without right-handed neutrinos. Heavy singlet neutrinos do not contribute to the electric dipole moment (EDM) of the electron either. The main contribution to EDM comes from SUSY-breaking terms, but only if one of the CP phases (θ and/or ϕ) introduced to SUSY-breaking sector is nonvanishing.

Chapter 1

Experimental survey

Neutrino oscillation experiments have provided undisputed evidence of lepton flavor violation (LFV) in the neutrino sector, pointing towards physics beyond the Standard Model (SM). Nevertheless, no evidence of LFV has been found in the charged lepton sector of SM, implying conservation of the individual lepton number associated with the electron e , the muon μ and the tau lepton τ . All past and current experiments were only able to report upper limits on observables of charged lepton flavor violation (CLFV). The experimental detection of CLFV would certenaly pave the way to the New Physics.

Measurements of the anomalous magnetic dipole moment of the muon (i.e. its deviation form the SM prediction, Δa_μ) can give an important constraint on model-building, since any New Physics contribution must remain within Δa_μ limit. Study of the electric dipole moment of the electron d_e is even more compelling, since the observation of non-zero (i.e. $\gtrsim 10^{-33} e\text{ cm}$) value for d_e would signify the existence of CP-violating physics beyond the Standard Model.

§ 1.1 Neutrino oscillations

When a neutrino is produced in some weak interaction process, and it propagates through some finite distance, there is a non-zero probability that it will change its flavor. This well established and observed fact is known as *neutrino oscillation* [1–3], due to the oscillatory dependence of the flavor change probability with respect to the neutrino energy and the distance of the propagation.

There are numerous neutrino experiments which report the lepton flavor violation in the neutrino sector, by observing the disappearances or the appearances of a particular neutrino flavor.

In solar neutrino experiments, first by Homestake [4] and later confirmed by others [5–12], the disappearance of the solar electron neutrino ν_e is observed. Atmospheric muon neutrinos ν_μ and antineutrinos $\bar{\nu}_\mu$ disappeared in Super-Kamiokande experiment [13, 14]. The disappearance of reactor electron antineutrinos $\bar{\nu}_e$ is observed in KamLAND reactor [15, 16] and in DOUBLE-CHOOZ experiment [17]. Muon neutrinos ν_μ disappeared in the long-baseline accelerator neutrino experiments MINOS [18, 19] and K2K [20]. Short-baseline reactor experiments Daya Bay [21, 22] and RENO [23] report the disappearance of the reactor electron antineutrinos $\bar{\nu}_e$.

The appearance of electron neutrino ν_e in a beam of muon neutrinos ν_μ in long-baseline accelerator is reported by T2K [24] and MINOS [25] experiments.

All these experiments have provided undisputed evidence for neutrino oscillations caused by finite (non-zero) neutrino masses and, consequently, neutrino mixing parameters. Since neutrinos are massive, the transition from the neutrino flavor eigenstate fields (ν_e , ν_μ , ν_τ) which makes the lepton charged current in weak interactions to the neutrino mass eigenstate fields (ν_1 , ν_2 , ν_3) is non-trivial:

$$\nu_l(x) = \sum_{i=1}^3 U_{li} \nu_i(x) , \quad l = e, \mu, \tau . \quad (1.1)$$

Unitary matrix U is known as Pontecorvo-Maki-Nakagawa-Sakata matrix [1–3] and is usually parametrized as

$$U_{PMNS} = \begin{pmatrix} c_{12}c_{13} & s_{12}c_{13} & s_{13}e^{-i\delta} \\ -s_{12}c_{23} - c_{12}s_{23}s_{13}e^{i\delta} & c_{12}c_{23} - s_{12}s_{23}s_{13}e^{i\delta} & s_{23}c_{13} \\ s_{12}s_{23} - c_{12}c_{23}s_{13}e^{i\delta} & -c_{12}s_{23} - s_{12}c_{23}s_{13}e^{i\delta} & c_{23}c_{13} \end{pmatrix} \cdot P, \quad (1.2)$$

where $P = \text{diag}(1, e^{i\alpha}, e^{i\beta})$, $c_{ij} \equiv \cos \theta_{ij}$ and $s_{ij} \equiv \sin \theta_{ij}$. θ_{12} denotes solar mixing angle, θ_{23} atmospheric mixing angle and θ_{13} reactor mixing angle. Phases δ , α and β stand for Dirac CP violating phase and two Majorana CP violating phases, respectively.

Nonzero values of θ_{13} reported in recent reactor neutrino oscillation experiments [17, 21, 23] strongly indicate a nontrivial neutrino-flavor structure and possibly CP violation.

§ 1.2 Searching for CLFV

The existence of lepton flavor violation (LFV) in the neutrino sector implies the possibility of LFV in the charged sector as well. However, in spite of intense experimental searches [26–37] no evidence of LFV in the charged lepton sector of the Standard Model (SM) has yet been found.

All past and current experiments searching for the charged lepton flavor violation (CLFV) were only able to report upper limits on the observables associated with CLFV. Recently, the MEG collaboration [26] has announced an improved upper limit on the branching ratio of the CLFV decay $\mu \rightarrow e\gamma$, with $B(\mu \rightarrow e\gamma) < 2.4 \times 10^{-12}$ at the 90% confidence level (CL). As also shown in Table 1.1, future experiments searching for the CLFV processes, $\mu \rightarrow e\gamma$, $\mu \rightarrow eee$, coherent $\mu \rightarrow e$ conversion in nuclei, $\tau \rightarrow e\gamma/\mu\gamma$, $\tau \rightarrow 3$ leptons and $\tau \rightarrow$ lepton + light meson, are expected to reach branching-ratio sensitivities to the level of 10^{-13} [38, 39] (10^{-14} [40]), 10^{-16} [41] (10^{-17} [40]), 10^{-17} [42–45] (10^{-18} [40, 46, 47]), 10^{-9} [48, 49], 10^{-10} [48] and 10^{-10} [48], respectively. The values in parentheses indicate the sensitivities that are ex-

pected to be achieved by the new generation CLFV experiments in the next decade. Most interestingly, the projected sensitivity for $\mu \rightarrow eee$ and $\mu \rightarrow e$ conversion in nuclei is expected to increase by five and six orders of magnitude, respectively. The history and current status of the experimental search for CLFV is very nicely exposed in Ref [50], which is highly recommended for further reading.

No.	Observable	Upper Limit	Future Sensitivity
1.	$B(\mu \rightarrow e\gamma)$	2.4×10^{-12} [26]	$1-2 \times 10^{-13}$ [38, 39], 10^{-14} [40]
2.	$B(\mu \rightarrow eee)$	10^{-12} [27]	10^{-16} [41], 10^{-17} [40]
3.	$R_{\mu e}^{\text{Ti}}$	4.3×10^{-12} [28]	$3-7 \times 10^{-17}$ [42–45], 10^{-18} [40, 46, 47]
4.	$R_{\mu e}^{\text{Au}}$	7×10^{-13} [29]	$3-7 \times 10^{-17}$ [42–45], 10^{-18} [40, 46, 47]
5.	$B(\tau \rightarrow e\gamma)$	3.3×10^{-8} [30–37]	$1-2 \times 10^{-9}$ [48, 49]
6.	$B(\tau \rightarrow \mu\gamma)$	4.4×10^{-8} [30–37]	2×10^{-9} [48, 49]
7.	$B(\tau \rightarrow eee)$	2.7×10^{-8} [30–37]	2×10^{-10} [48, 49]
8.	$B(\tau \rightarrow e\mu\mu)$	2.7×10^{-8} [30–37]	10^{-10} [48]
9.	$B(\tau \rightarrow \mu\mu\mu)$	2.1×10^{-8} [30–37]	2×10^{-10} [48, 49]
10.	$B(\tau \rightarrow \mu ee)$	1.8×10^{-8} [30–37]	10^{-10} [48]

Table 1.1: Current upper limits and future sensitivities of CLFV observables under study.

Given that CLFV is forbidden in the SM, its observation would constitute a clear signature for New Physics, which makes this field of investigation ever more exciting.

§ 1.3 Measuring lepton dipole moments

The anomalous magnetic dipole moment (MDM) of the muon, a_μ is a high precision observable extremely sensitive to physics beyond the Standard Model. Its current experimental value, according to PDG [37], is

$$a_\mu^{\text{exp}} = (116592089 \pm 63) \times 10^{-11}. \quad (1.3)$$

The Standard Model prediction of this observable reads

$$a_\mu^{\text{SM}} = (116591802 \pm 49) \times 10^{-11}. \quad (1.4)$$

The difference between measured and predicted value,

$$\Delta a_\mu \equiv a_\mu^{\text{exp}} - a_\mu^{\text{SM}} = (287 \pm 80) \times 10^{-11} \quad (1.5)$$

is at the 3.6σ confidence level (CL) and has therefore been called *the muon anomaly*. This value limits the allowed contributions of New Physics to MDM and consequently can be used as a strong constraint on model-building, or even eliminate some of the proposed New Physics models.

Likewise, the electric dipole moment (EDM) of the electron, d_e , constitutes a very sensitive probe for CP violation induced by new CP phases present in the physics beyond the Standard Model. The present upper limit on d_e is reported to be [37, 51, 52]

$$d_e < 10.5 \times 10^{-28} \text{ e cm}. \quad (1.6)$$

Future projected experiments utilizing paramagnetic systems, such as Cesium, Rubidium and Francium, may extend the current sensitivity to the $10^{-29} - 10^{-31}$ e cm level [52–59]. In the Standard Model, the predictions for d_e range from 10^{-38} e cm to 10^{-33} e cm depending on whether the Dirac CP phase in light neutrino mixing is zero or not (for details see Ref [60]). Therefore, any observation of non-zero value of d_e , i.e. value larger than 10^{-33} e cm, would signify the existence of CP-violating physics beyond the Standard Model.

For that reason, these observables are of great interest for the investigation of possible scenarios for the New Physics. The announced higher-precision measurement of a_μ by a factor of 4 in the future Fermilab experiment E989 [61–65] as well as the expected future sensitivities of the electron EDM down to the level of $\sim 10^{-31}$ e cm [52], renders the study of the dipole moments even more actual and interesting.

For further reading, the reader is encouraged to the excellent reviews provided by Refs [59, 66, 67].

Chapter 2

Theoretical framework

In this chapter we will expose some basic features of the theoretical framework which underlines the study of lepton flavor violation and anomalous dipole moments given in the thesis.

In the first section, we will give the basic structure of the Minimal Supersymmetric Standard Model (MSSM), as well as some main features regarding the Soft Supersymmetry Breaking in the MSSM. The notation used when discussing the Supersymmetry (SUSY) will correspond to the one used in Drees et al. [68], adapted to Petcov et al. [69]. For further reading regarding SUSY in general and MSSM in particular, the reader is encouraged to consult Refs [68, 70–73].

Second section is dedicated to the seesaw mechanisms, with the main focus on the low-scale version of the seesaw mechanism type I.

Finally, the the MSSM extended by low-scale right handed neutrinos (or ν_R MSSM) is introduced.

§ 2.1 Basic features of the MSSM

The basic idea behind all supersymmetric models is that there is a symmetry (conveniently called *supersymmetry*) which transforms a fermion into the boson and vice versa. The *Minimal Supersymmetric Standard Model* supersymmetrizes the SM with minimal extension of the SM particle spectrum: every SM particle is accompanied by one *superparticle* or a *superpartner*. The superpartners of matter fermions are spin zero particles, called *sfermions*. They can be further classified into the scalar leptons or *sleptons* and scalar quarks or *squarks*. Matter fermions and their superpartners are described by *chiral superfields*. The superpartners of SM gauge bosons are spin one-half particles called *gauginos*. They can be further classified into the strongly interacting *gluinos* and electroweak *zino* and *winos* (superpartners of Z and W bosons, respectively). Together with SM gauge bosons, they are described by *vector superfields*. Superpartners of Higgs bosons are spin one-half particles called *higgsinos* and, along with the latter, are described by chiral superfields. The electroweak symmetry breaking mixes the electroweak gauginos with higgsinos resulting in physical particles referred to as *charginos* and *neutralinos*. Table 2.1 displays full field contents of the MSSM, with the corresponding quantum numbers.

Field contents of the MSSM							
Superfield	Bosons		Fermions		$SU_c(3)$	$SU_L(2)$	$U_Y(1)$
gauge							
G^a	gluon	g^a	gluino	\tilde{g}^a	8	0	0
V^k	electroweak	$W^k (W^\pm, Z)$	wino, zino	$\tilde{\lambda}^k (\tilde{w}^\pm, \tilde{z})$	1	3	0
V'	hypercharge	$B (\gamma)$	bino	$\tilde{\lambda}_0 (\tilde{\gamma})$	1	1	0
matter							
L_i	sleptons	$\tilde{L}_i = (\tilde{\nu}, \tilde{e})_L$	leptons	$L_i = (\nu, e)_L$	1	2	-1
E_i		$\tilde{E}_i = \tilde{e}_R$		$E_i = e_R$	1	1	2
Q_i		$\tilde{Q}_i = (\tilde{u}, \tilde{d})_L$		$Q_i = (u, d)_L$	3	2	1/3
U_i	squarks	$\tilde{U}_i = \tilde{u}_R$	quarks	$U_i = u_R^c$	3*	1	-4/3
D_i		$\tilde{D}_i = \tilde{d}_R$		$D_i = d_R^c$	3*	1	2/3
Higgs							
H_1	Higgs bosons	H_1	Higgsinos	\tilde{H}_1	1	2	-1
H_2		H_2		\tilde{H}_2	1	2	1

Table 2.1: Superfields of the MSSM

As can be seen from Table 2.1, there are two Higgs superfields in the MSSM.

These can be written as

$$H_1 = \begin{pmatrix} H_1^1 \\ H_1^2 \end{pmatrix}, \quad H_2 = \begin{pmatrix} H_2^1 \\ H_2^2 \end{pmatrix}. \quad (2.1)$$

H_1 field is sometimes referred to as the down type Higgs ($Y = -1$), superfield containing h_1 and \tilde{h}_{1L} , while H_2 is referred to as the up type Higgs superfield containing h_2 and \tilde{h}_{2L} . The component fields denoted by lower case letters are given by

$$h_1 \equiv \begin{pmatrix} h_1^1 \\ h_1^2 \end{pmatrix} = \begin{pmatrix} h_1^0 \\ h_1^- \end{pmatrix}; \quad h_2 \equiv \begin{pmatrix} h_2^1 \\ h_2^2 \end{pmatrix} = \begin{pmatrix} h_2^+ \\ h_2^0 \end{pmatrix}, \quad (2.2)$$

$$\tilde{h}_{1L} \equiv \begin{pmatrix} \tilde{h}_1^1 \\ \tilde{h}_1^2 \end{pmatrix} = \begin{pmatrix} \tilde{h}_1^0 \\ \tilde{h}_1^- \end{pmatrix}_L; \quad \tilde{h}_{2L} \equiv \begin{pmatrix} \tilde{h}_2^1 \\ \tilde{h}_2^2 \end{pmatrix} = \begin{pmatrix} \tilde{h}_2^+ \\ \tilde{h}_2^0 \end{pmatrix}_L. \quad (2.3)$$

After the spontaneous breakdown of electroweak symmetry, the Higgs vacuum expectation values (VEVs) are given by real, positive quantities v_1 and v_2 ,

$$\langle h_1 \rangle = \frac{1}{\sqrt{2}} \begin{pmatrix} v_1 \\ 0 \end{pmatrix}; \quad \langle h_2 \rangle = \frac{1}{\sqrt{2}} \begin{pmatrix} 0 \\ v_2 \end{pmatrix}, \quad (2.4)$$

which arise from the minimization of the Higgs potential. The ratio of these values,

$$\frac{v_2}{v_1} \equiv \tan \beta \quad (2.5)$$

is considered to be a free parameter of the theory, at least regarding the fermion masses.

Let us proceed to the interaction and mass terms in the Lagrangian density $\mathcal{L}_{\text{MSSM}}$ which partly comes from the exact supersymmetrization of the SM. Full MSSM Lagrangian can be written as the sum of two parts,

$$\mathcal{L}_{\text{MSSM}} = \mathcal{L}_{\text{SUSY}} + \mathcal{L}_{\text{SSB}}. \quad (2.6)$$

While $\mathcal{L}_{\text{SUSY}}$ is fully supersymmetric, the \mathcal{L}_{SSB} contains terms which explicitly break the supersymmetry (acronym SSB stands for SuperSymmetry Breakdown).

Let's first take a look to the contents of $\mathcal{L}_{\text{SUSY}}$. The supersymmetric part of the MSSM Lagrangian can be further decomposed as

$$\mathcal{L}_{\text{SUSY}} = \mathcal{L}_g + \mathcal{L}_M + \mathcal{L}_H , \quad (2.7)$$

where \mathcal{L}_g , \mathcal{L}_M and \mathcal{L}_H are pure gauge, matter and Higgs-Yukawa parts, respectively. Detailed expressions for these terms can be found in the literature [68, pp 171-172]. The part which is most interesting for the purposes of this thesis is the *superpotential*, which constitutes important part of \mathcal{L}_H , and reads

$$\mathcal{W}_{\text{MSSM}} = \mu H_1 \cdot H_2 + \bar{E}_i \mathbf{h}_{ij}^e H_1 \cdot L_j + \bar{D}_i \mathbf{h}_{ij}^d H_1 \cdot Q_j + \bar{U}_i \mathbf{h}_{ij}^u H_2 \cdot Q_j , \quad (2.8)$$

where \mathbf{h} matrices are given by

$$\mathbf{h}_{ij}^{e\dagger} = \frac{g_2}{\sqrt{2}M_W \cos \beta} (\mathbf{m}_e)_{ij} , \quad (2.9)$$

$$\mathbf{h}_{ij}^{d\dagger} = \frac{g_2}{\sqrt{2}M_W \cos \beta} (\mathbf{m}_d)_{ij} , \quad (2.10)$$

$$\mathbf{h}_{ij}^{u\dagger} = \frac{g_2}{\sqrt{2}M_W \cos \beta} (\mathbf{m}_u)_{ij} . \quad (2.11)$$

Here, \mathbf{m}_e , \mathbf{m}_d and \mathbf{m}_u represent 3×3 lepton, down-quark and up-quark mass matrices, respectively. The dot products are defined in two-component notation [72, 74] as $A \cdot B \equiv \epsilon_{\alpha\beta} A^\alpha B^\beta$ ($\epsilon_{12} \equiv +1$). Second, third and fourth terms in right-hand side of Eq (2.8) are just supersymmetric generalization of the Yukawa couplings in the Standard Model Lagrangian (for this and other aspects of the SM see Ref [75]). The first term is however new, and can be thought of as a supersymmetric generalization of a higgsino mass term. It can be shown that the consistent incorporation of spontaneous electroweak symmetry breakdown requires μ to be of the order of the weak scale.

One more thing needs to be addressed at this point, and that is the implicit

assumption of the conservation of R -parity defined by a quantum number R_p given by

$$R_p = (-1)^{3(B-L)+2S}, \quad (2.12)$$

where B , L and S stand for barion number, lepton number and spin of the particle, respectively. The conservation of R_p in the MSSM may be posited as a natural assumption in a minimal supersymmetric extensions of the SM, due to the barion and lepton number conservations in the SM Lagrangian.

Let's now turn back to (2.6) and analyse the contents of the \mathcal{L}_{SSB} . There are several constraints which need to be put upon the supersymmetry breaking terms. First, they need to be “small” compared to the fully supersymmetric part $\mathcal{L}_{\text{SUSY}}$. Second, and most important, they must obey certain mass dimensional constraints in order to preserve the desired convergent behavior of the supersymmetric theory at high energies as well as the nonrenormalization of its superpotential couplings. According to the Symanzik's rule [76, pp 107–8] this turns out to be possible in all orders in perturbation theory only if the explicit supersymmetry breaking terms are *soft* [77–80], i.e. that every field operator occurring in \mathcal{L}_{SSB} has mass dimension strictly less than four. The Eq (2.6) is therefore usually written as

$$\mathcal{L}_{\text{MSSM}} = \mathcal{L}_{\text{SUSY}} + \mathcal{L}_{\text{SOFT}}. \quad (2.13)$$

Taking all this into account, one can write down the expression for $\mathcal{L}_{\text{SOFT}}$, by collecting all allowed soft SUSY-breaking terms [68, p 185],

$$\begin{aligned} -\mathcal{L}_{\text{SOFT}} = & \tilde{q}_{iL}^*(\mathcal{M}_{\tilde{q}}^2)_{ij}\tilde{q}_{jL} + \tilde{u}_{iR}^*(\mathcal{M}_u^2)_{ij}\tilde{u}_{jR} + \tilde{d}_{iR}^*(\mathcal{M}_d^2)_{ij}\tilde{d}_{jR} \\ & + \tilde{l}_{iL}^*(\mathcal{M}_{\tilde{l}}^2)_{ij}\tilde{l}_{jL} + \tilde{e}_{iR}^*(\mathcal{M}_{\tilde{e}}^2)_{ij}\tilde{e}_{jR} \\ & + \left[h_1 \cdot \tilde{l}_{iL}(A^e)_{ij}^T \tilde{e}_{jR}^* + h_1 \cdot \tilde{q}_{iL}(A^d)_{ij}^T \tilde{d}_{jR}^* \right. \\ & \left. + \tilde{q}_{iL} \cdot h_2 (A^u)_{ij}^T \tilde{u}_{jR}^* + \text{h.c.} \right] \\ & + m_1^2 |h_1|^2 + m_2^2 |h_2|^2 + (B\mu h_1 \cdot h_2 + \text{h.c.}) \\ & + \frac{1}{2} (M_1 \bar{\tilde{\lambda}}_0 P_L \tilde{\lambda}_0 + M_1^* \bar{\tilde{\lambda}}_0 P_R \tilde{\lambda}_0) \end{aligned}$$

$$\begin{aligned}
& + \frac{1}{2} (M_2 \bar{\tilde{\lambda}} P_L \tilde{\lambda} + M_2^* \bar{\tilde{\lambda}} P_R \tilde{\lambda}) \\
& + \frac{1}{2} (M_3 \bar{\tilde{g}}^a P_L \tilde{g}^a + M_3^* \bar{\tilde{g}}^a P_R \tilde{g}^a)
\end{aligned} \tag{2.14}$$

Practical calculations within the MSSM usually include several simplifying assumptions in order to drastically reduce the number of additional parameters in the model. Different assumptions result in different versions of the *Constrained Minimal Supersymmetric Standard Model* or CMSSM.

In this thesis, we will adopt the framework of *Minimal Super Gravity* (mSUGRA) model. Since MSSM fields alone cannot break supersymmetry spontaneously at the weak scale [68, pp 183-5], spontaneous supersymmetry breakdown needs to be effected in a sector of fields which are singlets with respect to the SM gauge group. This sector is known as the *hidden* or *secluded sector*. SUSY breaking is then transmitted to the gauge nonsinglet *observable* or *visible sector* by a messenger sector associated by a typical mass scale M_M . Unlike the details of the spontaneous SUSY-breaking in the hidden sector, the mechanism of its transmission from hidden sector to the MSSM fields does have an immediate impact on the observable sparticle spectrum and then also on the SUSY phenomenology. The most economical mechanism of this kind uses gravitational strength interactions based on local supersymmetry also known as *supergravity* [70, 81].

The great benefit in using the mSUGRA model is the fact that it reduces the extra one hundred and five parameters (compared to the nineteen parameters of the SM) to the set $\{p\}$ of just five parameters,

$$\{p\} = \{\text{sign}(\mu), m_0, M_{1/2}, A_0, \tan \beta\}, \tag{2.15}$$

where $\text{sign}(\mu)$ stands for the sign of the μ parameter in superpotential (2.8), m_0 constitute masses of the scalars ($m_{ij} = m_0 \delta_{ij}$), $M_{1/2}$ is common mass of all three MSSM gauginos, A_0 is common trilinear coupling constant (higgs-sfermion-sfermion) and $\tan \beta$ is ratio of VEVs defined by Eq (2.5). These parameters are also referred to as the *supersymmetry breaking parameters*. Their values are usually imposed on the scale of Grand Unification (GUT),

and then via Renormalization Group Equations (RGE) [69] transmitted down to the weak scale.

There are quite a few reasons to work in the framework of the MSSM with R -parity conserved. The MSSM provides a quantum-mechanically stable solution to the gauge hierarchy problem and predicts rather accurate unification of the SM gauge couplings close to the grand unified theory (GUT) scale. The lightest supersymmetric particle (LSP) is stable and, if neutral, such as the neutralino, could represent a good candidate for the dark matter in the Universe. Besides that, the MSSM typically predicts a SM-like Higgs boson lighter than 135 GeV, in agreement with the recent observations for a ~ 125 GeV Higgs boson, made by ATLAS [82] and CMS [83, 84] Collaborations.

§ 2.2 Seesaw mechanism

Neutrino oscillation experiments (see Chapter 1) have indisputably shown that neutrinos are not massless, as was once believed to be. This imposes the necessity to extend the Standard Model (as well as the MSSM) in a way that will consistently allow the existence of massive neutrinos. One of the most interesting extensions in that sense is provided by so-called seesaw mechanism. There are three realizations of the seesaw mechanism: the seesaw type one [85–90], the seesaw type two [90–95] and the seesaw type three [96]. These three scenarios differ by the nature of their seesaw messengers needed to explain the small neutrino masses. For the purpose of this thesis, we will explain and adopt a low-scale variant of the seesaw type-I realization, whose messengers are three singlet neutrinos $N_{1,2,3}$. But first let us examine the usual, high-scale variant, seesaw type-I mechanism in order to detect its weaknesses and to demonstrate how low-scale variant can overcome them.

The leptonic Yukawa sector of the SM with massless neutrinos is described

by

$$\mathcal{L}_Y^{(SM)} = - \left(\begin{matrix} \bar{\nu}'_i & \bar{l}'_i \end{matrix} \right)_L \mathbf{h}_{ij}^{(l)\dagger} \begin{pmatrix} \phi^+ \\ \phi^0 \end{pmatrix} l'_{jR} + \text{h.c.} \quad (2.16)$$

Here, the primes indicate that the fields are not written in the mass basis (so-called *physical states*), but rather in the interaction basis. $\mathbf{h}^{(l)}$ and $\mathbf{h}^{(\nu)}$ are 3×3 lepton and neutrino Yukawa matrices, respectively.

The consistent and straightforward extension of this sector by a right-handed neutrinos includes both the extra Yukawa neutrino term and the mass term which is singlet under the SM gauge group ,

$$\begin{aligned} \mathcal{L}_Y^{(SM+\nu_R)} = & - \left(\begin{matrix} \bar{\nu}'_i & \bar{l}'_i \end{matrix} \right)_L \mathbf{h}_{ij}^{(l)\dagger} \begin{pmatrix} \phi^+ \\ \phi^0 \end{pmatrix} l'_{jR} \\ & - \left(\begin{matrix} \bar{\nu}'_i & \bar{l}'_i \end{matrix} \right)_L \mathbf{h}_{ij}^{(\nu)\dagger} \begin{pmatrix} \phi^{0\dagger} \\ -\phi^{+\dagger} \end{pmatrix} \nu'_{jR} \\ & - \frac{1}{2} M \overline{(\nu'_R)^C} \nu'_R + \text{h.c.} \end{aligned} \quad (2.17)$$

After the spontaneous breakdowns of the electroweak symmetry,

$$\Phi(x) \rightarrow \frac{1}{\sqrt{2}} \begin{pmatrix} 0 \\ v \end{pmatrix}, \quad (2.18)$$

one ends with the well-known expression for lepton masses,

$$(m_l)_{ij} = \frac{v}{\sqrt{2}} \mathbf{h}_{ij}^{(l)\dagger}, \quad (m_D)_{ij} = \frac{v}{\sqrt{2}} \mathbf{h}_{ij}^{(\nu)\dagger}, \quad M. \quad (2.19)$$

Here m_l represents masses of the charged leptons, m_D stands for the Dirac mass matrix, and M is the Majorana mass matrix. The former two make

the mass term for neutrinos,

$$\mathcal{L}_\nu^{(mass)} = -\frac{1}{2} \begin{pmatrix} \overline{\nu'_L} & \overline{(\nu'_R)^C} \end{pmatrix} \underbrace{\begin{pmatrix} 0 & m_D \\ m_D^T & M \end{pmatrix}}_{\mathcal{M}_{D+M}} \begin{pmatrix} (\nu'_L)^C \\ \nu'_R \end{pmatrix}. \quad (2.20)$$

In order to get from the interaction to mass basis, i.e. to write the Lagrangian in terms of physical states, one needs to diagonalize the \mathcal{M}_{D+M} matrix. This is performed with unitary 6×6 matrix W ,

$$W^T \mathcal{M}_{D+M} W = \begin{pmatrix} \mathcal{M}_\nu & 0 \\ 0 & \mathcal{M}_N \end{pmatrix}. \quad (2.21)$$

This matrix equation is solved by Taylor expansion, order by order [97]. Keeping only the leading term, the solutions of Eq (2.21) read [98]

$$\mathcal{M}_\nu \simeq -m_D^T M^{-1} m_D, \quad \mathcal{M}_N \simeq M, \quad (2.22)$$

$$W \simeq \begin{pmatrix} \mathbf{1}_{3 \times 3} & (M^{-1} m_D)^\dagger \\ -M^{-1} m_d & \mathbf{1}_{3 \times 3} \end{pmatrix} \sim \begin{pmatrix} 1 & \sqrt{m_\nu/m_N} \\ \sqrt{m_\nu/m_N} & 1 \end{pmatrix}. \quad (2.23)$$

Matrix W transforms fields written in the interaction basis to the one written in the mass basis,

$$\begin{pmatrix} (\nu'_L)^C \\ \nu'_R \end{pmatrix} = W \begin{pmatrix} \nu_L^C \\ \nu_R \end{pmatrix} \quad (2.24)$$

Finally one can re-write the Lagrangian (2.20) in the mass basis,

$$\mathcal{L}_\nu^{(mass)} = -\frac{1}{2} \begin{pmatrix} \bar{\nu}_L & \bar{\nu}_R^C \end{pmatrix} \begin{pmatrix} \mathcal{M}_\nu & 0 \\ 0 & \mathcal{M}_N \end{pmatrix} \begin{pmatrix} \nu_L^C \\ \nu_R \end{pmatrix}. \quad (2.25)$$

If we allow the Yukawa matrices to be of arbitrary form, we have to face two

unpleasant consequences:

1. From Eq (2.22) we see that mass of light neutrinos is roughly given by $m_\nu \sim m_D^2/M$. Since the light neutrino masses are of the order $m_\nu \sim 0.1$ eV, and if we assume that Yukawa couplings are of order ~ 0.1 , it follows that the heavy singlet neutrinos must assume masses of order $\sim 10^{12-14}$ GeV. That is inconvenient by itself, since its direct detection is way beyond the reach of experiments in high energy physics.
2. From Eq (2.23) we see that the mixing between light and heavy neutrinos is of the order $\xi_{\nu N} \sim \sqrt{m_\nu/m_N} \sim 10^{-12}$, for light neutrino masses $m_\nu \sim 0.1$ eV. That means that the heavy neutrinos decouple from low-energy processes of CLFV in the SM with right-handed neutrinos, giving rise to extremely suppressed and unobservable rates.

One way to overcome these difficulties is to impose the presence of the approximate lepton flavor symmetries [99–105] in the theory. These symmetries result in a specific structure of Yukawa matrices which, if exact, can provide massless light neutrinos regardless of the masses of heavy neutrinos, so that

$$\mathcal{M}_\nu = -m_D^T M^{-1} m_D + \dots \equiv 0. \quad (2.26)$$

Small neutrino masses can then be reproduced by breaking the imposed symmetry by just the right amount. This scenario allows the heavy neutrino mass scale to be as low as 100 GeV. Unlike in the usual seesaw scenario, the light-to-heavy neutrino mixings $\xi_{\nu N}$ are not correlated to the light neutrino masses m_ν . Instead, $\xi_{\nu N}$ are free parameters, constrained by experimental limits on the deviations of the W^\pm and Z -boson couplings to leptons with respect to their SM values [106–109].

Approximate lepton flavor symmetries do not restrict the size of the LFV, and so potentially large phenomena of CLFV may be predicted. This feature is quite generic both in the SM [110] and in the MSSM [111, 112] extended with low-scale right-handed neutrinos. This new source of LFV, in addition

to the one resulting from the frequently considered soft SUSY breaking sector [113–119], will be in particular interest in the study provided in this thesis.

§ 2.3 MSSM extended with right-handed neutrinos

The SM and the MSSM extended by low-scale right-handed neutrinos in the presence of the approximate lepton-number symmetries will be denoted by ν_R SM and ν_R MSSM, respectively. Although some of the results displayed in this thesis may be applicable to the more general soft SUSY breaking scenarios, this study will be performed within the mSUGRA framework.

The ν_R MSSM has some interesting features compared with the MSSM. In particular, the heavy singlet sneutrinos may emerge as a new viable candidates of cold dark matter [120–124]. In addition, the mechanism of low-scale resonant leptogenesis [125–129] could provide a possible explanation for the observed baryon asymmetry in the Universe, as the parameter space for successful electroweak baryogenesis gets squeezed by the current LHC data [130, 131].

Given the multitude of quantum states mediating LFV in the ν_R MSSM, the predicted values for observables of CLFV in this model turn out to be generically larger than the corresponding ones in the ν_R SM, except possibly for $B(l \rightarrow l'\gamma)$ [111, 112], where $l, l' = e, \mu, \tau$. The origin of suppression for the latter branching ratios may partially be attributed to the SUSY no-go theorem due to Ferrara and Remiddi [132], which states that the magnetic dipole moment operator necessarily violates SUSY and it must therefore vanish in the supersymmetric limit of the theory.

In this section, we will describe the leptonic sector of the ν_R MSSM and introduce the neutrino Yukawa structure of two baseline scenarios based on approximate lepton-number symmetries and universal Majorana masses at the GUT scale. These scenarios will be used to present generic predictions of

the CLFV within the framework of mSUGRA, and to analyze the anomalous magnetic and electric dipole moments within the same framework.

The leptonic superpotential part of the ν_R MSSM reads:

$$W_{\text{lepton}} = \widehat{E}^C \mathbf{h}_e \widehat{H}_d \widehat{L} + \widehat{N}^C \mathbf{h}_\nu \widehat{L} \widehat{H}_u + \frac{1}{2} \widehat{N}^C \mathbf{m}_M \widehat{N}^C, \quad (2.27)$$

where $\widehat{H}_{u,d}$, \widehat{L} , \widehat{E} and \widehat{N}^C denote the two Higgs-doublet superfields, the three left- and right-handed charged-lepton superfields and the three right-handed neutrino superfields, respectively. The Yukawa couplings $\mathbf{h}_{e,\nu}$ and the Majorana mass parameters \mathbf{m}_M form 3×3 complex matrices. Here, the Majorana mass matrix \mathbf{m}_M is taken to be SO(3)-symmetric at the m_N scale, i.e. $\mathbf{m}_M = m_N \mathbf{1}_3$.

In the low-scale seesaw models models with the presence of approximate lepton symmetries, the neutrino induced LFV transitions from a charged lepton $l = \mu, \tau$ to another charged lepton $l' \neq l$ are functions of the ratios [110, 133–136]

$$\Omega_{l'l} = \frac{v_u^2}{2m_N^2} (\mathbf{h}_\nu^\dagger \mathbf{h}_\nu)_{l'l} = \sum_{i=1}^3 B_{l'N_i} B_{lN_i}, \quad (2.28)$$

and are not constrained by the usual seesaw factor m_ν/m_N , where $v_u/\sqrt{2} \equiv \langle H_u \rangle$ is the vacuum expectation value (VEV) of the Higgs doublet H_u , with $\tan \beta \equiv \langle H_u \rangle / \langle H_d \rangle$. The mixing matrix B_{lN_i} that occurs in the interaction of the W^\pm bosons with the charged leptons $l = e, \mu, \tau$ and the three heavy neutrinos $N_{1,2,3}$ is defined in Appendix A. It is important to note that the LFV parameters $\Omega_{l'l}$ do not directly depend on the RGE evolution of the soft SUSY-breaking parameters, except through the VEV v_u defined at the minimum of the Higgs potential.

In the electroweak interaction basis $\{\nu_{e,\mu,\tau L}, \nu_{1,2,3 R}^C\}$, the neutrino mass matrix in the ν_R MSSM takes on the standard seesaw type-I form:

$$\mathbf{M}_\nu = \begin{pmatrix} 0 & \mathbf{m}_D \\ \mathbf{m}_D^T & \mathbf{m}_M^* \end{pmatrix}, \quad (2.29)$$

where $\mathbf{m}_D = \sqrt{2}M_W \sin\beta g_w^{-1} \mathbf{h}_\nu^\dagger$ and \mathbf{m}_M are the Dirac- and Majorana-neutrino mass matrices, respectively. Complex conjugation of \mathbf{m}_M matrix is a consequence of the Majorana mass term in the superpotential W_{lepton} (2.27). In this thesis, we consider two baseline scenarios of neutrino Yukawa couplings. The first one realizes a U(1) leptonic symmetry [125–127] and is given by

$$\mathbf{h}_\nu = \begin{pmatrix} 0 & 0 & 0 \\ a e^{-\frac{i\pi}{4}} & b e^{-\frac{i\pi}{4}} & c e^{-\frac{i\pi}{4}} \\ a e^{\frac{i\pi}{4}} & b e^{\frac{i\pi}{4}} & c e^{\frac{i\pi}{4}} \end{pmatrix}. \quad (2.30)$$

In the second scenario, the structure of the neutrino Yukawa matrix \mathbf{h}_ν is motivated by the discrete symmetry group A_4 and has the following form [137]:

$$\mathbf{h}_\nu = \begin{pmatrix} a & b & c \\ a e^{-\frac{2\pi i}{3}} & b e^{-\frac{2\pi i}{3}} & c e^{-\frac{2\pi i}{3}} \\ a e^{\frac{2\pi i}{3}} & b e^{\frac{2\pi i}{3}} & c e^{\frac{2\pi i}{3}} \end{pmatrix}. \quad (2.31)$$

In Eqs (2.30) and (2.31), the Yukawa parameters a , b and c are assumed to be real. As was explained in the previous section, the small neutrino masses can be obtained by adding small symmetry-breaking terms into these matrices thus making the above mentioned symmetries approximate rather than exact. The predictions for CLFV observables, however, remain independent of the flavor structure of these small terms, needed to fit the low-energy neutrino data. For this reason, the particular symmetry breaking patterns of the above two baseline Yukawa scenarios will not be discussed in this thesis.

Another source of LFV in the models under consideration comes from sneutrino interactions. Specifically, the sneutrino mass Lagrangian in flavor and

mass bases is given by

$$\mathcal{L}^{(\tilde{\nu})} = (\tilde{\nu}_L^\dagger, \tilde{\nu}_R^{C\dagger}, \tilde{\nu}_L^T, \tilde{\nu}_R^{CT}) \mathbf{M}_{\tilde{\nu}}^2 \begin{pmatrix} \tilde{\nu}_L \\ \tilde{\nu}_R^C \\ \tilde{\nu}_L^* \\ \tilde{\nu}_R^{C*} \end{pmatrix} \quad (2.32)$$

$$= \tilde{N}^\dagger \mathcal{U}^{\tilde{\nu}\dagger} \mathbf{M}_{\tilde{\nu}}^2 \mathcal{U}^{\tilde{\nu}} \tilde{N} = \tilde{N}^\dagger \hat{\mathbf{M}}_{\tilde{\nu}}^2 \tilde{N}, \quad (2.33)$$

where $\mathbf{M}_{\tilde{\nu}}^2$ is a 12×12 Hermitian mass matrix in the flavor basis and $\hat{\mathbf{M}}_{\tilde{\nu}}^2$ is the corresponding diagonal mass matrix in the mass basis. More explicitly, in the flavor basis $\{\tilde{\nu}_{e,\mu,\tau L}, \tilde{\nu}_{1,2,3 R}^C, \tilde{\nu}_{e,\mu,\tau L}^*, \tilde{\nu}_{1,2,3 R}^{C*}\}$, the sneutrino mass matrix $\mathbf{M}_{\tilde{\nu}}^2$ may be cast into the following form:

$$\mathbf{M}_{\tilde{\nu}}^2 = \begin{pmatrix} \mathbf{H}_1 & \mathbf{N} & \mathbf{0} & \mathbf{M} \\ \mathbf{N}^\dagger & \mathbf{H}_2^T & \mathbf{M}^T & \mathbf{0} \\ \mathbf{0} & \mathbf{M}^* & \mathbf{H}_1^T & \mathbf{N}^* \\ \mathbf{M}^\dagger & \mathbf{0} & \mathbf{N}^T & \mathbf{H}_2 \end{pmatrix}, \quad (2.34)$$

where the block entries are the 3×3 matrices, namely

$$\begin{aligned} \mathbf{H}_1 &= \mathbf{m}_L^2 + \mathbf{m}_D \mathbf{m}_D^\dagger + \frac{1}{2} M_Z^2 \cos 2\beta \\ \mathbf{H}_2 &= \mathbf{m}_{\tilde{\nu}}^2 + \mathbf{m}_D^\dagger \mathbf{m}_D + \mathbf{m}_M \mathbf{m}_M^\dagger \\ \mathbf{M} &= \mathbf{m}_D (\mathbf{A}_\nu - \mu \cot \beta) \\ \mathbf{N} &= \mathbf{m}_D \mathbf{m}_M. \end{aligned} \quad (2.35)$$

Here, \mathbf{m}_L^2 , $\mathbf{m}_{\tilde{\nu}}^2$ and \mathbf{A}_ν are 3×3 soft SUSY-breaking matrices associated with the left-handed slepton doublets, the right-handed sneutrinos and their trilinear couplings, respectively.

In the supersymmetric limit, all the soft SUSY-breaking matrices are equal to zero, $\tan \beta = 1$ and $\mu = 0$. As a consequence, the sneutrino mass matrix $\mathbf{M}_{\tilde{\nu}}^2$ can be expressed in terms of the neutrino mass matrix \mathbf{M}_ν in (2.29) as

follows:

$$\mathbf{M}_{\tilde{\nu}}^2 \xrightarrow{\text{SUSY}} \begin{pmatrix} \mathbf{M}_\nu \mathbf{M}_\nu^\dagger & \mathbf{0}_{6 \times 6} \\ \mathbf{0}_{6 \times 6} & \mathbf{M}_\nu^\dagger \mathbf{M}_\nu \end{pmatrix}, \quad (2.36)$$

resulting with the expected equality between neutrino and sneutrino mixings. Sneutrino LFV mixings do depend on the RGE evolution of the ν_R MSSM parameters, but unlike the LFV mixings induced by soft SUSY-breaking terms, the sneutrino LFV mixings do not vanish at the GUT scale.

The sneutrino LFV mixings are obtained as combinations of unitary matrices which diagonalize the sneutrino, slepton and chargino mass matrices. It is interesting to notice that in the diagonalization of the sneutrino mass matrix $\mathbf{M}_{\tilde{\nu}}^2$ in (2.34), the sneutrino fields $\tilde{\nu}_{e,\mu,\tau L}$, $\tilde{\nu}_{1,2,3 R}^C$ and their complex conjugates $\tilde{\nu}_{e,\mu,\tau L}^*$, $\tilde{\nu}_{1,2,3 R}^{C*}$ are treated independently. As a result, the expressions for $\tilde{\nu}_{e,\mu,\tau L}$ and $\tilde{\nu}_{1,2,3 R}^C$, in terms of the real-valued mass eigenstates $\tilde{N}_{1,2,\dots,12}$, are not manifestly complex conjugates to $\tilde{\nu}_{e,\mu,\tau L}^*$ and $\tilde{\nu}_{1,2,3 R}^{C*}$, thus leading to a two-fold interpretation of the flavor basis fields,

$$\begin{aligned} \tilde{\nu}_i^* &= (\tilde{\nu}_i)^* = \mathcal{U}_{iA}^* \tilde{N}_A, \\ \tilde{\nu}_i^* &= \mathcal{U}_{i+6 A}^* \tilde{N}_A, \end{aligned} \quad (2.37)$$

where $\tilde{\nu}_{1,2,3} \equiv \tilde{\nu}_{e,\mu,\tau L}$ and $\tilde{\nu}_{4,5,6} \equiv \tilde{\nu}_{1,2,3 R}^C$, with $i = 1, 2, \dots, 6$ and $A = 1, 2, \dots, 12$. For this reason, in Appendix A we include all equivalent forms in which Lagrangians, such as $\mathcal{L}_{\tilde{e}\tilde{\chi}^- \tilde{N}}$ and $\mathcal{L}_{\tilde{N}\tilde{N}Z}$, can be written down.

Finally, a third source of LFV in the ν_R MSSM comes from soft SUSY-breaking LFV terms [113, 115]. These LFV terms are induced by RGE running and, in the mSUGRA framework, vanish at the GUT scale. Their size strongly depends on the interval of the RGE evolution from the GUT scale to the universal heavy neutrino mass scale m_N .

All the three different mechanisms of LFV, mediated by heavy neutrinos, heavy sneutrinos and soft SUSY-breaking terms, depend explicitly on the neutrino Yukawa matrix \mathbf{h}_ν and vanish in the limit $\mathbf{h}_\nu \rightarrow 0$.

We will end this chapter with a technical remark. The diagonalization of 12×12 sneutrino mass matrix $\mathbf{M}_{\tilde{\nu}}^2$ and the resulting interaction vertices will be evaluated numerically, without approximations. To perform the diagonalization of $\mathbf{M}_{\tilde{\nu}}^2$ numerically, the method developed in Ref [138] for the neutrino mass matrix will be used. This method becomes very efficient if one of the diagonal submatrices has eigenvalues larger than the entries in all other submatrices. It will therefore be assumed that the heavy neutrino mass scale m_N is of the order of, or larger than the scale of the other mass parameters in the ν_R MSSM.

Chapter 3

Charged lepton flavor violation

In this chapter, the results and key details regarding the calculations for a number of CLFV observables in the ν_R MSSM will be presented.

In the first section, the analytical results for the amplitudes of CLFV decays $l \rightarrow l'\gamma$ and $Z \rightarrow ll'^C$, as well as their branching ratios will be given. Second section gives analytical expressions for the neutrinoless three-body decays $l \rightarrow l'l_1l_2^C$ pertinent to muon and tau decays. Third section will deal with coherent $\mu \rightarrow e$ conversion in nuclei, giving analytical results for transition amplitudes. All analytical results are expressed in terms of one-loop functions and composite form factors defined in the appendices at the end of this thesis.

Finally, last section will present the numerical results for above mentioned processes, accompanied by the brief description of the numerical methods used and corresponding discussion regarding the very results.

These results are presented in Ref [139].

§ 3.1 The Decays $l \rightarrow l'\gamma$ and $Z \rightarrow ll'^C$

At the one-loop level, the effective $\gamma l'l$ and $Z l'l$ couplings are generated by the Feynman graphs shown in Fig 3.1. The general form of the transition amplitudes associated with these effective couplings is given by

$$\begin{aligned} \mathcal{T}_\mu^{\gamma l'l} &= \frac{e \alpha_w}{8\pi M_W^2} \bar{l}' \left[(F_\gamma^L)_{l'l} (q^2 \gamma_\mu - q^\nu q_\mu) P_L + (F_\gamma^R)_{l'l} (q^2 \gamma_\mu - q^\nu q_\mu) P_R \right. \\ &\quad \left. + (G_\gamma^L)_{l'l} i\sigma_{\mu\nu} q^\nu P_L + (G_\gamma^R)_{l'l} i\sigma_{\mu\nu} q^\nu P_R \right] l, \end{aligned} \quad (3.1)$$

$$\mathcal{T}_\mu^{Z l'l} = \frac{g_w \alpha_w}{8\pi \cos \theta_w} \bar{l}' \left[(F_Z^L)_{l'l} \gamma_\mu P_L + (F_Z^R)_{l'l} \gamma_\mu P_R \right] l, \quad (3.2)$$

where $P_{L(R)} = \frac{1}{2} [1 - (+) \gamma_5]$, $\alpha_w = g_w^2/(4\pi)$, e is the electromagnetic coupling constant, $M_W = g_w \sqrt{v_u^2 + v_d^2}/2$ is the W -boson mass, θ_w is the weak mixing angle and $q = p_{l'} - p_l$ is the photon momentum. The form factors $(F_\gamma^L)_{l'l}$, $(F_\gamma^R)_{l'l}$, $(G_\gamma^L)_{l'l}$, $(G_\gamma^R)_{l'l}$, $(F_Z^L)_{l'l}$ and $(F_Z^R)_{l'l}$ receive contributions from heavy neutrinos $N_{1,2,3}$, heavy sneutrinos $\tilde{N}_{1,2,3}$ and RGE induced soft SUSY-breaking terms. The analytical expressions for these three individual contributions are given in Appendix C. Note that, according to the normalization used, the composite form factors $(G_\gamma^L)_{l'l}$ and $(G_\gamma^R)_{l'l}$ have dimensions of mass, whilst all other form factors are dimensionless.

It is important to remark that the transition amplitudes (3.1) and (3.2) are also constituent parts of the leptonic amplitudes $l \rightarrow l' l_1 l_2^C$ and semileptonic amplitudes $l \rightarrow l' q_1 \bar{q}_2$, which will be discussed in more detail in Sections 3.2 and 3.3. To calculate the CLFV decay $l \rightarrow l'\gamma$, we only need to consider the dipole moment operators associated with the form factors $(G_\gamma^L)_{l'l}$ and $(G_\gamma^R)_{l'l}$ in (3.1). Taking this last fact into account, the branching ratios for $l \rightarrow l'\gamma$ and $Z \rightarrow ll'^C + l^C l'$ are given by

$$B(l \rightarrow l'\gamma) = \frac{\alpha_w^3 s_w^2}{256\pi^2} \frac{m_l^3}{M_W^4 \Gamma_l} \left(|(G_\gamma^L)_{l'l}|^2 + |(G_\gamma^R)_{l'l}|^2 \right), \quad (3.3)$$

$$B(Z \rightarrow l' l^C + l^C l) = \frac{\alpha_w^3 M_W}{768\pi^2 c_w^3 \Gamma_Z} \left(|(F_Z^L)_{l'l}|^2 + |(F_Z^R)_{l'l}|^2 \right). \quad (3.4)$$

The above expressions are valid up to the leading order in external charged

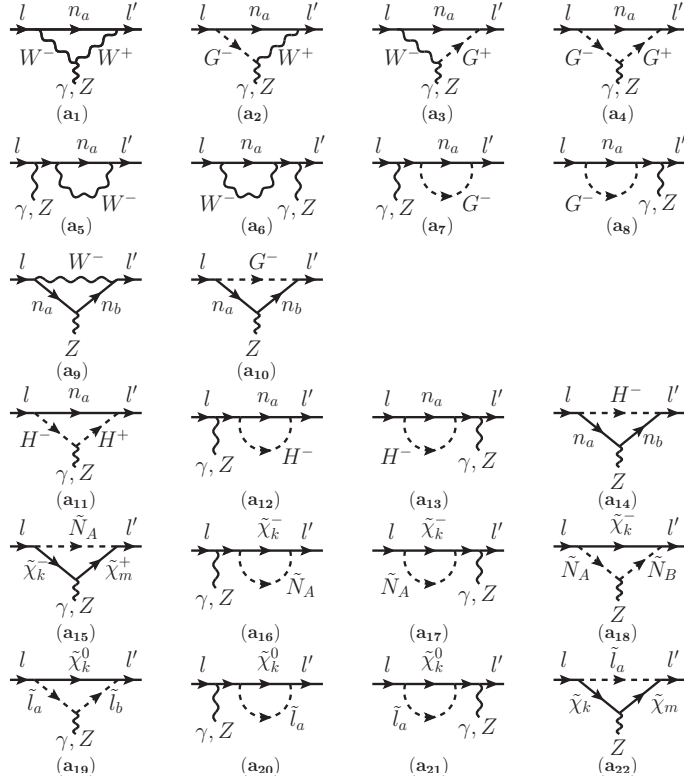


Figure 3.1: Feynman graphs contributing to $l \rightarrow l'\gamma$ and $Z \rightarrow ll'^C$ ($l \rightarrow Zl'$) amplitudes. Here n_a ($a = 1 \dots 6$) and \tilde{N}_A ($A = 1 \dots 12$) stand for neutrinos and snutrinos in mass basis, respectively.

lepton masses and external momenta, which constitutes an excellent approximation for our purposes. Thus, in (3.4) we have assumed that the Z -boson mass M_Z is much smaller than the SUSY and heavy neutrino mass scales, M_{SUSY} and m_N , and we have kept the leading term in an expansion of small momenta and masses for the external particles. In the decoupling regime of all soft SUSY-breaking and charged Higgs-boson masses, the low-energy sector of the ν_R MSSM becomes the ν_R SM. In this ν_R SM limit of the theory, the analytical expressions for $B(l \rightarrow l'\gamma)$ and $B(Z \rightarrow ll'^C + l'^Cl)$ take on the forms given in Refs [140] and [133–135], respectively.

§ 3.2 Three-Body Leptonic Decays $l \rightarrow l' l_1 l_2^C$

We now study the three-body CLFV decays $l \rightarrow l' l_1 l_2^C$, where l can be the muon or tau lepton, and l' , l_1 , l_2 denote other charged leptons to which l is allowed to decay kinematically.

The transition amplitude for $l \rightarrow l' l_1 l_2^C$ receives contributions from γ - and Z -boson-mediated graphs shown in Fig 3.1 and from box graphs displayed in Fig 3.2. The amplitudes for these three contributions are:

$$\mathcal{T}_\gamma^{ll'l_1l_2} = \frac{\alpha_w^2 s_w^2}{2M_W^2} \left\{ \delta_{l_1 l_2} \bar{l}' \left[(F_\gamma^L)_{l'l} \gamma_\mu P_L + (F_\gamma^R)_{l'l} \gamma_\mu P_R + \frac{(\not{p} - \not{p}')}{(p - p')^2} \right. \right. \\ \cdot \left. \left. \left((G_\gamma^L)_{l'l} \gamma_\mu P_L + (G_\gamma^R)_{l'l} \gamma_\mu P_R \right) \right] l \bar{l}_1 \gamma^\mu l_2^C - [l' \leftrightarrow l_1] \right\}, \quad (3.5)$$

$$\mathcal{T}_Z^{ll'l_1l_2} = \frac{\alpha_w^2}{2M_W^2} \left[\delta_{l_1 l_2} \bar{l}' \left((F_Z^L)_{l'l} \gamma_\mu P_L + (F_Z^R)_{l'l} \gamma_\mu P_R \right) l \right. \\ \cdot \left. \bar{l}_1 \left(g_L^l \gamma^\mu P_L + g_R^l \gamma^\mu P_R \right) l_2^C - (l' \leftrightarrow l_1) \right], \quad (3.6)$$

$$\mathcal{T}_{\text{box}}^{ll'l_1l_2} = -\frac{\alpha_w^2}{4M_W^2} \left(B_{\ell V}^{LL} \bar{l}' \gamma_\mu P_L l \bar{l}_1 \gamma^\mu P_L l_2^C + B_{\ell V}^{RR} \bar{l}' \gamma_\mu P_R l \bar{l}_1 \gamma^\mu P_R l_2^C \right. \\ + B_{\ell V}^{LR} \bar{l}' \gamma_\mu P_L l \bar{l}_1 \gamma^\mu P_R l_2^C + B_{\ell V}^{RL} \bar{l}' \gamma_\mu P_R l \bar{l}_1 \gamma^\mu P_L l_2^C \\ + B_{\ell S}^{LL} \bar{l}' P_L l \bar{l}_1 P_L l_2^C + B_{\ell S}^{RR} \bar{l}' P_R l \bar{l}_1 P_R l_2^C \\ + B_{\ell S}^{LR} \bar{l}' P_L l \bar{l}_1 P_R l_2^C + B_{\ell S}^{RL} \bar{l}' P_R l \bar{l}_1 P_L l_2^C \\ + B_{\ell T}^{LL} \bar{l}' \sigma_{\mu\nu} P_L l \bar{l}_1 \sigma^{\mu\nu} P_L l_2^C + B_{\ell T}^{RR} \bar{l}' \sigma_{\mu\nu} P_R l \bar{l}_1 \sigma^{\mu\nu} P_R l_2^C \left. \right) \quad (3.7)$$

$$\equiv -\frac{\alpha_w^2}{4M_W^2} \sum_{X,Y=L,R} \sum_{A=V,S,T} B_{\ell A}^{XY} \bar{l}' \Gamma_A^X l \bar{l}_1 \Gamma_A^Y l_2^C, \quad (3.8)$$

where $g_L^l = -1/2 + s_w^2$ and $g_R^l = s_w^2$ are Z -boson-lepton couplings and $s_w = \sin \theta_w$. The composite box form factors $B_{\ell A}^{XY}$ are given in Appendix C. The labels V , S and T denote the form factors of the vector, scalar and tensor combinations of the currents, while L and R distinguish between left and right chiralities of those currents. The box form factors contain both direct and Fierz-transformed contributions (see Appendix D). Equation (3.8) represents a shorthand expression that takes account of all individual contributions to the amplitude $\mathcal{T}_{\text{box}}^{ll'l_1l_2}$ induced by box graphs. Explicitly, the matrices Γ_A^X

appearing in (3.8) read:

$$(\Gamma_V^L, \Gamma_V^R, \Gamma_S^L, \Gamma_S^R, \Gamma_T^L, \Gamma_T^R) = (\gamma_\mu P_L, \gamma_\mu P_R, P_L, P_R, \sigma_{\mu\nu} P_L, \sigma_{\mu\nu} P_R) . \quad (3.9)$$

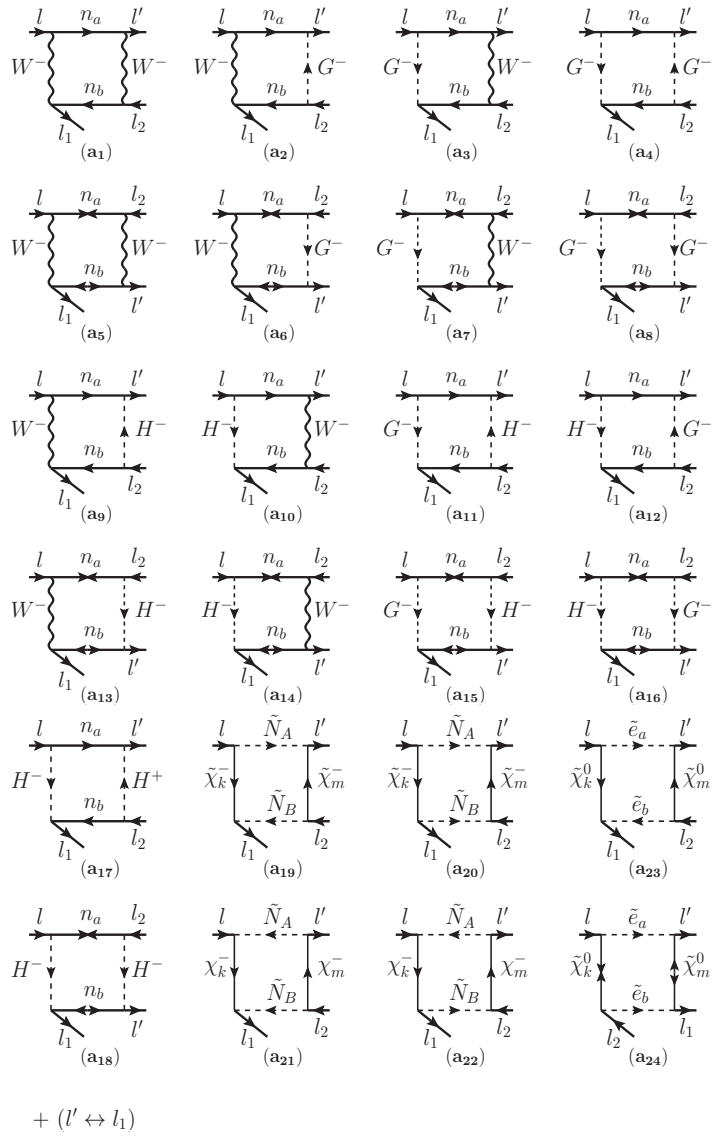


Figure 3.2: Feynman graphs contributing to the box $l \rightarrow l' l_1 l_2^C$ amplitudes.

As a consequence of the identity $\sigma^{\mu\nu}\gamma_5 = -\frac{i}{2}\varepsilon^{\mu\nu\rho\tau}\sigma_{\rho\tau}$, the tensor form factors $B_{\ell T}^{LR}$ and $B_{\ell T}^{RL}$ vanish in the sum (3.8), i.e. $B_{\ell T}^{LR} = B_{\ell T}^{RL} = 0$. A very similar chiral structure is found in the semileptonic box amplitudes defined in the

next section as well. It should also be said that the previous studies of these processes [114, 141] do not include in their calculations the chiral structures $P_L \times P_R$ and $P_R \times P_L$ and their corresponding form factors $B_{\ell S}^{LR}$ and $B_{\ell S}^{RL}$.

In a three-generation model, the transition amplitude for the decays $l \rightarrow l' l_1 l_2^C$ may fall in one of the following three classes or categories [110]: (i) $l' \neq l_1 = l_2$, (ii) $l' = l_1 = l_2$, and (iii) $l' = l_1 \neq l_2$. In the first two classes, total lepton number is conserved, whilst in the third class the total lepton number is violated by two units on the current level. Since the predictions for the observables in class (iii) turn out to be unobservably small in the ν_R MSSM, these processes will be ignored. Moreover, the universal indices $l' l$ which appear in the photon and Z -boson form factors, i.e. F_γ^L , F_γ^R , F_Z^L and F_Z^R , will be dropped out for the sake of readability. Given the above simplification and the notation of the box form factors (3.8), the branching ratios for the class (i) and (ii) of CLFV three-body decays are given by

$$\begin{aligned}
B(l \rightarrow l' l_1 l_2^C) &= \frac{m_l^5 \alpha_w^4}{24576 \pi^3 M_W^4 \Gamma_l} \left\{ \left[\left| 2s_w^2 (F_\gamma^L + F_Z^L) - F_Z^L - B_{\ell V}^{LL} \right|^2 \right. \right. \\
&+ \left| 2s_w^2 (F_\gamma^R + F_Z^R) - B_{\ell V}^{RR} \right|^2 + \left| 2s_w^2 (F_\gamma^L + F_Z^L) - B_{\ell V}^{LR} \right|^2 \\
&+ \left. \left| 2s_w^2 (F_\gamma^R + F_Z^R) - F_Z^R - B_{\ell V}^{RL} \right|^2 \right] \\
&+ \frac{1}{4} \left(|B_{\ell S}^{LL}|^2 + |B_{\ell S}^{RR}|^2 + |B_{\ell S}^{LR}|^2 + |B_{\ell S}^{RL}|^2 \right) \\
&+ 12 \left(|B_{\ell T}^{LL}|^2 + |B_{\ell T}^{RR}|^2 \right) \\
&+ \frac{32 s_w^4}{m_l} \left[\text{Re} \left((F_\gamma^R + F_Z^R) G_\gamma^{L*} \right) + \text{Re} \left((F_\gamma^L + F_Z^L) G_\gamma^{R*} \right) \right] \\
&- \frac{8 s_w^2}{m_l} \left[\text{Re} \left((F_Z^R + B_{\ell V}^{RR} + B_{\ell V}^{RL}) G_\gamma^{L*} \right) \right. \\
&+ \left. \text{Re} \left((F_Z^L + B_{\ell V}^{LL} + B_{\ell V}^{LR}) G_\gamma^{R*} \right) \right] \\
&- \left. \frac{32 s_w^4}{m_l^2} \left(|G_\gamma^L|^2 + |G_\gamma^R|^2 \right) \left(\ln \frac{m_l^2}{m_{l'}^2} - 3 \right) \right\}, \quad (3.10)
\end{aligned}$$

$$\begin{aligned}
B(l \rightarrow l' l' l'^C) &= \frac{m_l^5 \alpha_w^4}{24576 \pi^3 M_W^4 \Gamma_l} \left\{ 2 \left[\left| 2s_w^2 (F_\gamma^L + F_Z^L) - F_Z^L - \frac{1}{2} B_{\ell V}^{LL} \right|^2 \right. \right. \\
&+ \left| 2s_w^2 (F_\gamma^R + F_Z^R) - \frac{1}{2} B_{\ell V}^{RR} \right|^2 \left. \right] + \left| 2s_w^2 (F_\gamma^L + F_Z^L) - B_{\ell V}^{LR} \right|^2 \\
&+ \left| 2s_w^2 (F_\gamma^R + F_Z^R) - (F_Z^R + B_{\ell V}^{RL}) \right|^2 + \frac{1}{8} \left(|B_{\ell S}^{LL}|^2 + |B_{\ell S}^{RR}|^2 \right) \\
&+ 6 \left(|B_{\ell T}^{LL}|^2 + |B_{\ell T}^{RR}|^2 \right) \\
&+ \frac{48 s_w^4}{m_l} \left[\text{Re} \left((F_\gamma^R + F_Z^R) G_\gamma^{L*} \right) + \text{Re} \left((F_\gamma^L + F_Z^L) G_\gamma^{R*} \right) \right] \\
&- \frac{8 s_w^2}{m_l} \left[\text{Re} \left((F_Z^R + B_{\ell V}^{RR} + B_{\ell V}^{RL}) G_\gamma^{L*} \right) \right. \\
&+ \text{Re} \left((2F_Z^L + B_{\ell V}^{LL} + B_{\ell V}^{LR}) G_\gamma^{R*} \right) \left. \right] \\
&+ \left. \frac{32 s_w^4}{m_l^2} \left(|G_\gamma^L|^2 + |G_\gamma^R|^2 \right) \left(\ln \frac{m_l^2}{m_{l'}^2} - \frac{11}{4} \right) \right\}, \quad (3.11)
\end{aligned}$$

where m_l and $m_{l'}$, m_{l_1} , m_{l_2} are the masses of the initial- and final-state charged leptons and Γ_l is the decay width of the charged lepton l . It should be emphasized that the transition amplitudes (3.5), (3.6) and (3.7) as well as the branching ratios (3.10) and (3.11) have the most general chiral and form factor structure to the leading order in the external masses and momenta, which makes them applicable to most models of the New Physics containing CLFV. Even more general result can be found in the Appendix D.

These results have been checked in the ν_R SM limit of the theory in which the branching ratios (3.10) and (3.11) go over to the results presented in Ref [110].

§ 3.3 Coherent $\mu \rightarrow e$ Conversion in a Nucleus

The coherent $\mu \rightarrow e$ conversion in a nucleus corresponds to the process $J_\mu \rightarrow e^- J^+$, where J_μ is an atom of nucleus J with one orbital electron replaced by a muon and J^+ is the corresponding ion without the muon. The

transition amplitude for such a CLFV process,

$$\mathcal{T}^{\mu e;J} = \langle J^+ e^- | \mathcal{T}^{d\mu \rightarrow de} | J_\mu \rangle + \langle J^+ e^- | \mathcal{T}^{u\mu \rightarrow ue} | J_\mu \rangle , \quad (3.12)$$

depends on two effective box operators,

$$\begin{aligned} \mathcal{T}_{\text{box}}^{d\mu \rightarrow de} &= -\frac{\alpha_w^2}{4M_W^2} \sum_{X,Y=L,R} \sum_{A=V,S,T} B_{dA}^{XY} \bar{e} \Gamma_A^X \mu \bar{d} \Gamma_A^X d \\ &= -\frac{\alpha_w^2}{2M_W^2} (d^\dagger d) \bar{e} (V_d^R P_R + V_d^L P_L) \mu , \end{aligned} \quad (3.13)$$

$$\begin{aligned} \mathcal{T}_{\text{box}}^{u\mu \rightarrow ue} &= -\frac{\alpha_w^2}{4M_W^2} \sum_{X,Y=L,R} \sum_{A=V,S,T} B_{uA}^{XY} \bar{e} \Gamma_A^X \mu \bar{u} \Gamma_A^X u \\ &= -\frac{\alpha_w^2}{2M_W^2} (u^\dagger u) \bar{e} (V_u^R P_R + V_u^L P_L) \mu . \end{aligned} \quad (3.14)$$

Here μ and e are the muon and electron wave functions and d and u are field operators acting on the J_μ and J^+ states, respectively. The form factors B_{dA}^{XY} and B_{uA}^{XY} are given in the Appendix C. The composite form factors V_d^L , V_u^L , V_d^R , V_u^R may be written as

$$\begin{aligned} V_d^L &= -\frac{1}{3} s_w^2 \left(F_\gamma^L - \frac{1}{m_\mu} G_\gamma^R \right) + \left(\frac{1}{4} - \frac{1}{3} s_w^2 \right) F_Z^L \\ &\quad + \frac{1}{4} \left(B_{dV}^{LL} + B_{dV}^{LR} + B_{dS}^{RR} + B_{dS}^{RL} \right) , \end{aligned} \quad (3.15)$$

$$\begin{aligned} V_d^R &= -\frac{1}{3} s_w^2 \left(F_\gamma^R - \frac{1}{m_\mu} G_\gamma^L \right) + \left(\frac{1}{4} - \frac{1}{3} s_w^2 \right) F_Z^R \\ &\quad + \frac{1}{4} \left(B_{dV}^{RR} + B_{dV}^{RL} + B_{dS}^{LL} + B_{dS}^{LR} \right) , \end{aligned} \quad (3.16)$$

$$\begin{aligned} V_u^L &= \frac{2}{3} s_w^2 \left(F_\gamma^L - \frac{1}{m_\mu} G_\gamma^R \right) + \left(-\frac{1}{4} + \frac{2}{3} s_w^2 \right) F_Z^L \\ &\quad + \frac{1}{4} \left(B_{uV}^{LL} + B_{uV}^{LR} + B_{uS}^{RR} + B_{uS}^{RL} \right) , \end{aligned} \quad (3.17)$$

$$\begin{aligned} V_u^R &= \frac{2}{3} s_w^2 \left(F_\gamma^R - \frac{1}{m_\mu} G_\gamma^L \right) + \left(-\frac{1}{4} + \frac{2}{3} s_w^2 \right) F_Z^R \\ &\quad + \frac{1}{4} \left(B_{uV}^{RR} + B_{uV}^{RL} + B_{uS}^{LL} + B_{uS}^{LR} \right) , \end{aligned} \quad (3.18)$$

where F_γ^L , F_γ^R , F_Z^L , F_Z^R is the shorthand notation for $(F_\gamma^L)_{e\mu}$, $(F_\gamma^R)_{e\mu}$, $(F_Z^L)_{e\mu}$, $(F_Z^R)_{e\mu}$.

The next step aims to determine the nucleon matrix elements of the operators $u^\dagger u$ and $d^\dagger d$. These are given by

$$\begin{aligned}\langle J^+ e^- | u^\dagger u | J_\mu \rangle &= (2Z + N) F(-m_\mu^2), \\ \langle J^+ e^- | d^\dagger d | J_\mu \rangle &= (Z + 2N) F(-m_\mu^2),\end{aligned}\quad (3.19)$$

where the form factor $F(q^2)$ incorporates the recoil of the J^+ ion [142], and the factors $2Z + N$ and $Z + 2N$ count the number of u and d quarks in the nucleus J , respectively. Hence, the matrix element for $J_\mu \rightarrow J^+ \mu^-$ can be written down as

$$T^{J_\mu \rightarrow J^+ e^-} = -\frac{\alpha_w^2}{2M_W^2} F(-m_\mu^2) \bar{e} (Q_W^L P_R + Q_W^R P_L) \mu, \quad (3.20)$$

with

$$\begin{aligned}Q_W^L &= (2Z + N)V_u^L + (Z + 2N)V_d^L, \\ Q_W^R &= (2Z + N)V_u^R + (Z + 2N)V_d^R.\end{aligned}\quad (3.21)$$

Given the transition amplitude (3.20), the decay rate $J_\mu \rightarrow J^+ e^-$ is found to be

$$R_{\mu e}^J = \frac{\alpha^3 \alpha_w^4 m_\mu^5}{16\pi^2 M_W^4 \Gamma_{\text{capture}}} \frac{Z_{\text{eff}}^4}{Z} |F(-m_\mu^2)|^2 \left(|Q_W^L|^2 + |Q_W^R|^2 \right), \quad (3.22)$$

where Γ_{capture} is the capture rate of the muon by the nucleus, and Z_{eff} is the effective charge which takes into account coherent effects which can occur in the nucleus J due to its finite size. In this analysis, the values of Z_{eff} quoted in Ref [143] are used. Like before, the branching ratio (3.22) possesses the most general form factor structure to the leading order in external masses and momenta and is relevant to most models of New Physics with CLFV.

The analytical results presented in this section are found to be consistent with the results given in Refs [111, 144, 145] in the ν_R SM limit of the theory.

§ 3.4 Numerical Results

In this section, the numerical analysis of CLFV observables in the ν_R MSSM will be presented. In order to reduce the number of independent parameters, we adopt the constrained framework of mSUGRA, discussed in Chapter 2. In detail, the model parameters are: (i) the usual SM parameters, such as gauge coupling constants, the quark and charged-lepton Yukawa matrices inputted at the scale M_Z , (ii) the heavy neutrino mass m_N and the neutrino Yukawa matrix \mathbf{h}_ν evaluated at m_N , (iii) the universal mSUGRA parameters m_0 , $M_{1/2}$ and A_0 inputted at the GUT scale, and (iv) the ratio $\tan \beta$ of the Higgs VEVs and the sign of the superpotential Higgs-mixing parameter μ .

The allowed ranges of the soft SUSY-breaking parameters m_0 , $M_{1/2}$, A_0 and $\tan \beta$ are strongly constrained by a number of accelerator and cosmological data [82–84, 146–148]. For definiteness, we consider the following set of input parameters:

$$\begin{aligned} \tan \beta &= 10, & m_0 &= 1000 \text{ GeV}, \\ A_0 &= -3000 \text{ GeV}, & M_{1/2} &= 1000 \text{ GeV}. \end{aligned} \tag{3.23}$$

Here the μ parameter is taken to be positive, whilst its absolute value $|\mu|$ is derived from the minimization of the Higgs potential at the scale M_Z . Using Refs [149–152], one can verify that the parameter set (3.23) predicts a SM-like Higgs boson with $m_H \approx 125$ GeV, in agreement with the recent discovery at the LHC [82, 84, 147], and is compatible with the current lower limits on gluino and squark masses [84, 146, 147]. The set (3.23) is also in agreement with having the lightest neutralino as the Dark Matter in the Universe [148].

We employ the one-loop RGE equations given in Refs [69, 153] to evolve the gauge coupling constants and the quark and charged lepton Yukawa matrices from M_Z to the GUT scale, while the heavy neutrino mass matrix \mathbf{m}_M and the neutrino Yukawa matrix \mathbf{h}_ν are evolved from the heavy neutrino mass threshold m_N to the GUT scale. Furthermore, we assume that the heavy neutrino-sneutrino sector is approximately supersymmetric above m_N . For

purposes of RGE evolution, this is a good approximation for m_N larger than the typical soft SUSY-breaking scale [111]. At the GUT scale, the mSUGRA universality conditions are used to express the soft SUSY-breaking masses, in terms of m_0 , $M_{1/2}$ and A_0 . Hence, all scalar masses receive a soft SUSY-breaking mass m_0 , all gauginos are mass-degenerate to $M_{1/2}$, and all scalar trilinear couplings are of the form $\mathbf{h}_x A_0$, with $x = u, d, l, \nu$, where \mathbf{h}_x are the Yukawa matrices at the GUT scale. The sneutrino mass matrix acquires additional contributions from the heavy neutrino mass matrix. The sparticle mass matrices and trilinear couplings are evolved from the GUT scale to M_Z , except for the sneutrino masses which are evolved to the heavy neutrino threshold m_N . Having thus obtained all sparticle and sneutrino mass matrices, one can numerically evaluate all particle masses and interaction vertices in the ν_R MSSM, without approximations.

To simplify our numerical analysis, two representative scenarios of Yukawa textures discussed in Chapter 2 are considered. Specifically, the first scenario realizes the U(1)-symmetric Yukawa texture in (2.30), for which we take either $a = b$ and $c = 0$, or $a = c$ and $b = 0$, or $b = c$ and $a = 0$, thus giving rise to CLFV processes $\mu \rightarrow eX$, $\tau \rightarrow eX$ and $\tau \rightarrow \mu X$, respectively. Here X stands for the state(s) with zero net lepton number, e.g. $X = \gamma, e^+e^-, \mu^+\mu^-, q\bar{q}$. The second scenario is motivated by the A_4 group and uses the Yukawa texture (2.31), where the parameters a , b and c are taken to be all equal, i.e. $a = b = c$.

The heavy neutrino mass scale m_N strongly depends on the size of the symmetry-breaking terms in the Yukawa matrix \mathbf{h}_ν . For instance, for the model described by Eq (2.30), the typical values of the $U(1)$ -lepton-symmetry-breaking parameters $\epsilon_l \equiv \epsilon_{e,\mu,\tau}$ consistent with low-scale resonant leptogenesis is $\epsilon \lesssim 10^{-5}$ [125–127], leading to light-neutrino masses

$$m_\nu \sim \frac{\epsilon_l^2 v^2}{m_N} \sim 10^{-2} \text{ eV} \left(\frac{\epsilon_l}{10^{-6}} \right)^2 \left(\frac{1 \text{ TeV}}{m_N} \right). \quad (3.24)$$

Taking into account the constraint $m_\nu \gtrsim 10^{-1}$ eV generically derived from neutrino oscillation data, we may estimate that the heavy neutrino mass scale

m_N is typically restricted to be less than 10 TeV, for $\epsilon_l = 10^{-5}$. If the assumption of successful low-scale leptogenesis is relaxed, the symmetry-breaking parameters ϵ_l has only to be couple of orders in magnitude smaller than the Yukawa parameters a , b and c , with $a, b, c \lesssim 10$. Thus, for $\epsilon_l < 10^{-3} - 10^{-2}$, the heavy neutrino mass scale m_N may be as large as $10^7 - 10^9$ TeV, leading to the decoupling of heavy neutrinos from low-energy observables. As the main interest of this thesis is in the interplay between heavy neutrino, sneutrino and soft SUSY-breaking contributions to CLFV observables, the focus will be only on the parameter space in which $m_N < 10$ TeV.

In the present analysis, we consider that the symmetry-preserving Yukawa parameters a , b and c are limited by the perturbativity condition: $\text{Tr } \mathbf{h}_\nu^\dagger \mathbf{h}_\nu < 4\pi$, which is required to hold true for the entire interval of the RGE evolution: $\ln(M_Z/\text{TeV}) < t < \ln(M_{\text{GUT}}/\text{TeV})$. For the model described by Eq (2.30), this condition translates into the constraint: $a < 0.34$, and for the model described by Eq (2.31), to: $a < 0.23$. For that reason, the numerical values for points in parameter space for which the aforementioned perturbativity condition gets violated will not be displayed.

In Fig 3.3 are displayed numerical predictions for the μ -LFV observables $B(\mu \rightarrow eX)$: $B(\mu \rightarrow e\gamma)$ [blue (solid) line], $B(\mu \rightarrow eee)$ [red (dashed) line], $R_{\mu e}^{\text{Ti}}$ [violet (dotted) line] and $R_{\mu e}^{\text{Au}}$ [green (dash-dotted) line], as functions of $B(\mu \rightarrow e\gamma)$ (left pannels) and the Yukawa parameter a (right pannels), for $m_N = 400$ GeV and $\tan \beta = 10$. The upper two pannels assume the Yukawa texture in (2.30), with $a = b$ and $c = 0$, whilst the lower two pannels correspond to the Yukawa texture in (2.31), with $a = b = c$. In Fig 3.4, we give numerical estimates for the same set of μ -LFV observables, but for $m_N = 1$ TeV. In Figs 3.3 and 3.4, the Yukawa parameter a has been chosen, such that $10^{-20} < B(\mu \rightarrow e\gamma) < 10^{-10}$. Such a range of values includes both the present [26–29, 33, 36] and future [43–47, 49, 154–156] experimental limits. As can be seen from Figs 3.3 and 3.4, the CLFV observables under study depend quadratically on the Yukawa parameter a , namely they are proportional to a^2 . Instead, the quartic Yukawa terms proportional to a^4 [111] remain always small, which is a consequence of the imposed perturbativity

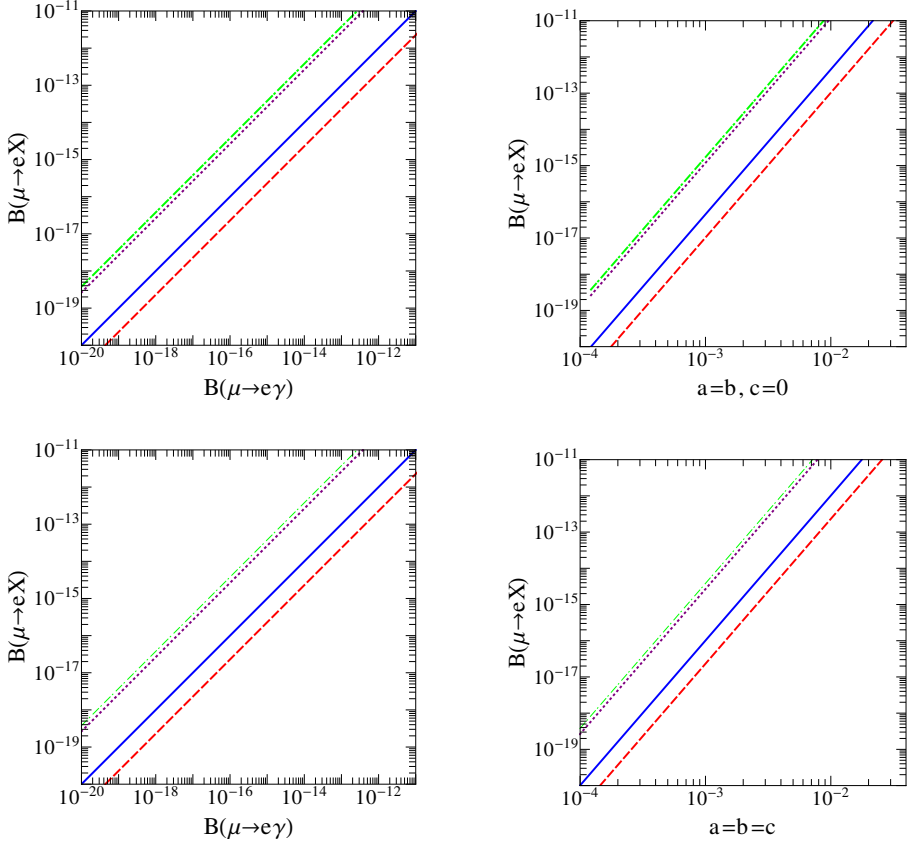


Figure 3.3: Numerical estimates of $B(\mu \rightarrow e\gamma)$ [blue (solid)], $B(\mu \rightarrow eee)$ [red (dashed)], $R_{\mu e}^{\text{Ti}}$ [violet (dotted)] and $R_{\mu e}^{\text{Au}}$ [green (dash-dotted)], as functions of $B(\mu \rightarrow e\gamma)$ (left pannels) and the Yukawa parameter a (right pannels), for $m_N = 400$ GeV and $\tan \beta = 10$. The upper two pannels correspond to the Yukawa texture (2.30), with $a = b$ and $c = 0$, and the lower two pannels to the Yukawa texture (2.31), with $a = b = c$.

constraint: $\text{Tr}(\mathbf{h}_\nu^\dagger \mathbf{h}_\nu) < 4\pi$, up to the GUT scale.

By analogy, Figs 3.5 and 3.6 present numerical estimates of the τ -LFV observables $B(\tau \rightarrow eX)$: $B(\tau \rightarrow e\gamma)$ [blue (solid) lines], $B(\tau \rightarrow eee)$ [red (dashed) lines] and $B(\tau \rightarrow e\mu\mu)$ [violet (dotted) lines], as functions of $B(\tau \rightarrow e\gamma)$ (left pannels) and the Yukawa parameter a (right pannels), for $m_N = 400$ GeV and $m_N = 1$ TeV, respectively. The predictions for the fully complementary observables $B(\tau \rightarrow \mu X)$: $B(\tau \rightarrow \mu\gamma)$, $B(\tau \rightarrow \mu\mu\mu)$ and $B(\tau \rightarrow \mu ee)$ are not displayed. The upper pannels give our predictions for the Yukawa tex-

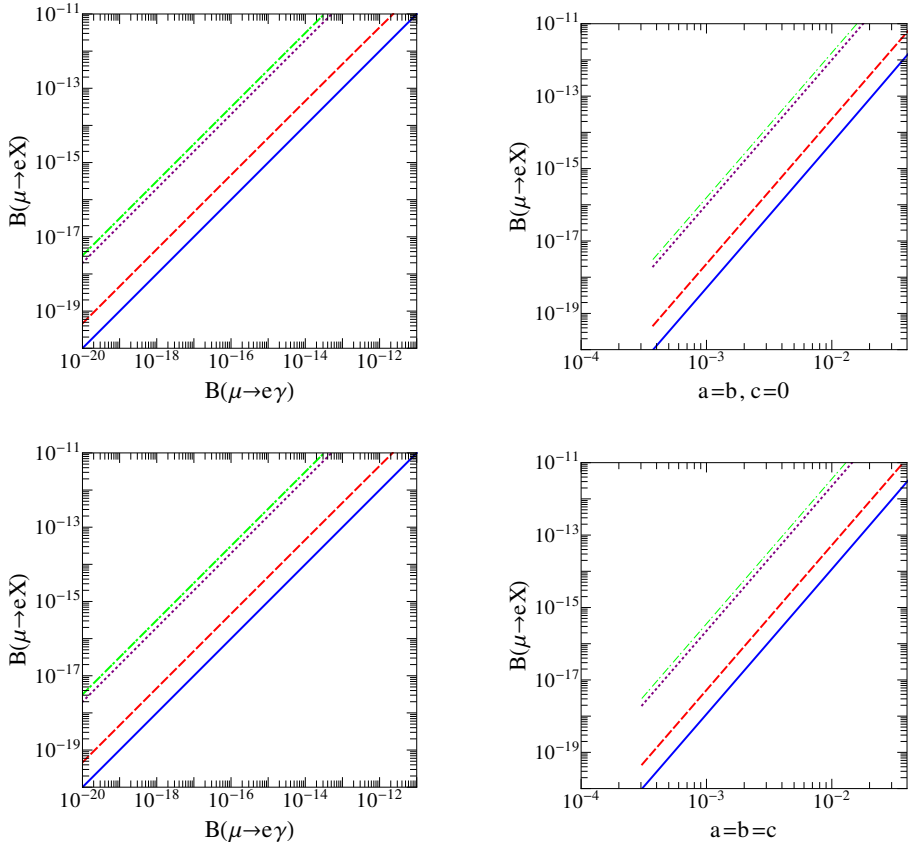


Figure 3.4: The same as in Fig 3.3, but for $m_N = 1$ TeV.

ture (2.30), with $a = c$ and $b = 0$, and the lower pannels for the Yukawa texture (2.31), with $a = b = c$. In both Figs 3.5 and 3.6, the Yukawa parameter a has been chosen, such that $10^{-16} < B(\tau \rightarrow e\gamma) < 10^{-7}$. As can be seen from Figs 3.5 and 3.6, all observables $B(\tau \rightarrow eX)$ of τ -LFV (with $X = \gamma, ee, \mu\mu$) exhibit similar quadratic dependence on the small Yukawa parameter a . However, close to the largest perturbatively allowed values of a , i.e. $a \lesssim 0.34$ for the model (2.30) and $a \lesssim 0.23$ for the model (2.31), some of the observables of τ -LFV exhibit either numerical instability, or the existence of a cancellation region in parameter space, as will be seen below.

Figure 3.7 presents numerical estimates of $B(\mu \rightarrow e\gamma)$ [blue (solid) line], $B(\mu \rightarrow eee)$ [red (dashed) line], $R_{\mu e}^{\text{Ti}}$ [violet (dotted) line] and $R_{\mu e}^{\text{Au}}$ [green (dash-dotted) line], as functions of $B(\mu \rightarrow e\gamma)$ (left pannels) and the heavy

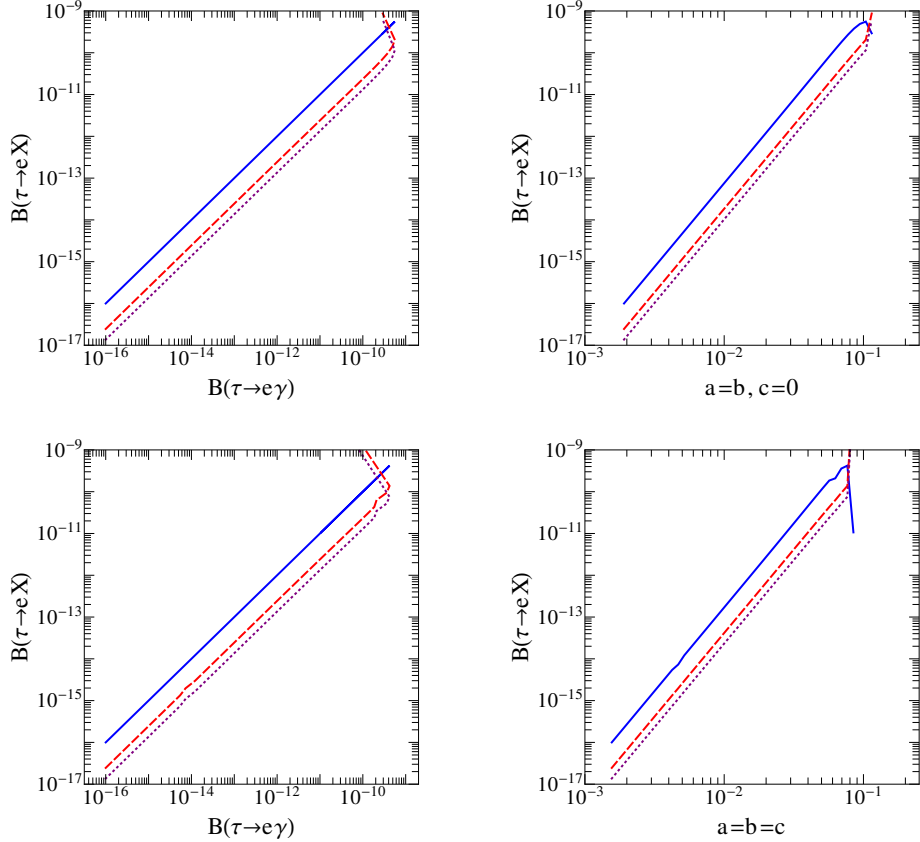


Figure 3.5: Numerical estimates of $B(\tau \rightarrow e\gamma)$ [blue (solid)], $B(\tau \rightarrow eee)$ [red (dashed)] and $B(\tau \rightarrow e\mu\mu)$ [violet (dotted)], as functions of $B(\tau \rightarrow e\gamma)$ (left panels) and the Yukawa parameter a (right panels), for $m_N = 400$ GeV and $\tan \beta = 10$. The upper panels present predictions for the Yukawa texture (2.30), with $a = c$ and $b = 0$, and the lower panels for the Yukawa texture (2.31), with $a = b = c$.

neutrino mass scale m_N (right panels). In all panels, the Yukawa parameter a is fixed by the condition $B(\mu \rightarrow e\gamma) = 10^{-12}$ for $m_N = 400$ GeV, using the benchmark value $\tan \beta = 10$. The upper panels display numerical values for the Yukawa texture (2.30), with $a = b$ and $c = 0$, and the lower panels for the Yukawa texture (2.31), with $a = b = c$. The heavy neutrino mass is varied within the LHC explorable range: $400 \text{ GeV} < m_N < 10 \text{ TeV}$. All observables $B(\mu \rightarrow eX)$ of μ -LFV (with $X = \gamma, ee, \text{Ti}, \text{Au}$) exhibit a non-trivial dependence on m_N . The branching ratio $B(\mu \rightarrow e\gamma)$ shows a dip at $m_N \approx 800$ GeV in both models (2.30) and (2.31), signifying the existence

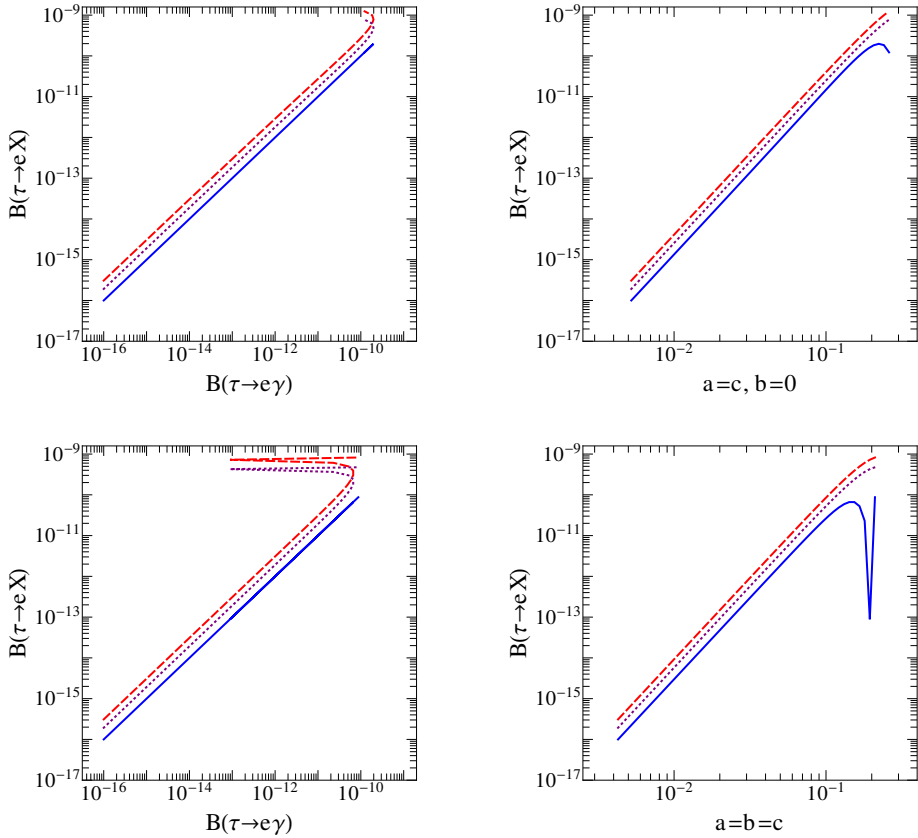


Figure 3.6: The same as in Fig 3.5, but for $m_N = 1$ TeV.

of a cancellation region in parameter space, due to the loops involving heavy neutrino, sneutrino and soft SUSY-breaking terms. For $m_N \gtrsim 3$ TeV, all observables tend to a constant value, as a result of the dominance of the soft SUSY-breaking contributions.

In Fig 3.8 we show contours of the Yukawa parameters (a, b, c) versus the heavy neutrino mass scale m_N , for $B(\mu \rightarrow e\gamma)$ [blue (solid) line], $B(\mu \rightarrow eee)$ [red (dashed) line], $R_{\mu e}^{\text{Ti}}$ [violet (dotted) line] and $R_{\mu e}^{\text{Au}}$ [green (dash-dotted) line]. The Yukawa parameter a and m_N are determined by the condition $B(\mu \rightarrow e\gamma) = 10^{-12}$. The labels in the vertical axes indicate the two Yukawa textures in (2.30) and (2.31), which we have adopted in our analysis. The contours for $B(\mu \rightarrow e\gamma)$ display a maximum for $m_N \approx 800$ GeV, as a consequence of cancellations between heavy neutrino, sneutrino and soft SUSY-

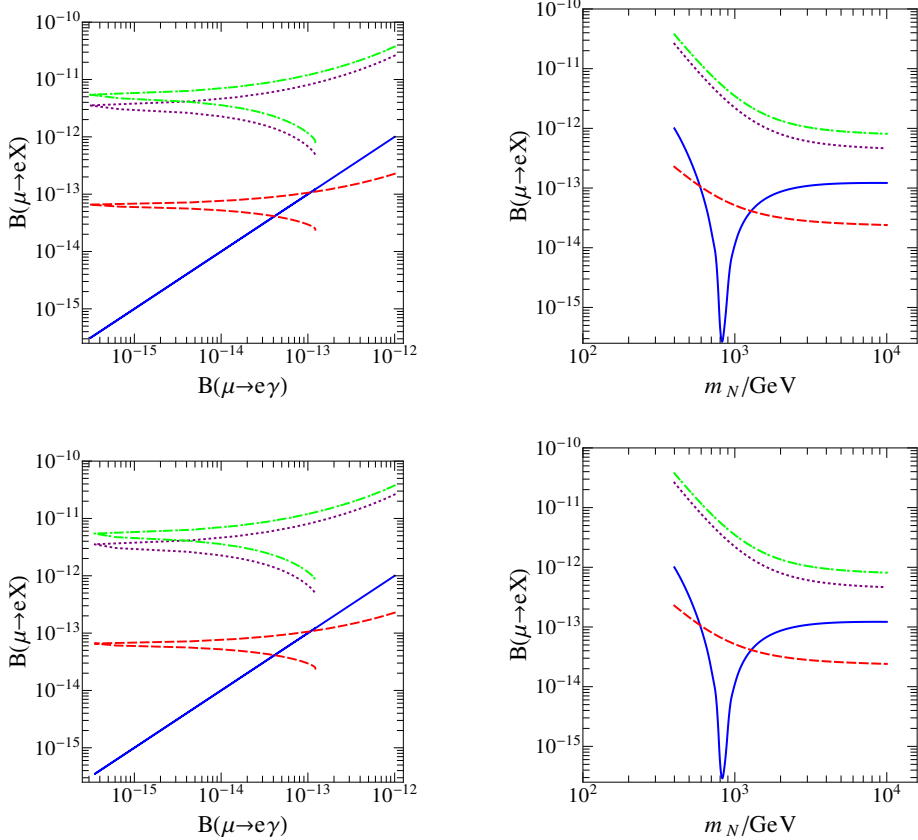


Figure 3.7: Numerical estimates of $B(\mu \rightarrow e\gamma)$ [blue (solid)], $B(\mu \rightarrow eee)$ [red (dashed)], $R_{\mu e}^{\text{Ti}}$ [violet (dotted)] and $R_{\mu e}^{\text{Au}}$ [green (dash-dotted)], as functions of $B(\mu \rightarrow e\gamma)$ (left panels) and the heavy neutrino mass scale m_N (right panels). In all panels, the Yukawa parameter a was kept fixed by the condition $B(\mu \rightarrow e\gamma) = 10^{-12}$ for $m_N = 400$ GeV, and $\tan \beta = 10$ was used. The upper panels display numerical values for the Yukawa texture (2.30), with $a = b$ and $c = 0$, and the lower panels for the Yukawa texture (2.31), with $a = b = c$.

breaking contributions (cf Fig 3.7).

Figure 3.9 shows contours of the Yukawa parameters (a, b, c) , as functions of m_N , for $B(\tau \rightarrow e\gamma)$ [blue (solid) line], where the parameters a and m_N are determined by the condition $B(\tau \rightarrow e\gamma) = 10^{-9}$. The numerical results for $B(\tau \rightarrow \mu\gamma)$ are not given, since these are fully complementary to the ones given for $B(\tau \rightarrow e\gamma)$. Given the above condition on $B(\tau \rightarrow e\gamma)$, no solution exists for the observables $B(\tau \rightarrow eee)$ and $B(\tau \rightarrow e\mu\mu)$.

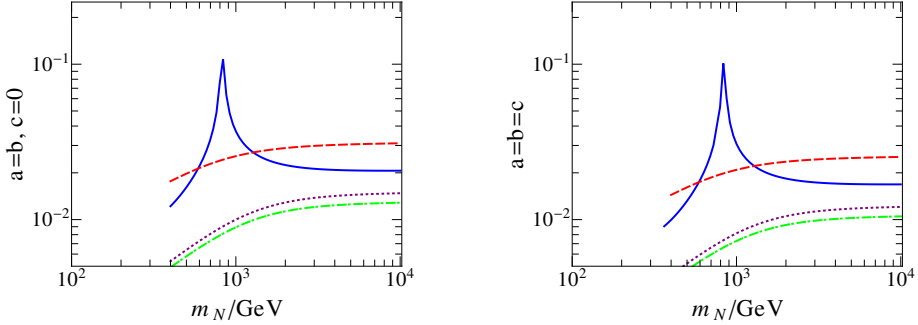


Figure 3.8: Contours of the Yukawa parameters (a, b, c) versus m_N , for $B(\mu \rightarrow e\gamma)$ [blue (solid)], $B(\mu \rightarrow eee)$ [red (dashed)], $R_{\mu e}^{\text{Ti}}$ [violet (dotted)] and $R_{\mu e}^{\text{Au}}$ [green (dash-dotted)], where a and m_N are determined by the condition $B(\mu \rightarrow e\gamma) = 10^{-12}$. All contours are evaluated with $\tan \beta = 10$ and for different Yukawa textures, as indicated by the vertical axes labels.

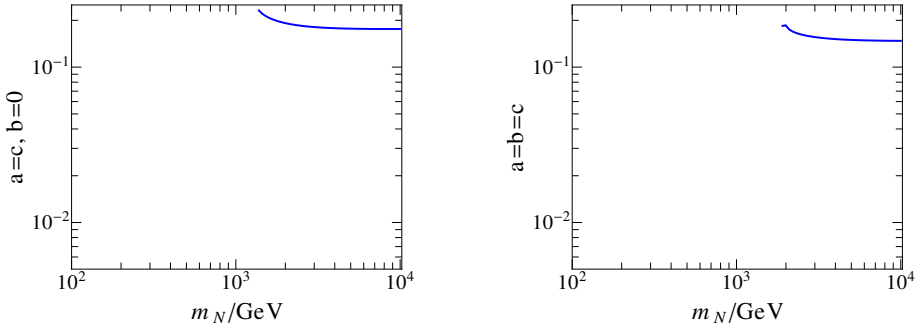


Figure 3.9: Contours of the Yukawa parameters (a, b, c) versus m_N , for $B(\tau \rightarrow e\gamma)$ [blue (solid)], where $\tan \beta = 10$ and a and m_N are determined by the condition $B(\tau \rightarrow e\gamma) = 10^{-9}$. No solutions have been found for $B(\tau \rightarrow eee)$ and $B(\tau \rightarrow e\mu\mu)$.

In the numerical analysis presented so far, the assumed value of $\tan \beta$ was fixed to its benchmark value given in (3.23), $\tan \beta = 10$. In Fig 3.10, this assumption is relaxed, and $\tan \beta$ is varied in the interval $5 \lesssim \tan \beta \lesssim 20$, while maintaining agreement with a SM-like Higgs boson mass $M_H \approx 125$ GeV and taking into account that the combined experimental and theoretical errors are currently of the order of 5–6 GeV. Specifically, in Fig 3.10 we display the dependence of $B(\mu \rightarrow e\gamma)$ [blue (solid) line], $B(\mu \rightarrow eee)$ [red (dashed) line], $R_{\mu e}^{\text{Ti}}$ [violet (dotted) line] and $R_{\mu e}^{\text{Au}}$ [green (dash-dotted) line] on $\tan \beta$. In all panels, the Yukawa parameter a is determined by the condition $B(\mu \rightarrow$

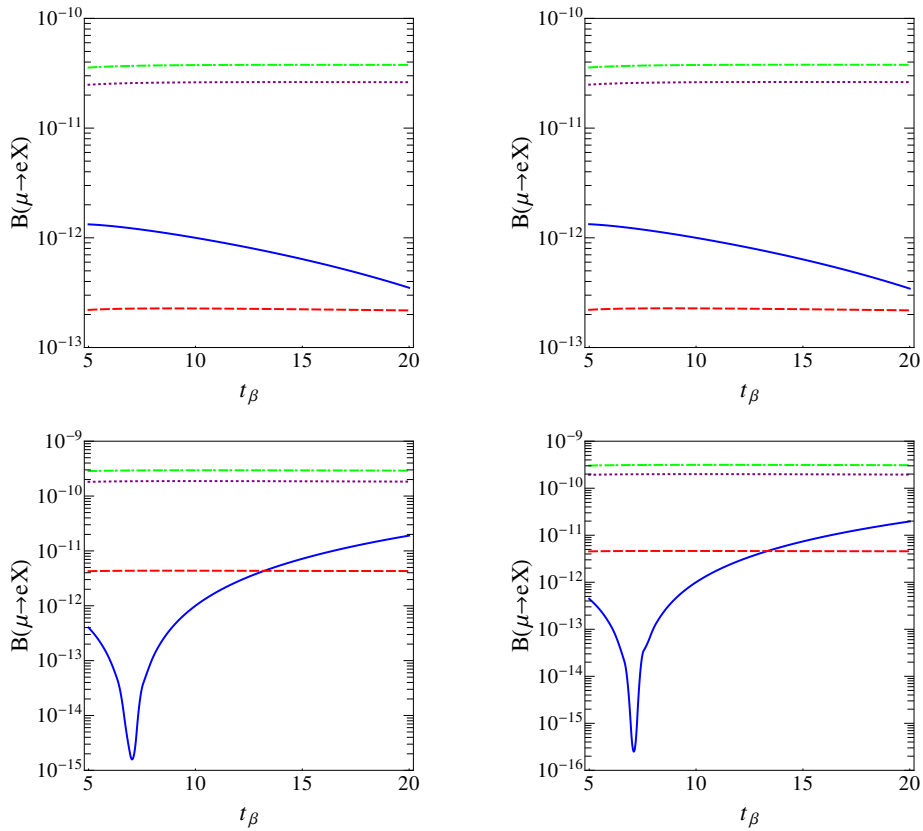


Figure 3.10: Numerical estimates of $B(\mu \rightarrow e\gamma)$ [blue (solid)], $B(\mu \rightarrow eee)$ [red (dashed)], $R_{\mu e}^{\text{Ti}}$ [violet (dotted)] and $R_{\mu e}^{\text{Au}}$ [green (dash-dotted)], as functions of $\tan \beta$. The upper pannels are obtained for $m_N = 400$ GeV and the lower pannels for $m_N = 1$ TeV. The left pannels use the Yukawa texture (2.30), with $a = b$ and $c = 0$, and the right pannels the Yukawa texture (2.31), with $a = b = c$. In all pannels, the Yukawa parameter a is determined by the condition $B(\mu \rightarrow e\gamma) = 10^{-12}$.

$e\gamma) = 10^{-12}$. The upper pannels in Fig 3.10 show numerical results for $m_N = 400$ GeV, while the lower pannels for $m_N = 1$ TeV. The left pannels give the predictions for the Yukawa texture (2.30), with $a = b$ and $c = 0$, and the right pannels for the Yukawa texture (2.31), with $a = b = c$. In the lower pannels, one can observe a suppression of $B(\mu \rightarrow e\gamma)$, for values $\tan \beta \approx 7$, due to the cancellation between heavy neutrino, sneutrino and soft SUSY-breaking effects.

It can be instructive to compare the contributions of the magnetic dipole form factors to the CLFV observables, with those originating from the remaining form factors. Specifically, if one assumes that only the magnetic dipole form factors $G_\gamma^{L,R}$ contribute in (3.10), (3.11) and (3.22), then the following analytical results are obtained for the ratios:

$$R_1 \equiv \frac{B(l \rightarrow l'l_1l_1^c)}{B(l \rightarrow l'\gamma)} = \frac{\alpha}{3\pi} \left(\ln \frac{m_l^2}{m_{l'}^2} - 3 \right) \quad (3.25)$$

$$R_2 \equiv \frac{B(l \rightarrow l'l'l'^c)}{B(l \rightarrow l'\gamma)} = \frac{\alpha}{3\pi} \left(\ln \frac{m_l^2}{m_{l'}^2} - \frac{11}{4} \right) \quad (3.26)$$

$$R_3 \equiv \frac{R_{\mu e}^J}{B(\mu \rightarrow e\gamma)} = 16\alpha^4 \frac{\Gamma_\mu}{\Gamma_{\text{capture}}} ZZ_{\text{eff}}^4 |F(-\mu^2)|^2. \quad (3.27)$$

According to the formulae (3.25)–(3.27), the predicted R_1 values for $\tau \rightarrow e\mu\mu$ and $\tau \rightarrow \mu ee$ are $1/90$ and $1/419$ respectively, the predicted R_2 values for $\mu \rightarrow eee$, $\tau \rightarrow eee$ and the $\tau \rightarrow \mu\mu\mu$ are $1/159$, $1/91$ and $1/460$ respectively, and the predicted R_3 values for Ti and Au are $1/198$ and $1/188$ respectively.

In Fig 3.11, the numerical estimates are given for the ratios $R_2(\mu \rightarrow eee)$, R_3^{Ti} and R_3^{Au} , as functions of m_N . The Yukawa parameter a is fixed by the condition $B(\mu \rightarrow e\gamma) = 10^{-12}$, for $m_N = 400$ GeV and $\tan \beta = 10$. In the upper pannel, thick lines show the predicted values obtained by a complete evaluation of $R_2(\mu \rightarrow eee)$ [blue (solid) line], R_3^{Ti} [red (dashed) line] and R_3^{Au} [violet (dotted) line], while the respective thin lines are obtained by keeping only the magnetic dipole form factors G_γ^L and G_γ^R . Hence, we see that going beyond the magnetic dipole moment approximation may enhance the ratios

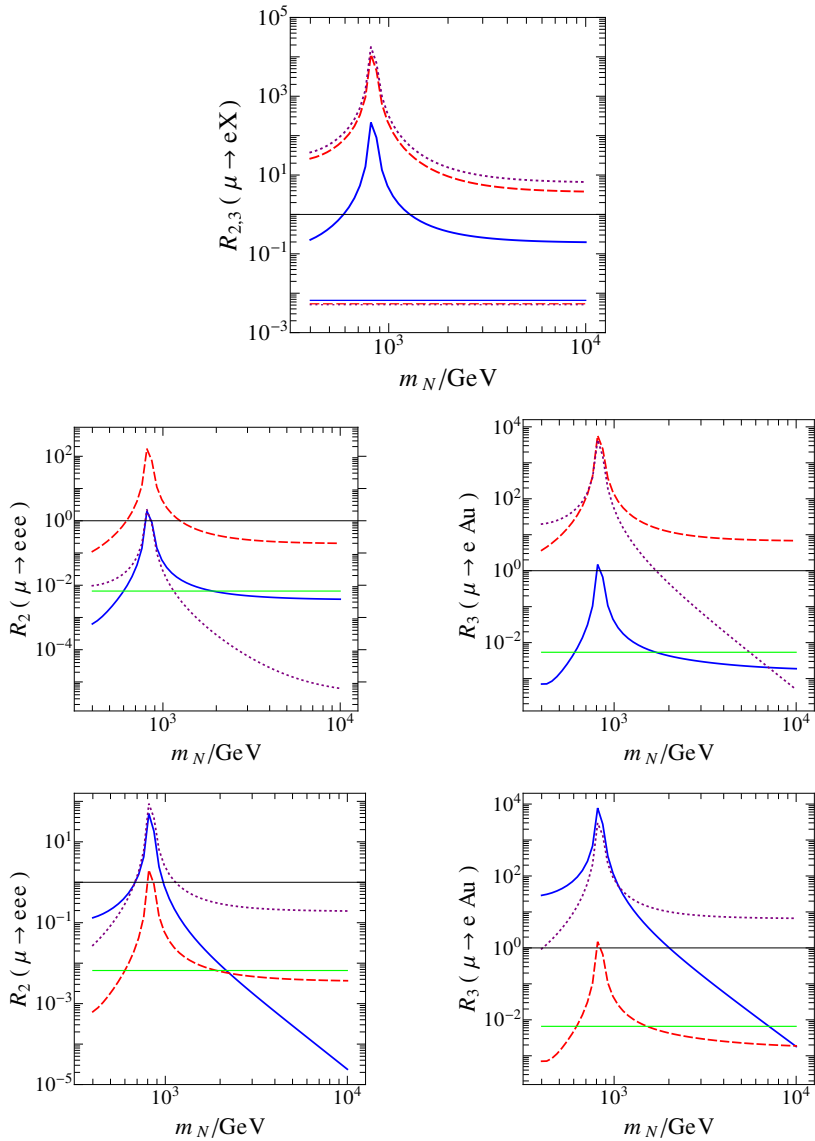


Figure 3.11: Numerical estimates of the ratios $R_2(\mu \rightarrow eee)$, R_3^{Ti} and R_3^{Au} , as functions of m_N . The Yukawa parameter a is fixed by the condition $B(\mu \rightarrow e\gamma) = 10^{-12}$, for $m_N = 400$ GeV and $\tan \beta = 10$. In the upper pannel, thick lines give the complete evaluation of $R_2(\mu \rightarrow eee)$ [blue (solid)], R_3^{Ti} [red (dashed)] and R_3^{Au} [violet (dotted)], while the respective thin lines are evaluated keeping only the magnetic dipole form factors G_γ^L and G_γ^R . The two middle pannels provide a form factor analysis of $R_2(\mu \rightarrow eee)$ and R_3^{Au} , in terms of contributions due to G_γ and F_γ [blue (solid)], F_Z [red (dashed)] and box form factors [violet (dotted)]. The lower two pannels show the separate contributions due to heavy neutrinos N [blue (solid)], sneutrinos \tilde{N} [red (dashed)] and soft SUSY-breaking LFV terms [violet (dotted)]. The green (horizontal) lines in the middle and lower pannels give the predicted values obtained by assuming that only the $G_\gamma^{L,R}$ form factors contribute to the amplitudes.

$R_{2,3}$ by more than two orders of magnitude.

The two middle pannels of Fig 3.11 provide a form factor analysis of $R_2(\mu \rightarrow eee)$ and R_3^{Au} , by considering separately the contributions due to G_γ and F_γ [blue (solid) line], F_Z [red (dashed) line] and box form factors [violet (dotted) line]. In particular, one observes that heavy neutrino contributions to the box form factors become comparable to and even larger than the Z -boson mediated graphs in $\mu \rightarrow e$ conversion in Gold, for heavy neutrino masses $m_N \lesssim 1$ TeV. We have checked that for $m_N \lesssim 1$ TeV, box graphs due to heavy neutrinos also dominate the process of $\mu \rightarrow e$ conversion in Titanium (not explicitly shown in Fig 3.11). Finally, the two lower pannels show the individual contributions due to the heavy neutrinos $N_{1,2,3}$ [blue (solid) line], sneutrinos $\tilde{N}_{1,2,\dots,12}$ [red (dashed) line] and soft SUSY-breaking LFV terms [violet (dotted) line]. From these two lower pannels, it is obvious that for heavy neutrino masses $m_N \gtrsim 1$ TeV, the soft SUSY-breaking effects dominate the CLFV form factors, which are tagged with the superscripts SB in Appendix C. Instead, for $m_N \lesssim 1$ TeV, heavy-neutrino effects start becoming the leading contribution to the CLFV observables associated with the muon. The green (horizontal) lines in the middle and lower pannels serve as reference values obtained by assuming that only the $G_\gamma^{L,R}$ form factors contribute to the amplitudes.

An important consistency check for this numerical analysis has been to *analytically* show that all soft SUSY-breaking effects on the form factors (C.4), (C.8) and (C.14) vanish in the limit of degenerate charged slepton masses. On the other hand, RGE effects from M_{GUT} to M_Z induce sizeable deviations to the charged slepton mass matrix from the unit matrix. As a consequence, unitarity cancellations due to the so-called GIM mechanism become less effective in this case and so render the SB part of the form factors, such as $F_{\nu' l Z}^{L,\text{SB}}$ and $F_{\nu' l Z}^{R,\text{SB}}$, rather large.

Another essential check was to show that under the assumptions adopted in part of Ref [157], the form factor $F_{\nu' l Z}^{L,\tilde{N}}$ given in Eq (C.7) reduces to $\frac{2c_W}{g} F_L^c$, where F_L^c is one of the form factors defined in [157, Eq (6)], which in turn can be shown to vanish. The assumptions in [157] are: (i) the standard

seesaw mechanism with ultra-heavy right neutrinos, (ii) no charged wino or higgsino mixing, and (iii) the dominance of the wino contribution. Under these three assumptions, the interaction vertices occurring in the form factor $F_{\nu l Z}^{L, \tilde{N}}$ simplify as follows:

$$\begin{aligned} \tilde{B}_{lmA}^{R,1}, \tilde{B}_{lmA}^{R,2} &\rightarrow -U_{lk}, \quad \tilde{C}_{AB}^1, \tilde{C}_{AB}^2, \tilde{C}_{AB}^3, \tilde{C}_{AB}^4 \rightarrow -\frac{1}{2} \delta_{kk'}, \\ V_{mk}^{\tilde{\chi}^- R} &\rightarrow c_w^2, \end{aligned} \tag{3.28}$$

where A, B now assume the restricted range of values $k, k' = 1, 2, 3$ and U is a 3×3 unitary matrix. Given the simplifications in Eq (3.28), we recover the expression given in Ref [157], resulting in the replacement: $F_{\nu l Z}^{L, \tilde{N}} \rightarrow \frac{2c_W}{g} F_L^c$. The above non-trivial checks provide firm support for the correctness of analytical and numerical results hereby presented. The full-fledged calculation in Ref [157] was performed without the above mentioned assumptions.

Chapter 4

Lepton Dipole Moments

In this chapter we perform the study of anomalous magnetic and electric dipole moments of charged leptons in ν_R MSSM, under the assumption that CP violation originates from complex soft SUSY-breaking bilinear and trilinear couplings associated with the right-handed sneutrino sector.

In the first section, the conventions and notation for the lepton dipole moments will be presented. This will be accompanied by the description of the new sources of CP violation which are considered within the ν_R MSSM.

Second section contains the numerical estimates for the anomalous magnetic moment of the muon (a_μ) and the electric dipole moment of the electron (d_e).

Technical details pertinent to the lepton-dipole moment form factors are to be found at the end of this chapter.

These results are presented in Ref [158].

§ 4.1 Magnetic and electric dipole moments

The anomalous MDM and EDM of a charged lepton l can be read off from the Lagrangian [159]:

$$\mathcal{L} = \bar{l} \left[\gamma_\mu (i\partial^\mu + eA^\mu) - m_l - \frac{e}{2m_l} \sigma^{\mu\nu} (F_l + iG_l\gamma_5) \partial_\nu A_\mu \right] l. \quad (4.1)$$

In the on-shell limit of the photon field A^μ , the form factor F_l defines the anomalous magnetic dipole moment (MDM) of the lepton l , i.e. $a_l \equiv F_l$, whilst the form factor G_l defines its electric dipole moment (EDM), i.e. $d_l \equiv eG_l/m_l$. Using Eq (3.1), one can write down the general form-factor decomposition of the photonic transition amplitude,

$$i\mathcal{T}^{\gamma ll} = i \frac{e\alpha_w}{8\pi M_W^2} \left[(G_\gamma^L)_l i\sigma_{\mu\nu} q^\nu P_L + (G_\gamma^R)_l i\sigma_{\mu\nu} q^\nu P_R \right]. \quad (4.2)$$

The anomalous MDM (a_l) and the EDM (d_l) of a lepton l are then respectively determined by:

$$a_l = \frac{\alpha_w m_l}{8\pi M_W^2} \left[(G_\gamma^L)_l + (G_\gamma^R)_l \right], \quad (4.3)$$

$$d_l = \frac{e\alpha_w}{8\pi M_W^2} i \left[(G_\gamma^L)_l - (G_\gamma^R)_l \right]. \quad (4.4)$$

Here and in the following, the notation for the couplings and the form-factors will correspond to the one used in Chapter 3.

As shown in Ref [160], the EDM d_l of the lepton vanishes in the MSSM with universal soft SUSY-breaking boundary conditions, if no CP phases are introduced. This result also holds true in the extensions of the MSSM with heavy neutrinos, as long as the sneutrino sector is universal and CP-conserving.

As a minimal departure from the above universal scenario, let it be assumed that *only* the sneutrino sector is CP-violating due to soft CP phases in the

bilinear and trilinear soft-SUSY breaking parameters:

$$\mathbf{b}_\nu \equiv \mathbf{B}_\nu \mathbf{m}_M = B_0 e^{i\theta} m_N \mathbf{1}_3, \quad (4.5)$$

$$\mathbf{A}_\nu = \mathbf{h}_\nu A_0 e^{i\phi}, \quad (4.6)$$

where B_0 and A_0 are real parameters determined at the GUT scale, m_N is a real parameter inputed at the scale m_N , and θ and ϕ are physical, flavor-blind CP-odd phases, and \mathbf{h}_ν is the 3×3 neutrino Yukawa matrix given by Eq (2.31). The soft SUSY breaking terms corresponding to the \mathbf{b}_ν and \mathbf{A}_ν are obtained from the Lagrangian terms

$$-(\mathbf{A}_\nu)^{ij} \tilde{\nu}_{iR}^c (h_{uL}^+ \tilde{e}_{jL} - h_{uL}^0 \tilde{\nu}_{jL}) \quad (4.7)$$

and

$$(\mathbf{b}_\nu \mathbf{m}_M)_{ii} \tilde{\nu}_{Ri} \tilde{\nu}_{Ri}, \quad (4.8)$$

respectively. Correspondingly, $\tilde{\nu}_{iR}^c$, \tilde{e}_{jL} , h_{uL}^+ and h_{uL}^0 denote the heavy sneutrino, selectron, charged Higgs and neutral Higgs fields. The $O(3)$ flavor symmetry of the model for the heavy neutrinos assures that the heavy neutrino mass matrix \mathbf{m}_N is proportional to the unit matrix $\mathbf{1}_3$ with eigenvalues m_N , up to small renormalization-group effects. To keep things simple, we also assume that the 3×3 soft bilinear mass matrix \mathbf{b}_ν is proportional to $\mathbf{1}_3$. In the standard SUSY seesaw scenarios with ultra-heavy neutrinos of mass m_N , the CP-violating sneutrino contributions to electron EDM d_e scale as B_0/m_N and A_0/m_N at the one-loop level, and practically decouple for heavy-neutrino masses m_N close to the GUT scale. Hence, sizeable effects on d_e should only be expected in low-scale seesaw scenarios, in which m_N can become comparable to B_0 and A_0 .

Note that the bilinear soft 3×3 matrix \mathbf{b}_ν was neglected in the previous chapter, where it was tacitly assumed that it was small compared to the other soft SUSY-breaking parameters in sneutrino mass matrix given by Eq (2.34). Here, this term will be taken into the account, but with the restricted size of the universal bilinear mass parameter B_0 , such that the sneutrino masses remain always positive and hence physical.

The generation of a non-zero lepton EDM d_l results from the soft sneutrino CP-odd phases θ and ϕ , as well as from complex neutrino Yukawa couplings \mathbf{h}_ν . All these CP-odd phases are present in the photon dipole form factors $G_{ll\gamma}^{L,\tilde{N}}$ and $G_{ll\gamma}^{R,\tilde{N}}$, whose analytical forms may be found in Appendix C. In fact, it can be noticed that d_l may be generated by products of vertices that are not relatively complex conjugate to each other, since they contain the factors

$$\Delta_{\text{CP}}^{LR} = \tilde{B}_{lkA}^{L,1} \tilde{B}_{lkA}^{R,1*} + \tilde{B}_{lkA}^{L,2} \tilde{B}_{lkA}^{R,2*}, \quad \Delta_{\text{CP}}^{RL} = \tilde{B}_{lkA}^{R,1} \tilde{B}_{lkA}^{L,1*} + \tilde{B}_{lkA}^{R,2} \tilde{B}_{lkA}^{L,2*}, \quad (4.9)$$

as can be seen from the Eq (C.3),

In the exact supersymmetric limit of softly-broken SUSY theories, the anomalous MDM (as well as EDM) operator is forbidden. This comes as a consequence of the Ferrara and Remiddi no-go theorem [132], which is verified for every particle and its SUSY-counterpart contribution to the anomalous MDM a_μ . Besides the SM contribution, there are three additional contributions in the ν_R MSSM, which originate from: (i) heavy neutrinos, (ii) sneutrinos and (iii) soft SUSY-breaking parameters. In the supersymmetric limit, the latter contribution (iii) vanishes. In the same limit, the heavy neutrino and sneutrino contributions read:

$$\begin{aligned} (G_\gamma^{ll})^N &\rightarrow \frac{7}{6} B_{lN_a} B_{lN_a}^*, \\ (G_\gamma^{ll})^{\tilde{N}} &\rightarrow -\frac{7}{6} B_{lN_a} B_{lN_a}^*, \end{aligned} \quad (4.10)$$

where B_{lN_a} are the lepton-to-heavy neutrino mixings defined in Refs [104, 105, 110]. Obviously, the sum $(G_\gamma^{ll})^N + (G_\gamma^{ll})^{\tilde{N}}$ vanishes, thereby confirming the above mentioned theorem proposed by Ferrara and Remiddi.

In the MSSM, the leading contribution to a_l behaves as [161–163]

$$a_l^{\text{MSSM}} \propto \frac{m_l^2}{M_{\text{SUSY}}^2} \tan \beta \text{ sign}(\mu M_{1,2}), \quad (4.11)$$

where M_{SUSY} is a typical soft SUSY-breaking mass scale, $\tan \beta = v_2/v_1$ is

the ratio of the neutral Higgs vacuum expectation values, and $M_{1,2}$ are the soft gaugino masses associated with the $U(1)_Y$ and $SU(2)$ gauge groups, respectively. As will be seen in the next section, the MSSM contribution (4.11) to a_μ remains dominant in the ν_R MSSM as well.

From Eqs (4.3) and (4.11), one naively expects d_l at the one-loop level to behave

$$d_l^{\text{MSSM}} \propto \sin(\phi_{\text{CP}}) \frac{m_l}{M_{\text{SUSY}}^2} \tan \beta , \quad (4.12)$$

where ϕ_{CP} is a generic soft SUSY-breaking CP-odd phase. Although there are different dependencies of d_l on $\tan \beta$ possible in the MSSM beyond the one-loop approximation [160, 164] it will be shown that within the ν_R MSSM, the $\tan \beta$ dependence is linear at the one loop level.

§ 4.2 Numerical results

In this numerical analysis, we will adopt the procedure established in Chapter 3. As a benchmark model, we choose a minimally extended scenario of minimal supergravity (mSUGRA), in which we allow for the bilinear and trilinear soft SUSY-breaking terms, \mathbf{B}_ν and \mathbf{A}_ν , to acquire at the GUT scale overall CP-violating phases denoted as θ and ϕ , respectively. Like before, we choose the sign of the μ -parameter to be positive. As for the neutrino Yukawa coupling matrix \mathbf{h}_ν , we consider the A_4 -symmetric models introduced in previous chapter [see Eq (2.31)].

For definiteness, our numerical analysis in this section is based on the following baseline scenario:

$$\begin{aligned} m_0 &= 1 \text{ TeV}, & M_{1/2} &= 1 \text{ TeV}, & A_0 &= -4 \text{ TeV}, & \tan \beta &= 20, \\ m_N &= 1 \text{ TeV}, & B_0 &= 0.1 \text{ TeV}, & a = b = c &= 0.05, \end{aligned} \quad (4.13)$$

where m_0 , $M_{1/2}$ and A_0 are the standard universal soft SUSY-breaking parameters [cf Eq (2.15)]. All mass parameters except m_N are defined at the

GUT scale and m_N is intaken at m_N scale. It is understood that parameters which are not explicitly quoted in the text assume their default values stated in (4.13).

We will analyze the deviation of a_μ from the SM value due to the ν_R MSSM, denoted by δa_μ , as well as d_e on several key theoretical parameters, by varying them around their baseline value given in (4.13), while keeping the remaining parameters fixed. In doing so, it will be made sure that the displayed parameters can accommodate the LHC data for a SM-like Higgs boson with mass $m_H = 125.5 \pm 2$ GeV [82, 84, 147] and satisfy the current lower limits on gluino and squark masses [146, 147], i.e. $m_{\tilde{g}} > 1500$ GeV and $m_{\tilde{t}} > 500$ GeV.

§ 4.2.1 Results for a_μ

The numerical estimates for δa_μ exhibit a direct quadratic dependence on the muon mass m_μ . In fact, one finds that for the same set of soft SUSY-breaking parameters m_0 , $M_{1/2}$ and A_0 , the ratio $\delta a_\mu/\delta a_e$ remains constant to a good approximation, i.e. $\delta a_\mu/\delta a_e \approx m_\mu^2/m_e^2 \approx 42752.0$. In order to understand this parameter dependence, one has to carefully analyze the soft SUSY-breaking contributions to the form-factors:

$$\begin{aligned} G_{ll\gamma}^{L,\text{SB}} &= \tilde{V}_{lma}^{0\ell R} \tilde{V}_{lma}^{0\ell R*} \left[m_l \lambda_{\tilde{e}_a} J_{41}^1(\lambda_{\tilde{e}_a}, \lambda_{\tilde{\chi}_m^0}) \right] + \tilde{V}_{lma}^{0\ell L} \tilde{V}_{lma}^{0\ell L*} \left[m_l \lambda_{\tilde{e}_a} J_{41}^1(\lambda_{\tilde{e}_a}, \lambda_{\tilde{\chi}_m^0}) \right] \\ &\quad + \tilde{V}_{lma}^{0\ell L} \tilde{V}_{lma}^{0\ell R*} \left[2m_{\tilde{\chi}_m^0} \lambda_{\tilde{e}_a} J_{31}^0(\lambda_{\tilde{e}_a}, \lambda_{\tilde{\chi}_m^0}) \right], \end{aligned} \quad (4.14)$$

$$\begin{aligned} G_{ll\gamma}^{R,\text{SB}} &= \tilde{V}_{lma}^{0\ell L} \tilde{V}_{lma}^{0\ell L*} \left[m_l \lambda_{\tilde{e}_a} J_{41}^1(\lambda_{\tilde{e}_a}, \lambda_{\tilde{\chi}_m^0}) \right] + \tilde{V}_{lma}^{0\ell R} \tilde{V}_{lma}^{0\ell R*} \left[m_l \lambda_{\tilde{e}_a} J_{41}^1(\lambda_{\tilde{e}_a}, \lambda_{\tilde{\chi}_m^0}) \right] \\ &\quad + \tilde{V}_{lma}^{0\ell R} \tilde{V}_{lma}^{0\ell L*} \left[2m_{\tilde{\chi}_m^0} \lambda_{\tilde{e}_a} J_{31}^0(\lambda_{\tilde{e}_a}, \lambda_{\tilde{\chi}_m^0}) \right], \end{aligned} \quad (4.15)$$

where the different terms that occur in Eq (4.14) and (4.15) are defined in Chapter 3 as well as at the end of this chapter. It is important to note that the neutralino vertices induce a term which is not manifestly proportional to the charged lepton mass, but to the neutralino mass. However, we have numerically confirmed that δa_μ is proportional to m_l^2 , which means that

the products of the mixing matrices $\tilde{V}_{lma}^{0\ell R}\tilde{V}_{lma}^{0\ell R*}$ and $\tilde{V}_{lma}^{0\ell R}\tilde{V}_{lma}^{0\ell L*}$, as well as $G_{ll\gamma}^{L,\text{SB}}$ and $G_{ll\gamma}^{R,\text{SB}}$, are themselves proportional to the charged lepton mass m_l (cf Ref [163]). The latter provides a non-trivial powerful check for the correctness of the results presented in this thesis.

In addition, this numerical analysis shows that the contribution to the muon anomalous MDM is almost independent of the neutrino-Yukawa parameters a , b and c , the heavy neutrino mass m_N and the soft trilinear parameter A_0 . Hence, our results are almost insensitive to a particular choice for a neutrino Yukawa texture, e.g. as given in (2.30) and (2.31), and also independent of the CP-odd phases θ and ϕ .

In Fig 4.1, the numerical estimates for δa_μ are given, as a function of the key theoretical parameters: $\tan \beta$, $M_{1/2}$, m_0 and m_N . In the frame (a) of this figure, we see that δa_μ depends linearly on $\tan \beta$, as expected from (4.11). Likewise, in Fig 4.1 we have investigated the dependence of δa_μ on the soft SUSY-breaking parameters m_0 and $M_{1/2}$, for different kinematic situations, and obtained results consistent with the scaling behaviour of $1/M_{\text{SUSY}}^2$ in (4.11).

In the pannel (e) of Fig 4.1, we observe that the effect of the heavy right-handed neutrinos (N) and sneutrinos (\tilde{N}) on δa_μ is negative, but small, in agreement with our discussion above. The size of their contributions alone to a_μ ranges from -10^{-12} to -4.8×10^{-15} , for $m_N = 0.5 - 10$ TeV. On the other hand, the left-handed sneutrino contributions to a_μ are approximately independent of the heavy Majorana mass m_N , reaching values $\approx 8.5 \times 10^{-11}$. The soft SUSY-breaking contributions are also approximately independent of the heavy Majorana mass m_N and have values $\approx 1.1 \times 10^{-12}$. Note that the light sneutrino contribution to the anomalous magnetic moment is the largest in magnitude, and it is already present in the MSSM contributions to a_μ .

Finally, we have checked the dominance of the MSSM contributions by looking at the dependence of the parameter:

$$\delta' a_\mu = a_\mu^{\nu_R \text{MSSM}} - a_\mu^{\text{MSSM}}. \quad (4.16)$$

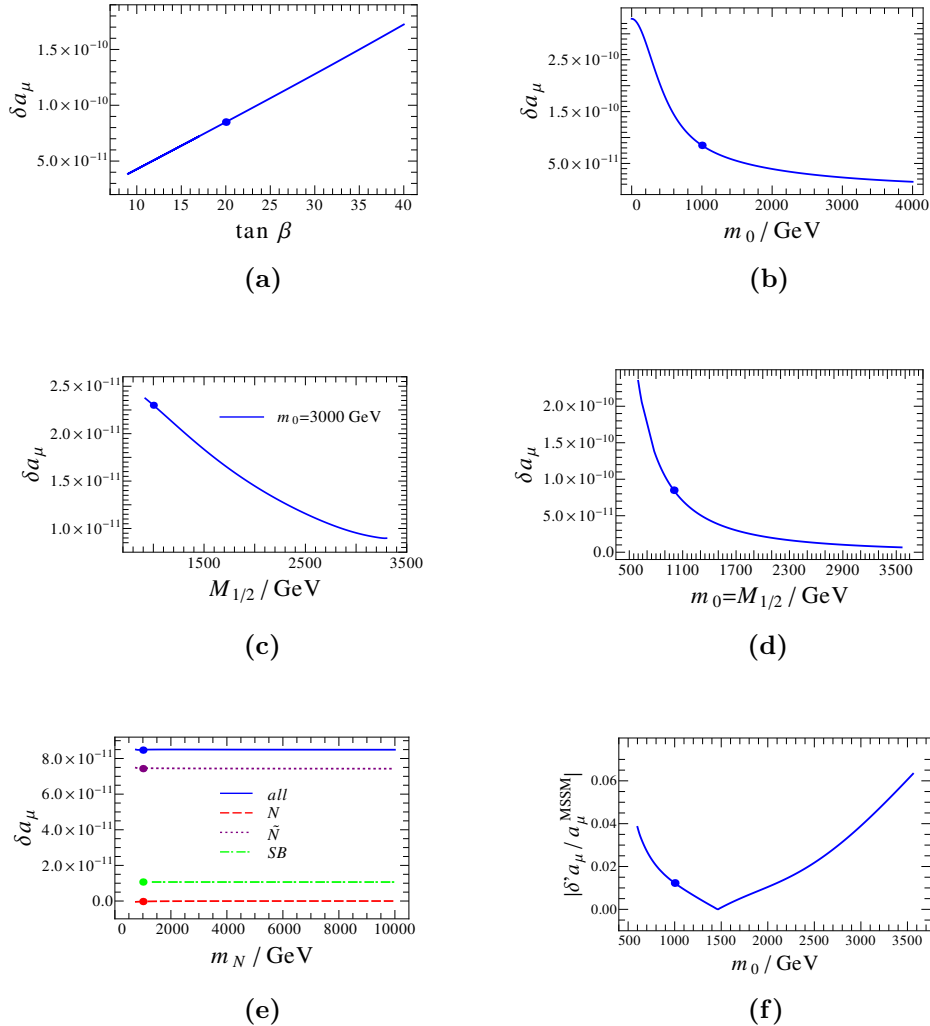


Figure 4.1: Numerical estimates for the contribution to the muon anomalous MDM, as functions of $\tan \beta$, $M_{1/2}$, m_N , m_0 and $m_0 = M_{1/2}$, in the ν_R MSSM. The default parameter set of the baseline model is given in (4.13). The panel (e) shows the heavy neutrino (N), sneutrino (\tilde{N}), soft SUSY-breaking (SB) and *all* contributions to δa_μ , as a function of m_N . The panel (f) displays the absolute value of the relative deviation $\delta' a_\mu / a_\mu$ of the ν_R MSSM and MSSM predictions for a_μ [cf. (4.16)], as a function of m_0 . The range of input parameters in all plots satisfy the current LHC constraints on Higgs, gluino and squark masses. The heavy dots on the curves give the predicted values evaluated for the default parameters (4.13).

The difference $\delta' a_\mu$ of the predictions for a_μ within the ν_R MSSM and the MSSM divided by a_μ is evaluated, and the absolute values of the results are displayed in the pannel (f) of Fig 4.1, as a function of $m_0 = M_{1/2}$. The largest deviation from the MSSM is found for largest allowed parameter value, $m_0 = 3600$ GeV, in which case $\delta' a_\mu/a_\mu^{\text{MSSM}}$ is as large as 6.2×10^{-2} .

§ 4.2.2 Results for d_e

We will now study the dependence of the electron EDM d_e on several key model parameters, such as m_0 , $M_{1/2}$, B_0 , A_0 , $\tan\beta$, θ and ϕ . The predictions for d_μ may be obtained by using the naive scaling relation: $d_\mu \approx (m_\mu/m_e) d_e \approx 205 d_e$. It is found this scaling behaviour is numerically satisfied very well. The maximal numerical values for d_e obtained are of the order $\sim 10^{-27}$ e cm. The predicted values for d_μ are therefore always found to be less than $\sim 10^{-25}$ e cm, which is several orders of magnitude below the present experimental upper bound: $d_\mu = 0.1 \pm 0.9 \times 10^{-19}$ e cm [37].

It is noted that heavy singlet neutrinos N do not contribute to d_e , even if the soft SUSY-breaking CP-odd phases ϕ and θ are taken to be non-zero. On the other hand, soft SUSY-breaking and right handed neutrino effects induce non-vanishing d_e , if either θ or ϕ are non-zero. If both $\phi = 0$ and $\theta = 0$, lepton EDMs d_l numerically vanish. Therefore, the complex products of vertices (4.9) emerging in the ν_R MSSM do not induce the CP violation at one loop level, in accord with the result of Ref [160] obtained in the MSSM with a high-scale seesaw mechanism.

In Fig 4.2, the present numerical estimates of d_e on the ν_R MSSM parameters $\tan\beta$, m_0 , $M_{1/2}$ and m_N , for maximal A_0 phase, $\phi = \pi/2$ are presented. The value of θ is set to zero, since the dependence of d_e on B_0 is weaker than the dependence on A_0 . As shown in pannel (a) of Fig 4.2 d_e exhibits a linear dependence on $\tan\beta$ confirming the $\tan\beta$ naive scaling behaviour in Eq (4.12).

Further, d_e is a decreasing function of m_0 . As a function of $m_0 = M_{1/2}$, d_e assumes both positive and negative values, and is roughly proportional to

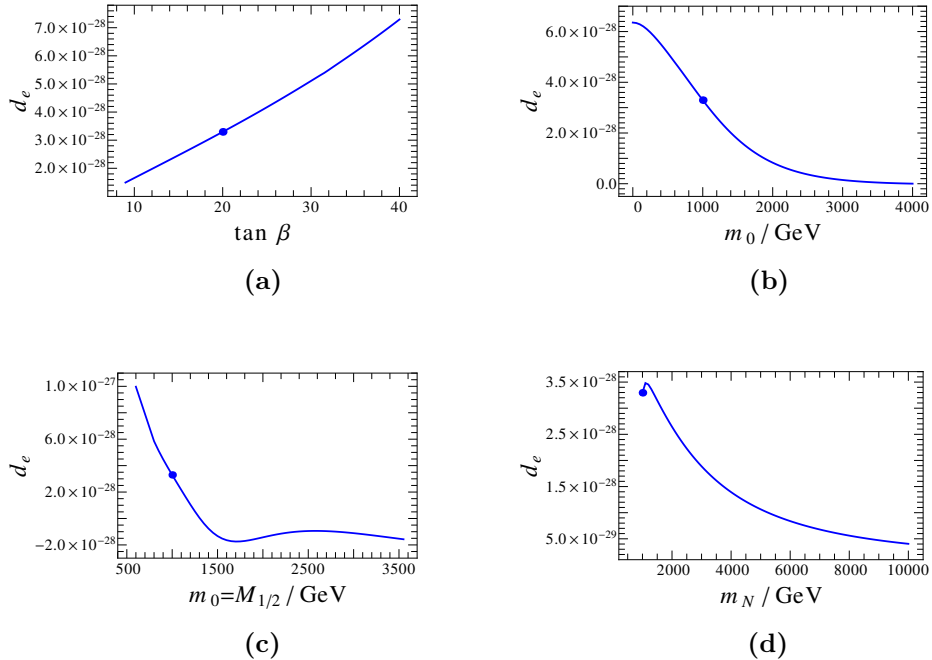


Figure 4.2: Numerical estimates of the electron EDM d_e in the ν_R MSSM, as functions of $\tan \beta$, m_0 , $m_0 = M_{1/2}$ and m_N , for $\phi = \pi/2$. The remaining parameters not shown assume the baseline values in (4.13). All input parameters are chosen so as to satisfy the LHC constraints on Higgs, gluino and squark masses. The heavy dots on the curves indicate the predicted values for d_e evaluated for the default parameters (4.13).

$-1 - 2.4 \text{ TeV}/m_0 + 6.3 \text{ TeV}^2/m_0^2$. There is also a small region of parameter space for $m_0 = M_{1/2} \lesssim 800$ GeV, for which the prediction for d_e is of the order of the experimental upper limit on d_e (1.6). In addition, d_e decreases with increasing m_N : for the m_N values from the pannel (d) of Fig 4.2 this behavior can roughly approximated by a function $-0.13 + \text{TeV}^{\frac{2}{3}} m_N^{-\frac{2}{3}}$, in the m_N -range $10 \text{ TeV} < m_N < 100 \text{ TeV}$ d_e roughly scales as $1/m_N$, and above $m_N = 100 \text{ TeV}$ it becomes very slowly decreasing function in m_N .

In Fig 4.3, we show the predicted numerical values for d_e , as functions of the soft SUSY-breaking parameters A_0 and B_0 , and their corresponding CP phases ϕ and θ . In all pannels except the pannel (c), where $\phi = 0$ and θ is a variable, ϕ assumes value $\pi/2$ or it is a variable and θ is taken to be equal zero. In the pannel (a) of Fig 4.3, the soft trilinear parameter A_0 is

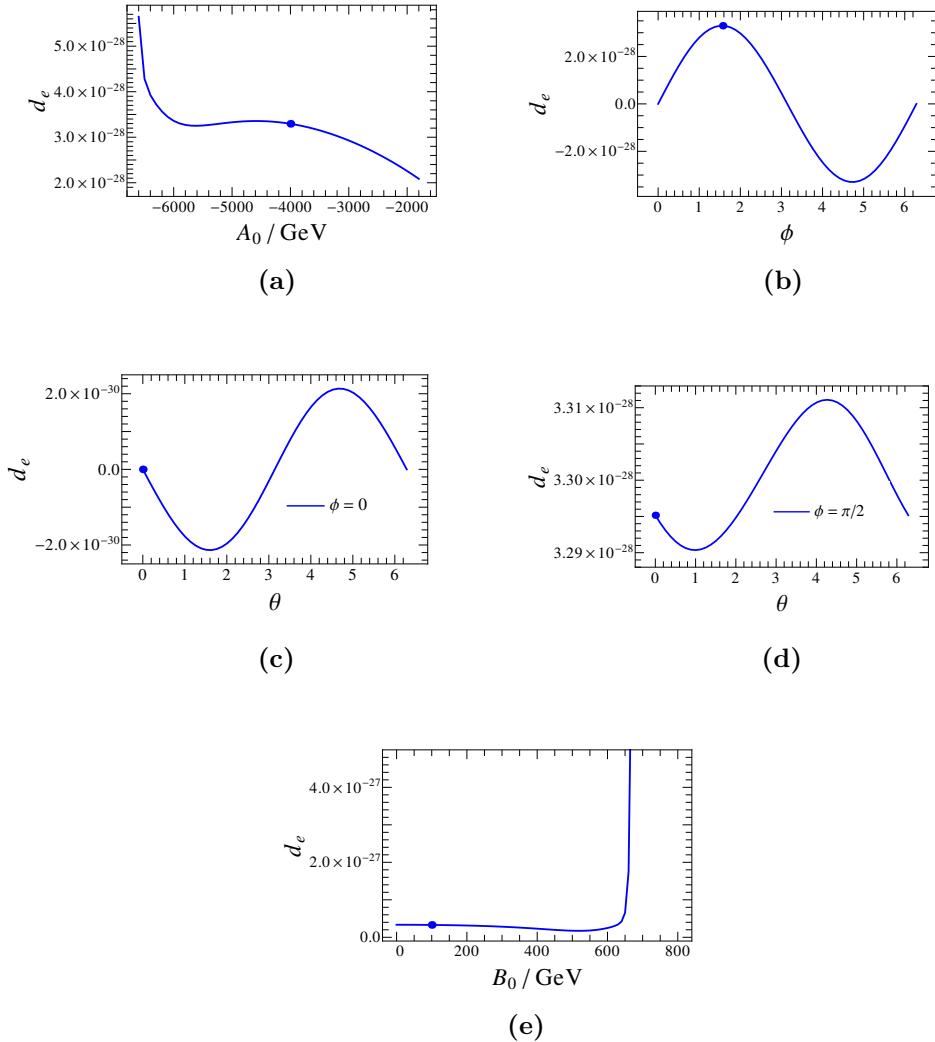


Figure 4.3: Predicted numerical values for the electron EDM d_e versus the soft SUSY breaking parameters A_0 and B_0 and their corresponding soft CP-odd phases ϕ and θ in the ν_R MSSM, for the baseline scenario in (4.13). If not shown ϕ assumes value $\pi/2$. The range of input parameters shown in the plots is compatible with the LHC constraints on Higgs, gluino and squark masses. The heavy dots show the predicted values for d_e , using the default parameters (4.13).

constrained by the LHC data pertinent to Higgs, gluino and squark masses. The electron EDM d_e is a complicated function of $|A_0|$ that slowly rises for $|A_0|$ between 1.8 TeV and 4.5 TeV, slowly decreases for $|A_0|$ between 4.5 TeV and 6 TeV, and steeply rises for $|A_0| > 6$ TeV. This function cannot be pre-

cisely described by a simple Laurent series in $|A_0|$, but in the largest part of the allowed $|A_0|$ interval it can roughly be approximated by a constant. The ϕ dependence of d_e is almost sinusoidal with an amplitude few times smaller than the experimental upper bound (1.6). Moreover, d_e is approximately constant function of B_0 , up to $B_0 \approx 600$ GeV. For larger values, i.e. $B_0 \gtrsim 600$ GeV, d_e steeply rises, suggesting the numerical instability in the diagonalization of the sneutrino mass matrix, which probably makes the results in this regime invalid. For $\phi = \pi/2$, the electron EDM d_e attains values of order the experimental upper limit (1.6), but for $\phi = \theta = 0$, the predictions are numerically consistent with zero. The dependence of d_e on θ is sinusoidal with an amplitude of order $\text{few} \times 10^{-30}$, while its average value strongly depends on the chosen value ϕ . From Figs 4.2 and 4.3, the following dependence of d_l on m_l , $m_0 = M_{1/2}$, m_N and $\tan \beta$ may be deduced:

$$d_l \propto \tan \beta \cdot m_l \cdot \frac{f(m_0)}{m_N^x}, \quad m_N < 10 \text{ TeV}, \quad (4.17)$$

where x assumes values between $2/3$ and 1 , and $f(m_0)$ is roughly proportional to the function $-1 - 2.4 \text{ TeV}/m_0 + 6.3 \text{ TeV}^2/m_0^2$. The last factor in Eq (4.17) corresponds to the scaling factor $1/M_{SUSY}^2$ in the naive approximation (4.12), and in the approximate expressions for lepton EDM derived in Ref [160].

§ 4.3 Technical remarks

Let's end this chapter with several technical remarks, including the detailed analytical expressions for all the quantities that appear in the form factors $G_{ll\gamma}^{L,SB}$ and $G_{ll\gamma}^{R,SB}$, given in (4.14) and (4.15), respectively. To start with, the variables λ_X are defined as $\lambda_X = m_X^2/M_W^2$, for instance $\lambda_{\tilde{e}} = m_{\tilde{e}}^2/M_W^2$. The integrals J_{bc}^a derived from loop integrations (see Appendix B) are UV finite. These are given by

$$J_{bc}^a = (-1)^{a-n_b-n_c} \int_0^\infty \frac{dx x^{1+a}}{(x + \lambda_b)^{n_b} (x + \lambda_c)^{n_c}}. \quad (4.18)$$

The couplings $\tilde{V}_{lma}^{0\ell L}$ and $\tilde{V}_{lma}^{0\ell R}$ read:

$$\tilde{V}_{lma}^{0\ell L} = -\sqrt{2}t_w Z_{m1}^*(R_R^{\tilde{e}})_{al}^* - \frac{(m_e)_l}{\sqrt{2}c_\beta M_W} Z_{m3}^*(R_L^{\tilde{e}})_{al}^*, \quad (4.19)$$

$$\tilde{V}_{lma}^{0\ell R} = \frac{1}{\sqrt{2}c_w}(c_w Z_{m2} + s_w Z_{m1})(R_L^{\tilde{e}})_{al}^* - \frac{(m_e)_l}{\sqrt{2}c_\beta M_W} Z_{m3}(R_R^{\tilde{e}})_{al}^*, \quad (4.20)$$

where $t_w = \tan \theta_w$, $c_w = \cos \theta_w$, $s_w = \sin \theta_w$, $c_\beta = \cos \beta$. The unitary matrices \mathcal{U} and \mathcal{V} , which diagonalize the chargino mass matrix, and the unitary matrix Z diagonalizing the neutralino mass matrix are taken from Ref [68].

Finally, the following lepton-slepton disalignment matrices may be defined:

$$\begin{aligned} R_{ak}^{\tilde{e}L} &= U_{ia}^{\tilde{e}} U_{ik}^{e_L*}, \\ R_{ak}^{\tilde{e}R} &= U_{i+3a}^{\tilde{e}} U_{ik}^{e_R*}, \end{aligned} \quad (4.21)$$

where U^{e_L} , U^{e_R} and $U^{\tilde{e}}$ are unitary matrices diagonalizing the lepton and slepton mass matrices, with $a = 1, \dots, 6$ and $i, k = 1, 2, 3$.

Chapter 5

Conclusions

In Chapter 3 Charged Lepton Flavor Violation was analysed in the MSSM extended by low-scale singlet heavy neutrinos, paying special attention to the individual loop contributions due to the heavy neutrinos $N_{1,2,3}$, sneutrinos $\tilde{N}_{1,2,\dots,12}$ and soft SUSY-breaking terms. In this analysis, we have, for the first time, included the complete set of box diagrams, in addition to the photon and the Z -boson mediated interactions. We have also derived the complete set of chiral amplitudes and their associate form factors related to the neutrinoless three-body CLFV decays of the muon and tau, such as $\mu \rightarrow eee$, $\tau \rightarrow \mu\mu\mu$, $\tau \rightarrow e\mu\mu$ and $\tau \rightarrow ee\mu$, and to the coherent $\mu \rightarrow e$ conversion in nuclei. Our analytical results are general and can be applied to most of the New Physics models with CLFV. In this context, we emphasize that this systematic analysis has revealed the existence of two new box formfactors, which have not been considered before in the existing literature of New Physics theories with CLFV.

This detailed study has shown that the soft SUSY-breaking effects in the Z -boson-mediated graphs dominate the CLFV observables, for appreciable regions of the ν_R MSSM parameter space in mSUGRA. Nevertheless, there is a significant portion of parameter space for heavy neutrino masses $m_N \lesssim 1$ TeV, where box diagrams involving heavy neutrinos in the loop can be comparable to, or even larger than the corresponding Z -boson-exchange diagrams

in $\mu \rightarrow eee$ and in $\mu \rightarrow e$ conversion in nuclei (cf. Fig 3.11). In the same kinematic regime, due to accidental numerical cancellations, we have also observed a suppression of the branching ratios for the photonic CLFV decays $\mu \rightarrow e\gamma$, as well as for the decays $\tau \rightarrow e\gamma$ and $\tau \rightarrow \mu\gamma$. As was already mentioned, such a suppression in low-scale seesaw models is a consequence of a cancellation between particle and sparticle contributions due to the approximate realization of the SUSY no-go theorem due to Ferrara and Remiddi [132]. Instead, in high-scale seesaw models such cancellations can only occur for a particular choice of the neutrino-Yukawa and Majorana-mass textures [119, 141]. Hence, the results obtained within supersymmetric low-scale seesaw type-I models, with $m_N \lesssim 10$ TeV, support the original findings in Ref [111], where the usual paradigm with the photon dipole-moment operators dominating the CLFV observables in high-scale seesaw models [114–118] gets radically modified, such that $\mu \rightarrow eee$ and $\mu \rightarrow e$ conversion may also represent sensitive probes of CLFV.

We have found that, unlike heavy neutrinos, CLFV effects induced by sneutrinos remain subdominant for the entire region of the mSUGRA parameter space. In addition, the perturbativity constraint on the neutrino Yukawa couplings \mathbf{h}_ν up to the GUT scale renders the quartic coupling contributions of order $(\mathbf{h}_\nu)^4$ small. This study has focused on providing numerical predictions for relatively small and intermediate values of $\tan \beta$, i.e. $\tan \beta \lesssim 20$, where neutral Higgs-mediated interactions constrained by the recent LHCb observation of the decay $B_s \rightarrow \mu\mu$ are not expected to give sizeable contributions. A global analysis that includes large $\tan \beta$ effects on CLFV observables and LHC constraints is one of the goals of the future researches.

Chapter 4 presented the systematical study of the one-loop contributions to the muon anomalous MDM a_μ and the electron EDM d_e in the ν_R MSSM. In particular, special attention was paid to the effect of the sneutrino soft SUSY-breaking parameters, \mathbf{B}_ν and \mathbf{A}_ν , and their universal CP phases, θ and ϕ , on a_μ and d_e . As far as one can tell, lepton dipole moments have not been analyzed in detail before, within SUSY models with low scale singlet (s)neutrinos.

For the deviation of a_μ from the SM value due to the ν_R MSSM (δa_μ) it is found that the heavy singlet neutrino and sneutrino contributions to δa_μ are small, typically one to two orders of magnitude below the muon anomaly Δa_μ . Instead, left-handed sneutrinos and sleptons give the largest effect on Δa_μ , exactly as is the case in the MSSM. The dependence of δa_μ on the muon mass m_μ , $\tan \beta$ and the soft SUSY-breaking mass scale M_{SUSY} have been carefully analyzed and their scaling behaviour according to Eq (4.11) has been confirmed. Finally, the dependence of δa_μ on the universal soft trilinear parameter A_0 , the neutrino Yukawa couplings \mathbf{h}_ν and the heavy neutrino mass m_N are negligible.

Furthermore, the electron EDM d_e in the ν_R MSSM is analysed. The heavy singlet neutrinos do not contribute to d_e , and soft SUSY-breaking and sneutrino terms contribute only if the phases ϕ and/or θ have a nonzero value. The contribution from the possible CP violating terms arising from the relatively complex products of the vertices exposed in (4.9) is numerically shown to be equal zero. On the other hand, the contribution due to a non-zero value of ϕ is the largest and may give rise to values for the electron EDM d_e comparable to its present experimental upper limit. The effect of the CP-odd phase θ on d_e is approximately one to two orders of magnitude smaller than that of ϕ . The size of d_e increases with $\tan \beta$ and mass of the lepton m_l , it is approximatively independent of A_0 and B_0 , but it generically decreases, as functions of the soft SUSY-breaking parameters m_0 , $M_{1/2}$.

Based on this numerical results, the approximate semi-analytical expressions are derived, which differ from those presented in the existing literature for SUSY models realizing a high-scale seesaw mechanism. Specifically, the flavor-blind CP-odd phases lead to a scaling of the lepton EDM $d_l \propto m_l \tan \beta / m_N^y$, where $2/3 < y < 1$. While it is true that d_l generally decreases with M_{SUSY} , this dependence cannot be described with a simple scaling law. The dependences on SUSY breaking parameters A_0 and B_0 are weak in the largest part of the parameter space. The linear dependence on $\tan \beta$ and the dependence on heavy neutrino mass are new results arising from this study.

In comparison, the $\tan \beta$ dependence in Ref [160] is, depending on its magnitude, either cubic or constant. Given the current experimental limits on d_e , a significant portion of the ν_R MSSM parameter space is identified with maximal CP phase $\phi = \pi/2$, where the electron EDM d_e can have values comparable to the present and future experimental sensitivities. The effect of sneutrino-sector CP violation on the neutron and Mercury EDMs is expected to be suppressed, which is a distinctive feature for the class of the ν_R MSSM scenarios studied in this thesis.

In his brief review regarding the future of Particle Physics [165], Nobel Prize winner Sheldon Lee Glashow emphasized six points which he personally finds most important for the future of High Energy Physics research. Among others, those include charged lepton flavor violation processes, anomalous magnetic dipole moment of the muon $a_\mu = g_\mu - 2$ and electric dipole moment of the electron d_e . The author of this thesis couldn't agree more.

Appendices

Appendix A

Interaction vertices

In this appendix, the Lagrangians describing the interaction vertices required to calculate the transition amplitudes for the CLFV processes under study are listed. The corresponding interaction vertices for the SM and the MSSM are obtained by adopting the conventions of the public code FeynArts-3.3 [166], `FVMSSM.mod` [167, 168], adapted to the notation used by Petcov et al. [69]. The Lagrangians of interest to this study include:

1. Vertices from 2HDM sector of the MSSM involving SM particles only,

$$\mathcal{L}_{\bar{d}uH^-} + \text{h.c.} = \frac{g_w}{\sqrt{2}M_W} V_{ij}^* \bar{d}_j \left(t_\beta m_{d_j} P_L + t_\beta^{-1} m_{u_i} P_R \right) u_i H^- + \text{h.c.} \quad (\text{A.1})$$

Here H^- is the negatively charged Higgs scalar, V is the Cabibbo–Kobayashi–Maskawa matrix, m_{d_i} and m_{u_i} are the quark masses and $c_w = \cos \theta_w$.

2. Vertices of singlet neutrinos in the ν_R SM sector of the MSSM,

$$\mathcal{L}_{\bar{e}nG^-} + \text{h.c.} = \frac{g_w}{\sqrt{2}M_W} B_{ia} \bar{e}_i \left(-m_{e_i} P_L + m_{n_a} P_R \right) n_a G^- + \text{h.c.}, \quad (\text{A.2})$$

$$\mathcal{L}_{\bar{e}nW^-} + \text{h.c.} = -\frac{g_w}{\sqrt{2}} B_{ia} \bar{e}_i \gamma^\mu P_L n_a W_\mu^- + \text{h.c.}, \quad (\text{A.3})$$

$$\mathcal{L}_{\bar{n}nZ} = -\frac{g_w}{2c_W} C_{ab} \bar{n}_a \gamma^\mu P_L n_b Z_\mu. \quad (\text{A.4})$$

Here n_a and m_{n_a} denote the neutrino mass-eigenstates and their respective

masses and B and C are lepton flavor mixing matrices defined in Refs [104, 105, 110]. The matrices B and C satisfy the following set of relations:

$$\begin{aligned} B_{la}B_{l'a}^* &= \delta_{ll'}, & C_{ac}C_{bc} &= C_{ab}, & B_{lb}C_{ba} &= B_{la}, & B_{l'a}^*B_{lb} &= C_{ab}, \\ m_aC_{ac}C_{bc} &= 0, & m_aB_{lb}C_{ba}^* &= 0, & m_aB_{la}B_{l'a} &= 0. \end{aligned} \quad (\text{A.5})$$

3. Vertices from the 2HDM sector of the MSSM involving Majorana neutrinos,

$$\mathcal{L}_{\bar{e}nH^-} + \text{h.c.} = \frac{g_w}{\sqrt{2}M_W} B_{ia} \bar{e}_i \left(t_\beta m_{e_i} P_L + t_\beta^{-1} m_{n_a} P_R \right) n_a H^- + \text{h.c.} \quad (\text{A.6})$$

4. MSSM vertices with sparticles,

$$\mathcal{L}_{\bar{d}\tilde{\chi}^-\tilde{u}} + \text{h.c.} = g_w \bar{d}_j \left(\tilde{V}_{jma}^{-dL} P_L + \tilde{V}_{jma}^{-dR} P_R \right) \tilde{\chi}_m^- \tilde{u}_a + \text{h.c.}, \quad (\text{A.7})$$

$$\mathcal{L}_{\bar{u}\tilde{\chi}^+\tilde{d}} + \text{h.c.} = g_w \bar{u}_j \left(\tilde{V}_{jma}^{+uL} P_L + \tilde{V}_{jma}^{+uR} P_R \right) \tilde{\chi}_m^+ \tilde{d}_a + \text{h.c.}, \quad (\text{A.8})$$

$$\mathcal{L}_{\bar{\tilde{\chi}}^-\tilde{\chi}^-A} + \mathcal{L}_{\bar{\tilde{\chi}}^+\tilde{\chi}^+A} = e \bar{\tilde{\chi}}_m^- \gamma^\mu \tilde{\chi}_m^- A_\mu - e \bar{\tilde{\chi}}_m^+ \gamma^\mu \tilde{\chi}_m^+ A_\mu, \quad (\text{A.9})$$

$$\begin{aligned} \mathcal{L}_{\bar{\tilde{\chi}}^-\tilde{\chi}^-Z} + \mathcal{L}_{\bar{\tilde{\chi}}^+\tilde{\chi}^+Z} &= \frac{g_w}{c_W} \bar{\tilde{\chi}}_m^- \gamma^\mu \left(V_{mk}^{\tilde{\chi}^-L} P_L + V_{mk}^{\tilde{\chi}^-R} P_R \right) \tilde{\chi}_k^- Z_\mu \\ &- \frac{g_w}{c_W} \bar{\tilde{\chi}}_m^+ \gamma^\mu \left(V_{mk}^{\tilde{\chi}^-L*} P_R + V_{mk}^{\tilde{\chi}^-R*} P_L \right) \tilde{\chi}_k^+ Z_\mu, \end{aligned} \quad (\text{A.10})$$

$$\mathcal{L}_{\bar{\tilde{\chi}}^0\tilde{\chi}^0Z} = \frac{g}{c_w} \bar{\tilde{\chi}}_m^0 \left(\gamma^\mu P_L V_{mk}^{\tilde{\chi}^0L} + \gamma^\mu P_R V_{mk}^{\tilde{\chi}^0R} \right) \tilde{\chi}_k^0 Z_\mu, \quad (\text{A.11})$$

$$\mathcal{L}_{\tilde{e}^*\tilde{e}Z} = g_w \tilde{V}_{ab}^{\tilde{e}} \tilde{e}_a^* i \overleftrightarrow{\partial}^\mu \tilde{e}_b Z_\mu, \quad (\text{A.12})$$

$$\mathcal{L}_{\bar{e}\tilde{\chi}^0\tilde{e}} + \mathcal{L}_{\bar{\tilde{\chi}}^0e\tilde{e}^*} = g_w \bar{e}_j (P_L \tilde{V}_{jma}^{0eL} + P_R \tilde{V}_{jma}^{0eR}) \tilde{\chi}^0 \tilde{e}_a + \text{h.c.}, \quad (\text{A.13})$$

$$\mathcal{L}_{\bar{u}\tilde{\chi}^0\tilde{u}} + \mathcal{L}_{\bar{\tilde{\chi}}^0u\tilde{u}^*} = g_w \bar{u}_j (P_L \tilde{V}_{jma}^{0uL} + P_R \tilde{V}_{jma}^{0uR}) \tilde{\chi}^0 \tilde{u}_a + \text{h.c.}, \quad (\text{A.14})$$

$$\mathcal{L}_{\bar{d}\tilde{\chi}^0\tilde{d}} + \mathcal{L}_{\bar{\tilde{\chi}}^0d\tilde{d}^*} = g_w \bar{d}_j (P_L \tilde{V}_{jma}^{0dL} + P_R \tilde{V}_{jma}^{0dR}) \tilde{\chi}^0 \tilde{d}_a + \text{h.c.}, \quad (\text{A.15})$$

where

$$\begin{aligned} \tilde{V}_{jma}^{-dL} &= \frac{m_{d_j}}{\sqrt{2}c_\beta M_W} \mathcal{U}_{m2}^* V_{ij}^* (R_L^{\tilde{u}})_{ai}^*, \\ \tilde{V}_{jma}^{-dR} &= -\mathcal{V}_{m1} V_{ij}^* (R_L^{\tilde{u}})_{ai}^* + \frac{m_{u_i}}{\sqrt{2}s_\beta M_W} \mathcal{V}_{m2} V_{ij}^* (R_R^{\tilde{u}})_{ai}^*, \end{aligned} \quad (\text{A.16})$$

$$\begin{aligned}\tilde{V}_{jma}^{+uL} &= \frac{m_{uj}}{\sqrt{2}s_\beta M_W} \mathcal{V}_{m2}^* V_{ji} (R_L^d)_{ai}^*, \\ \tilde{V}_{jma}^{+uR} &= -\mathcal{U}_{m1} V_{ji} (R_L^d)_{ai}^* + \frac{m_{di}}{\sqrt{2}c_\beta M_W} \mathcal{U}_{m2} V_{ji} (R_R^d)_{ai}^*,\end{aligned}\tag{A.17}$$

$$\begin{aligned}V_{mk}^{\tilde{\chi}^- L} &= \mathcal{U}_{m1} \mathcal{U}_{k1}^* + \frac{1}{2} \mathcal{U}_{m2} \mathcal{U}_{k2}^* - \delta_{mk} s_w^2, \\ V_{mk}^{\tilde{\chi}^- R} &= \mathcal{V}_{m1}^* \mathcal{V}_{k1} + \frac{1}{2} \mathcal{V}_{m2}^* \mathcal{V}_{k2} - \delta_{mk} s_w^2,\end{aligned}\tag{A.18}$$

$$V_{mk}^{\tilde{\chi}^0 L} = -\frac{1}{4} (Z_{m3} Z_{k3}^* - Z_{m4} Z_{k4}^*),\tag{A.19}$$

$$V_{mk}^{\tilde{\chi}^0 R} = \frac{1}{4} (Z_{m3}^* Z_{k3} - Z_{m4}^* Z_{k4}),\tag{A.20}$$

$$\tilde{V}_{ab}^{\tilde{e}} = \frac{c_{2w}}{c_w} (R_L^{\tilde{e}})_{ai} (R_L^{\tilde{e}})_{bi}^* - \frac{s_w^2}{c_w} (R_R^{\tilde{e}})_{ai} (R_R^{\tilde{e}})_{bi}^*,\tag{A.21}$$

$$\tilde{V}_{jma}^{0\ell L} = -\sqrt{2} t_w Z_{m1}^* (R_R^{\tilde{e}})_{aj}^* - \frac{(m_e)_j}{\sqrt{2}c_\beta M_W} Z_{m3} (R_L^{\tilde{e}})_{aj}^*,\tag{A.22}$$

$$\tilde{V}_{jma}^{0\ell R} = \frac{1}{\sqrt{2}c_W} (c_W Z_{m2} + s_W Z_{m1}) (R_L^{\tilde{e}})_{aj}^* - \frac{(m_e)_j}{\sqrt{2}c_\beta M_W} Z_{m3} (R_R^{\tilde{e}})_{aj}^*,\tag{A.23}$$

$$\tilde{V}_{jma}^{0uL} = \frac{2\sqrt{2}}{3} t_w Z_{m1}^* (R_R^{\tilde{u}})_{aj}^* - \frac{(m_u)_j}{\sqrt{2}s_\beta M_W} Z_{m4} (R_L^{\tilde{u}})_{aj}^*,\tag{A.24}$$

$$\tilde{V}_{jma}^{0uR} = -\frac{1}{2c_W} (c_W Z_{m2} + \frac{1}{3} s_W Z_{m1}) (R_L^{\tilde{u}})_{aj}^* - \frac{(m_u)_j}{\sqrt{2}s_\beta M_W} Z_{m4} (R_R^{\tilde{u}})_{aj}^*,\tag{A.25}$$

$$\tilde{V}_{jma}^{0dL} = -\frac{\sqrt{2}}{3} t_w Z_{m1}^* (R_R^{\tilde{d}})_{aj}^* - \frac{(m_d)_j}{\sqrt{2}c_\beta M_W} Z_{m3} (R_L^{\tilde{d}})_{aj}^*,\tag{A.26}$$

$$\tilde{V}_{jma}^{0dR} = \frac{1}{2c_W} (c_W Z_{m2} - \frac{1}{3} s_W Z_{m1}) (R_L^{\tilde{d}})_{aj}^* - \frac{(m_d)_j}{\sqrt{2}c_\beta M_W} Z_{m3} (R_R^{\tilde{d}})_{aj}^*,\tag{A.27}$$

and $c_{2w} = \cos 2\theta_w$. The unitary matrices diagonalizing the chargino mass matrix \mathcal{U} and \mathcal{V} and the unitary matrix diagonalizing the neutralino mass matrix Z are taken from [68]. The matrices

$$R_{ak}^{\tilde{f}L} \equiv U_{ia}^{\tilde{f}} U_{ik}^{fL*}, \quad R_{ak}^{\tilde{f}R} \equiv U_{i+3a}^{\tilde{f}} U_{ik}^{fR*},\tag{A.28}$$

with $f = d, u, e$, $a = 1, 2, \dots, 6$ and $i, k = 1, 2, 3$, quantify the disalignment between fermions and sfermions. Here U^{fL} , U^{fR} and $U^{\tilde{f}}$ are unitary matrices that diagonalize the fermion and sfermion mass matrices, respectively.

5. Sneutrino vertices in the ν_R MSSM,

$$\begin{aligned}\mathcal{L}_{\bar{e}\tilde{\chi}^-\tilde{N}} + \text{h.c.} &= g_w \tilde{N}_A \bar{\ell}_l \left(P_L \frac{m_l}{\sqrt{2}c_\beta M_W} \tilde{B}_{lmA}^{L,1} + P_R \tilde{B}_{lmA}^{R,1} \right) \tilde{\chi}_m^- + \text{h.c.} \\ &= g_w \tilde{N}_A^* \bar{\ell}_l \left(P_L \frac{m_l}{\sqrt{2}c_\beta M_W} \tilde{B}_{lmA}^{L,2} + P_R \tilde{B}_{lmA}^{R,2} \right) \tilde{\chi}_m^- + \text{h.c.},\end{aligned}\quad (\text{A.29})$$

$$\begin{aligned}\mathcal{L}_{\tilde{N}\tilde{N}Z} &= \frac{g_w}{c_W} \tilde{C}_{AB}^1 \tilde{N}_A^* i \overleftrightarrow{\partial}^\mu \tilde{N}_B Z_\mu \\ &= \frac{g_w}{c_W} \tilde{C}_{AB}^2 \tilde{N}_A^* i \overleftrightarrow{\partial}^\mu \tilde{N}_B^* Z_\mu \\ &= \frac{g_w}{c_W} \tilde{C}_{AB}^3 \tilde{N}_A i \overleftrightarrow{\partial}^\mu \tilde{N}_B Z_\mu \\ &= \frac{g_w}{c_W} \tilde{C}_{AB}^4 \tilde{N}_A i \overleftrightarrow{\partial}^\mu \tilde{N}_B^* Z_\mu,\end{aligned}\quad (\text{A.30})$$

where

$$\begin{aligned}\tilde{B}_{lmA}^{L,1} &= \mathcal{U}_{m2} U_{il}^{\ell_R*} \mathcal{U}_{iA}^{\tilde{\nu}}, \\ \tilde{B}_{lmA}^{L,2} &= \mathcal{U}_{m2} U_{il}^{\ell_R*} \mathcal{U}_{i+6A}^{\tilde{\nu}*}, \\ \tilde{B}_{lmA}^{R,1} &= -\mathcal{U}_{iA}^{\tilde{\nu}} U_{il}^{\ell_L*} \mathcal{V}_{m1} + \frac{m_{n_a}}{\sqrt{2}s_\beta M_W} \mathcal{V}_{m2} \mathcal{U}_{i+9A}^{\tilde{\nu}} U_{i+3a}^{\nu*} B_{la}, \\ \tilde{B}_{lmA}^{R,2} &= -\mathcal{U}_{i+6A}^{\tilde{\nu}*} U_{il}^{\ell_L*} \mathcal{V}_{m1} + \frac{m_{n_a}}{\sqrt{2}s_\beta M_W} \mathcal{V}_{m2} \mathcal{U}_{i+3A}^{\tilde{\nu}*} U_{i+3a}^{\nu*} B_{la}, \\ \tilde{C}_{AB}^1 &= -\frac{1}{2} \mathcal{U}_{iA}^{\tilde{\nu}*} \mathcal{U}_{iB}^{\tilde{\nu}}, \\ \tilde{C}_{AB}^2 &= -\frac{1}{2} \mathcal{U}_{iA}^{\tilde{\nu}*} \mathcal{U}_{i+6B}^{\tilde{\nu}*}, \\ \tilde{C}_{AB}^3 &= -\frac{1}{2} \mathcal{U}_{i+6A}^{\tilde{\nu}} \mathcal{U}_{iB}^{\tilde{\nu}}, \\ \tilde{C}_{AB}^6 &= -\frac{1}{2} \mathcal{U}_{i+6A}^{\tilde{\nu}} \mathcal{U}_{i+6B}^{\tilde{\nu}*}.\end{aligned}\quad (\text{A.31})$$

In the above, $\mathcal{U}^{\tilde{\nu}}$ is the unitary matrix diagonalizing the sneutrino mass matrix.

Notice that the weak coupling constant g_w are factored out from all interaction vertices defined above. To better identify chirality-flip mass effects in the CLFV amplitudes, factor $m_l/(\sqrt{2}c_\beta M_W)$ is also pulled out from the interaction vertex \tilde{B}_{lmA}^L .

Appendix B

Loop functions

The CLFV amplitudes are expressed in terms of leading-order one-loop functions. We expand the loop functions with respect to the momenta and masses of the external charged leptons, while keeping only the leading non-zero terms. The leading terms may then be expressed, in terms of the dimensionless loop integrals

$$\begin{aligned} \bar{J}_{n_1 n_2 \dots n_k}^m(\lambda_1, \lambda_2, \dots, \lambda_k) &= \frac{(\mu^2)^{2-D/2}}{(M_W^2)^{-D/2-m+\sum_i n_i}} \int \frac{d^D \ell}{(2\pi)^D} \frac{(\ell^2)^m}{\prod_{i=1}^k (\ell^2 - m_i^2)^{n_i}} \\ &= \frac{i(-1)^{m-\sum_i n_i}}{(4\pi)^{D/2} \Gamma(\frac{D}{2})} \left(\frac{\mu^2}{M_W^2}\right)^{2-D/2} \int_0^\infty \frac{dx x^{D/2-1+m}}{\prod_{i=1}^k (x + \lambda_i)^{n_i}}, \end{aligned} \quad (\text{B.1})$$

where m_i are loop particle masses, n_i are the exponents of the propagator denominators, $\lambda_i = m_i^2/M_W^2$ are dimensionless mass parameters and μ is 't Hooft's renormalization mass scale. Parameter μ is chosen to be M_W , even though any other scale can be chosen equally well as a reference scale for any of the integrals. For the amplitudes dealt with in this thesis, the integrals are either divergent and satisfy $m + 2 - \sum_i n_i = 0$, or they are convergent with $m + 2 - \sum_i n_i < 0$. For convergent integrals, one may set $D = 4$, whilst for divergent integrals one takes $D = 4 - 2\epsilon$. Factor $i/(4\pi)^2$ is

pulled out from all integrals. Thus, for finite integrals one obtains:

$$\bar{J}_{n_1 n_2 \dots n_k}^m(\lambda_1, \lambda_2, \dots, \lambda_k) \equiv \frac{i}{(4\pi)^2} J_{n_1 n_2 \dots n_k}^m(\lambda_1, \lambda_2, \dots, \lambda_k). \quad (\text{B.2})$$

Instead, the divergent integrals are written down as a sum of a divergent and constant term and a finite mass-dependent term:

$$\bar{J}_{n_1 n_2 \dots n_k}^m(\lambda_1, \lambda_2, \dots, \lambda_k) \equiv \frac{i}{(4\pi)^2} \left[\frac{1}{\varepsilon} + \text{const} + J_{n_1 n_2 \dots n_k}^m(\lambda_1, \lambda_2, \dots, \lambda_k) \right]. \quad (\text{B.3})$$

In the CLFV amplitudes, the “divergent+constant” terms vanish in the total sum, or as a result of a GIM-like mechanism. Therefore, all CLFV amplitudes can be expressed in terms of finite mass dependent functions $J_{n_1 n_2 \dots}^m(\lambda_1, \lambda_2, \dots)$, which we call the *basic integrals*. Those integrals are analytically calculated using *Wolfram Mathematica* package. We will now describe the procedure used in the calculation and present the exact results thus obtained.

There are three types of J -functions which are used in this study:

$$J_{bc}^a(x, y) = K \cdot (-1)^{a+b+c} \cdot \int \frac{dt}{(t+x)^b (t+y)^c} t^{D/2-1+a}, \quad (\text{B.4})$$

$$J_{bcd}^a(x, y, z) = K \cdot (-1)^{a+b+c+d} \cdot \int \frac{dt}{(t+x)^b (t+y)^c (t+z)^d} t^{D/2-1+a}, \quad (\text{B.5})$$

$$J_{bcde}^a(x, y, z, w) = K \cdot (-1)^{a+b+c+d+e} \cdot \int \frac{dt}{(t+x)^b (t+y)^c (t+z)^d (t+w)^e} t^{D/2-1+a}, \quad (\text{B.6})$$

where

$$K = \frac{i 2^{-D} \pi^{-D/2} \mu^{4-D}}{\Gamma(D/2)}. \quad (\text{B.7})$$

The calculation of these integrals is performed in three steps. In the first step, the integral is exactly calculated using `Integrate` function. In the second step, the constant term is isolated from the expression. Because of the specific identities obeyed by the flavor-mixing matrices (see Eqs (2.9) and (2.10) in Ref [110]) the constant terms can effectively be ignored. Finally,

the third step gets rid of these constant terms, and gives simplified result in the zeroth order over ϵ , with factor $i/16\pi^2$ dropped for better readability of the result.

♦ For calculation of the J -functions type (B.4), these steps are performed by the following *Mathematica* functions:

Step one.

```
INT3[a_, b_, c_] := (-1)^(a + b + c)*
Assuming[{x > 0, y > 0, D <= 2 (b + c - a - 1)}, 
Integrate[
t^(D/2 - 1 + a)/(((t + x)^b) ((t + y)^c)), {t, 0, \[Infinity]}]]
```

Step two.

```
CteExtract3[expr_] := Module[{},
cstep1 = Collect[Expand[expr /. Log[x] -> 0], x];
cstep2 = cstep1 /. x^n__ -> 0 /. x -> 0;
cstep3 = cstep2 /. Log[y] -> 0 /. y^n__ -> 0]
```

Step three.

```
ProcInt3[a_, b_, c_] := Module[{},
step1 =
Series[INT3[a, b, c]*Ofa[D]*(16 \[Pi]^2)/I /.
D -> 4 - 2 \[Epsilon], {\[Epsilon], 0, 0}] // FullSimplify //
Normal;
cte = CteExtract3[step1];
step2 = step1 - cte // FullSimplify]
```

In order to evaluate function $J_{bc}^a(x, y)$, one only needs to call the function defined in Step three, e.g. $J241[x_, y_] = ProcInt3[2, 4, 1]$. The analogous procedure is applied for other types of J loop-functions as well.

♦ For calculation of the J -functions type (B.5):

Step one.

```
INT4[a_, b_, c_, d_] := (-1)^(a + b + c + d)*
Assuming[{x > 0, y > 0, z > 0, D <= 2 (b + c + d - a - 1)}, 
Integrate[
t^(D/2 - 1 + a)/((t + x)^b (t + y)^c (t + z)^d), {t, 0, \[Infinity]}]]
```

Step two.

```
CteExtract4[expr_] := Module[{ },
  cstep1 = Collect[Expand[expr /. Log[x] -> 0], x];
  cstep2 = cstep1 /. x^n__ -> 0 /. x -> 0;
  cstep3 = Collect[Expand[cstep2 /. Log[y] -> 0], y];
  cstep4 = cstep3 /. y^n__ -> 0 /. y -> 0;
  cstep5 = cstep4 /. Log[z] -> 0 /. z^n__ -> 0]
```

Step three.

```
ProcInt4[a_, b_, c_, d_] := Module[{ },
  step1 =
  Series[INT4[a, b, c, d]*Ofa[D]*(16 \[Pi]^2)/I /.
    D -> 4 - 2 \[Epsilon], {\[Epsilon], 0, 0}] // FullSimplify //
  Normal;
  cte = CteExtract4[step1];
  step2 = step1 - cte // FullSimplify]
```

♦ For calculation of the J -functions type (B.6):

Step one.

```
INT5[a_, b_, c_, d_, e_] := (-1)^(a + b + c + d + e)*
Assuming[{x > 0, y > 0, z > 0, w > 0, D < 1},
Integrate[t^( $\frac{D}{2} - 1 + a$ ) / ((t + x)^b (t + y)^c (t + z)^d (t + w)^e),
{t, 0, \[Infinity]}]]
```

Step two.

```
CteExtract5[expr_] := Module[{ },
  cstep1 = Collect[Expand[expr /. Log[x] -> 0], x];
  cstep2 = cstep1 /. x^n__ -> 0 /. x -> 0;
  cstep3 = Collect[Expand[cstep2 /. Log[y] -> 0], y];
  cstep4 = cstep3 /. y^n__ -> 0 /. y -> 0;
  cstep5 = Collect[Expand[cstep4 /. Log[z] -> 0], z];
  cstep6 = cstep5 /. z^n__ -> 0 /. z -> 0;
  cstep7 = cstep6 /. Log[w] -> 0 /. w^n__ -> 0]
```

Step three.

```

ProcInt5[a_, b_, c_, d_, e_] := Module[{},

  step1 =
  Series[INT5[a, b, c, d, e]*OFa[D]*(16 \[Pi]^2)/I /.
    D -> 4 - 2 \[Epsilon], {\[Epsilon], 0, 0}] // FullSimplify //.
    Normal;

  cte = CteExtract5[step1];
  step2 = step1 - cte // FullSimplify]

```

In all these expressions, $OFa[D]$ is defined as factor K in the Eq (B.7).

Using this procedure, one comes out with the following results:

$$\begin{aligned}
J_{11}^0(x, y) &= \frac{y \log(y) - x \log(x)}{x - y}, \\
J_{21}^0(x, y) &= \frac{y \log(x) - x + y - y \log(y)}{(x - y)^2}, \\
J_{31}^0(x, y) &= \frac{x^2 - 2xy(\log(x) - \log(y)) - y^2}{2x(x - y)^3}, \\
J_{21}^1(x, y) &= -\frac{x(x - y) + x(x - 2y) \log(x) + y^2 \log(y)}{(x - y)^2}, \\
J_{31}^1(x, y) &= \frac{2y^2(\log(y) - \log(x)) - (x - 3y)(x - y)}{2(x - y)^3}, \\
J_{41}^1(x, y) &= \frac{(x - y)(x^2 - 5xy - 2y^2) + 6xy^2(\log(x) - \log(y))}{6x(x - y)^4}, \\
J_{41}^2(x, y) &= \frac{6y^3(\log(x) - \log(y)) - (x - y)(2x^2 - 7xy + 11y^2)}{6(x - y)^4}, \quad (B.8)
\end{aligned}$$

$$\begin{aligned}
J_{111}^0(x, y, z) &= \frac{x \log(x)(z - y) + y(x - z) \log(y) + z(y - x) \log(z)}{(x - y)(x - z)(y - z)}, \\
J_{211}^0(x, y, z) &= \frac{1}{(x - y)^2(x - z)^2(y - z)} \left[\log(x)(y - z)(x^2 - yz) \right. \\
&\quad \left. + z(x - y)^2 \log(z) + (x - z)(y(z - x) \log(y) - (x - y)(y - z)) \right], \\
J_{111}^1(x, y, z) &= \frac{x^2 \log(x)(y - z) + y^2(z - x) \log(y) + z^2(x - y) \log(z)}{(x - y)(x - z)(z - y)},
\end{aligned}$$

$$\begin{aligned}
J_{211}^1(x, y, z) = & \frac{1}{(x-y)^2(x-z)^2(y-z)} \\
& \cdot \left[(x-z)(y^2(z-x)\log(y) + x(x-y)(z-y)) \right. \\
& \left. + z^2(x-y)^2\log(z) + x\log(x)(y-z)(x(y+z)-2yz) \right],
\end{aligned} \tag{B.9}$$

$$\begin{aligned}
J_{1111}^0(x, y, z, w) = & -\frac{w\log(w)}{(w-x)(w-y)(w-z)} + \frac{x\log(x)}{(w-x)(x-y)(x-z)} \\
& + \frac{y\log(y)}{(w-y)(y-x)(y-z)} + \frac{z\log(z)}{(w-z)(x-z)(y-z)}, \\
J_{1111}^1(x, y, z, w) = & -\frac{w^2\log(w)}{(w-x)(w-y)(w-z)} + \frac{x^2\log(x)}{(w-x)(x-y)(x-z)} \\
& + \frac{y^2\log(y)}{(w-y)(y-x)(y-z)} + \frac{z^2\log(z)}{(w-z)(x-z)(y-z)}.
\end{aligned} \tag{B.10}$$

These functions are often evaluated in the limit in which two or more variables are equal to each other or equal to zero. This is easily performed with the `Limit` function, although it can be rather time consuming. To avoid time consumption, we have evaluated all possible limits only once and then used those results to define the one-loop form factors expressed in Appendix C.

Appendix C

One-loop form factors

Here we present the complete analytical form of the CLFV form factors F_γ , F_Z and F_{box} defined in Chapter 3, in the Feynman–t’ Hooft gauge. In the following, the usual summation convention over repeated indices is implied. The interaction vertices and loop functions used here are given in Appendices A and B, respectively.

§ C.1 Photon Form factors

The form factors F_γ^L , F_γ^R , G_γ^L and G_γ^R may be explicitly written as follows:

$$\begin{aligned} (F_\gamma^L)_{ll'} &= F_{ll'\gamma}^N + F_{ll'\gamma}^{L,\tilde{N}} + F_{ll'\gamma}^{L,\text{SB}}, \\ (F_\gamma^R)_{ll'} &= F_{ll'\gamma}^N + F_{ll'\gamma}^{R,\tilde{N}} + F_{ll'\gamma}^{R,\text{SB}}, \\ (G_\gamma^L)_{ll'} &= m_{l'}(G_{ll'\gamma}^N + G_{ll'\gamma}^{L,\tilde{N}}) + G_{ll'\gamma}^{L,\text{SB}}, \\ (G_\gamma^R)_{ll'} &= m_l(G_{ll'\gamma}^N + G_{ll'\gamma}^{R,\tilde{N}}) + G_{ll'\gamma}^{R,\text{SB}}, \end{aligned} \quad (\text{C.1})$$

where

$$\begin{aligned}
F_{l'l\gamma}^N &= B_{l'a}B_{la}^* \left[2 \left(J_{31}^1(1, \lambda_{n_a}) - \frac{1}{6} J_{41}^2(1, \lambda_{n_a}) \right) \right. \\
&\quad \left. - \frac{1}{6} \lambda_{n_a} J_{41}^2(1, \lambda_{n_a}) - \frac{1}{6t_\beta^2} \lambda_{n_a} J_{41}^2(\lambda_{H^+}, \lambda_{n_a}) \right], \\
G_{l'l\gamma}^N &= B_{l'a}B_{la}^* \left[J_{31}^1(1, \lambda_{n_a}) + J_{41}^2(1, \lambda_{n_a}) + \lambda_{n_a} \left(\frac{1}{2} J_{41}^1(1, \lambda_{n_a}) - J_{31}^0(1, \lambda_{n_a}) \right) \right. \\
&\quad \left. + \lambda_{n_a} \lambda_{H^+} \left(\frac{1}{2t_\beta^2} J_{41}^1(\lambda_{H^+}, \lambda_{n_a}) + J_{31}^0(\lambda_{H^+}, \lambda_{n_a}) \right) \right], \tag{C.2} \\
F_{l'l\gamma}^{L,\tilde{N}} &= \frac{1}{2} (\tilde{B}_{l'kA}^{R,1} \tilde{B}_{lkA}^{R,*} + \tilde{B}_{l'kA}^{R,2} \tilde{B}_{lkA}^{R,2*}) \left[-\frac{2}{3} J_{41}^2(\lambda_{\tilde{\chi}_k}, \lambda_{\tilde{N}_A}) + \lambda_{\tilde{\chi}_k} J_{41}^1(\lambda_{\tilde{\chi}_k}, \lambda_{\tilde{N}_A}) \right], \\
F_{l'l\gamma}^{R,\tilde{N}} &= \frac{m_l m_{l'}}{4c_\beta^2 M_W^2} (\tilde{B}_{l'kA}^{L,1} \tilde{B}_{lkA}^{L,1*} + \tilde{B}_{l'kA}^{L,2} \tilde{B}_{lkA}^{L,2*}) \\
&\quad \cdot \left[-\frac{2}{3} J_{41}^2(\lambda_{\tilde{\chi}_k}, \lambda_{\tilde{N}_A}) + \lambda_{\tilde{\chi}_k} J_{41}^1(\lambda_{\tilde{\chi}_k}, \lambda_{\tilde{N}_A}) \right], \\
G_{l'l\gamma}^{L,\tilde{N}} &= \frac{1}{2} (\tilde{B}_{l'kA}^{L,1} \tilde{B}_{lkA}^{L,1*} + \tilde{B}_{l'kA}^{L,2} \tilde{B}_{lkA}^{L,2*}) \left[-\frac{m_l^2}{2c_\beta^2 M_W^2} \lambda_{\tilde{\chi}_k} J_{41}^1(\lambda_{\tilde{\chi}_k}, \lambda_{\tilde{N}_A}) \right] \\
&\quad + \frac{1}{2} (\tilde{B}_{l'kA}^{R,1} \tilde{B}_{lkA}^{R,1*} + \tilde{B}_{l'kA}^{R,2} \tilde{B}_{lkA}^{R,2*}) \left[-\lambda_{\tilde{\chi}_k} J_{41}^1(\lambda_{\tilde{\chi}_k}, \lambda_{\tilde{N}_A}) \right] \\
&\quad + \frac{1}{2} (\tilde{B}_{l'kA}^{L,1} \tilde{V}_{lkA}^{R,1*} + \tilde{B}_{l'kA}^{L,2} \tilde{V}_{lkA}^{R,2*}) \left[\frac{\sqrt{2}}{c_\beta} \sqrt{\lambda_{\tilde{\chi}_k}} J_{31}^1(\lambda_{\tilde{\chi}_k}, \lambda_{\tilde{N}_A}) \right], \\
G_{l'l\gamma}^{R,\tilde{N}} &= \frac{1}{2} (\tilde{B}_{l'kA}^{L,1} \tilde{B}_{lkA}^{L,1*} + \tilde{B}_{l'kA}^{L,2} \tilde{B}_{lkA}^{L,2*}) \left[-\frac{m_{l'}^2}{2c_\beta^2 M_W^2} \lambda_{\tilde{\chi}_k} J_{41}^1(\lambda_{\tilde{\chi}_k}, \lambda_{\tilde{N}_A}) \right] \\
&\quad + \frac{1}{2} (\tilde{B}_{l'kA}^{R,1} \tilde{B}_{lkA}^{R,1*} + \tilde{B}_{l'kA}^{R,2} \tilde{B}_{lkA}^{R,2*}) \left[-\lambda_{\tilde{\chi}_k} J_{41}^1(\lambda_{\tilde{\chi}_k}, \lambda_{\tilde{N}_A}) \right] \\
&\quad + \frac{1}{2} (\tilde{B}_{l'kA}^{R,1} \tilde{V}_{lkA}^{L,1*} + \tilde{B}_{l'kA}^{R,2} \tilde{V}_{lkA}^{L,2*}) \left[\frac{\sqrt{2}}{c_\beta} \sqrt{\lambda_{\tilde{\chi}_k}} J_{31}^1(\lambda_{\tilde{\chi}_k}, \lambda_{\tilde{N}_A}) \right], \tag{C.3} \\
F_{l'l\gamma}^{L,\text{SB}} &= \tilde{V}_{l'ma}^{0\ell R} \tilde{V}_{lma}^{0\ell R*} \left[-\frac{1}{3} J_{41}^2(\lambda_{\tilde{e}_a}, \lambda_{\tilde{\chi}_m^0}) \right], \\
F_{l'l\gamma}^{R,\text{SB}} &= \tilde{V}_{l'ma}^{0\ell L} \tilde{V}_{lma}^{0\ell L*} \left[-\frac{1}{3} J_{41}^2(\lambda_{\tilde{e}_a}, \lambda_{\tilde{\chi}_m^0}) \right], \\
G_{l'l\gamma}^{L,\text{SB}} &= \tilde{V}_{l'ma}^{0\ell R} \tilde{V}_{lma}^{0\ell R*} \left[m_{l'} \lambda_{\tilde{e}_a} J_{41}^1(\lambda_{\tilde{e}_a}, \lambda_{\tilde{\chi}_m^0}) \right] + \tilde{V}_{l'ma}^{0\ell L} \tilde{V}_{lma}^{0\ell L*} \left[m_l \lambda_{\tilde{e}_a} J_{41}^1(\lambda_{\tilde{e}_a}, \lambda_{\tilde{\chi}_m^0}) \right] \\
&\quad + \tilde{V}_{l'ma}^{0\ell L} \tilde{V}_{lma}^{0\ell R*} \left[+ 2m_{\tilde{\chi}_m^0} \lambda_{\tilde{e}_a} J_{31}^0(\lambda_{\tilde{e}_a}, \lambda_{\tilde{\chi}_m^0}) \right],
\end{aligned}$$

$$\begin{aligned} G_{l'l\gamma}^{R,\text{SB}} &= \tilde{V}_{l'ma}^{0\ell L} \tilde{V}_{lma}^{0\ell L*} \left[m_{l'} \lambda_{\tilde{e}_a} J_{41}^1(\lambda_{\tilde{e}_a}, \lambda_{\tilde{\chi}_m^0}) \right] + \tilde{V}_{l'ma}^{0\ell R} \tilde{V}_{lma}^{0\ell R*} \left[m_l \lambda_{\tilde{e}_a} J_{41}^1(\lambda_{\tilde{e}_a}, \lambda_{\tilde{\chi}_m^0}) \right] \\ &+ \tilde{V}_{l'ma}^{0\ell R} \tilde{V}_{lma}^{0\ell L*} \left[+ 2m_{\tilde{\chi}_m^0} \lambda_{\tilde{e}_a} J_{31}^0(\lambda_{\tilde{e}_a}, \lambda_{\tilde{\chi}_m^0}) \right]. \end{aligned} \quad (\text{C.4})$$

§ C.2 *Z*-Boson Form factors

The form factors F_Z^L and F_Z^R may be decomposed as follows:

$$\begin{aligned} (F_Z^L)_{l'l} &= F_{l'lZ}^N + F_{l'lZ}^{L,\tilde{N}} + F_{l'lZ}^{L,\text{SB}}, \\ (F_\gamma^R)_{l'l} &= F_{l'lZ}^N + F_{l'lZ}^{R,\tilde{N}} + F_{l'lZ}^{R,\text{SB}}, \end{aligned} \quad (\text{C.5})$$

where

$$\begin{aligned} F_{l'lZ}^{L,N} &= B_{l'a} B_{la}^* \left[\frac{5}{2} \lambda_{n_a} J_{21}^0(1, \lambda_{n_a}) \right] \\ &+ B_{l'b} C_{ba} B_{la}^* \left[-\frac{1}{2} J_{111}^1(1, \lambda_{n_b}, \lambda_{n_a}) + \frac{1}{2} \lambda_{n_a} \lambda_{n_b} J_{111}^0(1, \lambda_{n_b}, \lambda_{n_a}) \right. \\ &\quad \left. + \frac{1}{2t_\beta^2} \lambda_{n_a} \lambda_{n_b} J_{111}^0(\lambda_{H^+}, \lambda_{n_b}, \lambda_{n_a}) \right], \\ F_{l'lZ}^{R,N} &= -\frac{m_l m_{l'} t_\beta^2}{4M_W^2} B_{l'b} C_{ba} B_{la}^* J_{111}^1(\lambda_{H^+}, \lambda_{n_b}, \lambda_{n_a}), \\ F_{l'lZ}^{L,\tilde{N}} &= \frac{1}{2} (\tilde{B}_{l'mA}^{R,1} \tilde{V}_{mk}^{\tilde{\chi}^- R} \tilde{B}_{lkA}^{R,1*} + \tilde{B}_{l'mA}^{R,2} \tilde{V}_{mk}^{\tilde{\chi}^- R} \tilde{B}_{lkA}^{R,2*}) J_{111}^1(\lambda_{\tilde{\chi}_m}, \lambda_{\tilde{\chi}_k}, \lambda_{\tilde{N}_A}) \\ &- (\tilde{B}_{l'mA}^{R,1} \tilde{V}_{mk}^{\tilde{\chi}^- L} \tilde{B}_{lmA}^{R,1*} + \tilde{B}_{l'mA}^{R,2} \tilde{V}_{mk}^{\tilde{\chi}^- L} \tilde{B}_{lmA}^{R,2*}) \sqrt{\lambda_{\tilde{\chi}_m} \lambda_{\tilde{\chi}_k}} J_{111}^0(\lambda_{\tilde{\chi}_m}, \lambda_{\tilde{\chi}_k}, \lambda_{\tilde{N}_A}) \\ &+ \frac{1}{2} (\tilde{B}_{l'mA}^{R,1} \tilde{B}_{lkA}^{R,1*} + \tilde{B}_{l'mA}^{R,2} \tilde{B}_{lkA}^{R,2*}) \\ &\quad \cdot \left(\frac{1}{2} - s_w^2 \right) (J_{21}^1(\lambda_{\tilde{\chi}_k}, \lambda_{\tilde{N}_A}) - 2J_{11}^0(\lambda_{\tilde{\chi}_k}, \lambda_{\tilde{N}_A})) \\ &+ \frac{1}{4} (\tilde{B}_{l'kA}^{R,1} \tilde{C}_{BA}^1 \tilde{B}_{lkA}^{R,1*} + \tilde{B}_{l'kA}^{R,1} \tilde{C}_{BA}^2 \tilde{B}_{lkA}^{R,2*} + \tilde{B}_{l'mA}^{R,2} \tilde{C}_{BA}^3 \tilde{B}_{lkA}^{R,1*} \\ &\quad + \tilde{B}_{l'mA}^{R,2} \tilde{C}_{BA}^4 \tilde{B}_{lkA}^{R,2*}) J_{111}^1(\lambda_{\tilde{\chi}_k}, \lambda_{\tilde{N}_B}, \lambda_{\tilde{N}_A}), \\ F_{l'lZ}^{R,\tilde{N}} &= \frac{m_l m_{l'}}{2s_\beta^2 M_W^2} \left[\frac{1}{2} (\tilde{B}_{l'mA}^{L,1} \tilde{V}_{mk}^{\tilde{\chi}^- L} \tilde{B}_{lkA}^{L,1*} + \tilde{B}_{l'mA}^{L,2} \tilde{V}_{mk}^{\tilde{\chi}^- L} \tilde{B}_{lkA}^{L,2*}) J_{111}^1(\lambda_{\tilde{\chi}_m}, \lambda_{\tilde{\chi}_k}, \lambda_{\tilde{N}_A}) \right. \\ &\quad \left. - (\tilde{B}_{l'mA}^{L,1} \tilde{V}_{mk}^{\tilde{\chi}^- R} \tilde{B}_{lmA}^{L,1*} + \tilde{B}_{l'mA}^{L,2} \tilde{V}_{mk}^{\tilde{\chi}^- R} \tilde{B}_{lmA}^{L,2*}) \sqrt{\lambda_{\tilde{\chi}_m} \lambda_{\tilde{\chi}_k}} J_{111}^0(\lambda_{\tilde{\chi}_m}, \lambda_{\tilde{\chi}_k}, \lambda_{\tilde{N}_A}) \right] \end{aligned} \quad (\text{C.6})$$

$$\begin{aligned}
& + \frac{1}{2} (\tilde{B}_{l'mA}^{L,1} \tilde{B}_{lkA}^{L,1*} + \tilde{B}_{l'mA}^{L,2} \tilde{B}_{lkA}^{L,2*}) (-s_w^2) (J_{21}^1(\lambda_{\tilde{\chi}_k}, \lambda_{\tilde{N}_A}) - 2J_{11}^0(\lambda_{\tilde{\chi}_k}, \lambda_{\tilde{N}_A})) \\
& + \frac{1}{4} (\tilde{B}_{l'kA}^{L,1} \tilde{C}_{BA}^1 \tilde{B}_{lkA}^{L,1*} + \tilde{B}_{l'kA}^{L,1} \tilde{C}_{BA}^2 \tilde{B}_{lkA}^{L,2*} + \tilde{B}_{l'mA}^{L,2} \tilde{C}_{BA}^3 \tilde{B}_{lkA}^{L,1*} \\
& + \tilde{B}_{l'mA}^{L,2} \tilde{C}_{BA}^4 \tilde{B}_{lkA}^{L,2*}) J_{111}^1(\lambda_{\tilde{\chi}_k}, \lambda_{\tilde{N}_B}, \lambda_{\tilde{N}_A}) \Big], \tag{C.7}
\end{aligned}$$

$$\begin{aligned}
F_{l'lZ}^{L,\text{SB}} &= -\tilde{V}_{l'ma}^{0\ell R} \tilde{V}_{mk}^{\tilde{\chi}^0 R} \tilde{V}_{lka}^{0\ell R*} J_{111}^1(\lambda_{\tilde{\chi}_m^0}, \lambda_{\tilde{\chi}_k^0}, \lambda_{\tilde{e}_a}) \\
&+ \tilde{V}_{l'ma}^{0\ell R} \tilde{V}_{mk}^{\tilde{\chi}^0 L} \tilde{V}_{lka}^{0\ell R*} 2\sqrt{\lambda_{\tilde{\chi}_m} \lambda_{\tilde{\chi}_k}} J_{111}^0(\lambda_{\tilde{\chi}_m^0}, \lambda_{\tilde{\chi}_k^0}, \lambda_{\tilde{e}_a}) \\
&+ \tilde{V}_{l'ka}^{0\ell R} \tilde{V}_{lka}^{0\ell R*} \left(\frac{1}{2} - s_w^2 \right) \left(-\frac{1}{2} J_{21}^1(\lambda_{\tilde{\chi}_k^0}, \lambda_{\tilde{e}_a}) + J_{11}^0(\lambda_{\tilde{\chi}_k^0}, \lambda_{\tilde{e}_a}) \right) \\
&- \frac{1}{2} \tilde{V}_{l'kb}^{0\ell L} \tilde{V}_{ba}^{\tilde{e}} \tilde{V}_{lka}^{0\ell L*} J_{111}^1(\lambda_{\tilde{\chi}_k^0}, \lambda_{\tilde{e}_b}, \lambda_{\tilde{e}_a}), \\
F_{l'lZ}^{R,\text{SB}} &= -\tilde{V}_{l'ma}^{0\ell L} \tilde{V}_{mk}^{\tilde{\chi}^0 L} \tilde{V}_{lka}^{0\ell L*} J_{111}^1(\lambda_{\tilde{\chi}_m^0}, \lambda_{\tilde{\chi}_k^0}, \lambda_{\tilde{e}_a}) \\
&+ \tilde{V}_{l'ma}^{0\ell L} \tilde{V}_{mk}^{\tilde{\chi}^0 R} \tilde{V}_{lka}^{0\ell L*} 2\sqrt{\lambda_{\tilde{\chi}_m} \lambda_{\tilde{\chi}_k}} J_{111}^0(\lambda_{\tilde{\chi}_m^0}, \lambda_{\tilde{\chi}_k^0}, \lambda_{\tilde{e}_a}) \\
&+ \tilde{V}_{l'ka}^{0\ell L} \tilde{V}_{lka}^{0\ell L*} (-s_w^2) \left(-\frac{1}{2} J_{21}^1(\lambda_{\tilde{\chi}_k^0}, \lambda_{\tilde{e}_a}) + J_{11}^0(\lambda_{\tilde{\chi}_k^0}, \lambda_{\tilde{e}_a}) \right) \\
&- \frac{1}{2} \tilde{V}_{l'kb}^{0\ell R} \tilde{V}_{ba}^{\tilde{e}} \tilde{V}_{lka}^{0\ell R*} J_{111}^1(\lambda_{\tilde{\chi}_k^0}, \lambda_{\tilde{e}_b}, \lambda_{\tilde{e}_a}). \tag{C.8}
\end{aligned}$$

§ C.3 Leptonic Box Form factors

The leptonic box amplitudes are expressed in terms of the chiral structures: $\bar{l}\Gamma_A^X l \bar{l}_1\Gamma_A^Y l_2^C$ [cf Eq (3.8)]. There are two distinct contributions to the chiral amplitudes. The first one has *direct* relevance to the original structure given above and that one is denoted with a subscript D . The second contribution comes from a chiral amplitude of the form $\bar{l}_1\Gamma_A^X l \bar{l}\Gamma_A^Y l_2^C$, which contributes to the original amplitude $\bar{l}\Gamma_A^X l \bar{l}_1\Gamma_A^Y l_2^C$, after performing a Fierz transformation. This Fierz-transformed contribution is indicated with a subscript F . More explicitly, the leptonic box form factors are given by

$$\begin{aligned}
B_{\ell V}^{LL} &= B_{\ell V,D}^{LL} + B_{\ell V,F}^{LL}, & B_{\ell V}^{RR} &= B_{\ell V,D}^{RR} + B_{\ell V,F}^{RR}, \\
B_{\ell V}^{LR} &= B_{\ell V,D}^{LR} - \frac{1}{2} B_{\ell S,F}^{LR}, & B_{\ell V}^{RL} &= B_{\ell V,D}^{RL} - \frac{1}{2} B_{\ell S,F}^{RL}, \\
B_{\ell S}^{LL} &= B_{\ell S,D}^{LL} + \frac{1}{2} B_{\ell S,F}^{LL} + \frac{3}{2} B_{\ell T,F}^{LL}, & B_{\ell S}^{RR} &= B_{\ell S,D}^{RR} + \frac{1}{2} B_{\ell S,F}^{RR} + \frac{3}{2} B_{\ell T,F}^{RR},
\end{aligned}$$

$$\begin{aligned} B_{\ell S}^{LR} &= B_{\ell S,D}^{LR} - 2B_{\ell V,F}^{LR}, & B_{\ell S}^{RL} &= B_{\ell S,D}^{RL} - 2B_{\ell V,F}^{RL}, \\ B_{\ell T}^{LL} &= B_{\ell T,D}^{LL} - \frac{1}{2}B_{\ell T,F}^{LL} + \frac{1}{2}B_{\ell S,F}^{LL}, & B_{\ell T}^{RR} &= B_{\ell T,D}^{RR} - \frac{1}{2}B_{\ell T,F}^{RR} + \frac{1}{2}B_{\ell S,F}^{RR}. \end{aligned} \quad (\text{C.9})$$

The *direct* and Fierz-transformed contributions to the form factors are related by the exchange of outgoing leptons

$$B_{\ell A,F}^{XY} = B_{\ell A,D}^{XY}(l' \leftrightarrow l_1). \quad (\text{C.10})$$

The *direct* contributions have *direct* N , SB and Fierz-transformed \tilde{N} contributions:

$$\begin{aligned} B_{\ell V,D}^{LL} &= B_{\ell V,D}^{LL,N} + B_{\ell V,F}^{LL,\tilde{N}} + B_{\ell V,D}^{LL,SB}, & B_{\ell V,D}^{RR} &= B_{\ell V,D}^{RR,SB}, \\ B_{\ell V,D}^{LR} &= B_{\ell V,D}^{LR,SB}, & B_{\ell V,D}^{RL} &= -\frac{1}{2}B_{\ell S,F}^{RL,\tilde{N}} + B_{\ell V,D}^{RL,SB}, \\ B_{\ell S,D}^{LL} &= B_{\ell S,D}^{LL,SB}, & B_{\ell S,D}^{RR} &= \frac{1}{2}B_{\ell S,F}^{RR,\tilde{N}} + B_{\ell S,D}^{RR,SB}, \\ B_{\ell S,D}^{LR} &= B_{\ell S,D}^{LR,SB}, & B_{\ell S,D}^{RL} &= B_{\ell S,D}^{RL,N} - 2B_{\ell V,F}^{RL,\tilde{N}} + B_{\ell S,D}^{RL,SB}, \\ B_{\ell T,D}^{LL} &= B_{\ell T,D}^{LL,SB}, & B_{\ell T,D}^{RR} &= \frac{1}{2}B_{\ell S,F}^{RR,\tilde{N}} + B_{\ell T,D}^{RR,SB}. \end{aligned} \quad (\text{C.11})$$

The form factor contributions from Eq (C.11) read:

$$\begin{aligned} B_{\ell V,D}^{LL,N} &= B_{la}^* B_{l_2 b}^* B_{l' a} B_{l_1 b} \left[- \left(1 + \frac{\lambda_{n_a} \lambda_{n_b}}{4} \right) J_{211}^1(1, \lambda_{n_a}, \lambda_{n_b}) \right. \\ &\quad + 2\lambda_{n_a} \lambda_{n_b} J_{211}^0(1, \lambda_{n_a}, \lambda_{n_b}) - 2\lambda_{n_a} \lambda_{n_b} t_\beta^{-2} J_{1111}^0(1, \lambda_{H^+}, \lambda_{n_a}, \lambda_{n_b}) \\ &\quad \left. - \frac{1}{2} \lambda_a \lambda_b t_\beta^{-2} J_{1111}^1(1, \lambda_{H^+}, \lambda_{n_a}, \lambda_{n_b}) - \frac{1}{4} \lambda_a \lambda_b t_\beta^{-4} J_{211}^1(\lambda_{H^+}, \lambda_{n_a}, \lambda_{n_b}) \right], \\ B_{\ell V,D}^{RL,N} &= -B_{la}^* B_{l_2 b}^* B_{l' a} B_{l_1 b} \frac{m_l m_{l_1} t_\beta^2}{M_W^2} \\ &\quad \cdot \left(J_{1111}^1(1, \lambda_{H^+}, \lambda_{n_a}, \lambda_{n_b}) + \lambda_a \lambda_b J_{1111}^0(\lambda_{H^+}, \lambda_{n_a}, \lambda_{n_b}) \right), \end{aligned} \quad (\text{C.12})$$

$$\begin{aligned} B_{\ell V,F}^{LL,\tilde{N}} &= (\tilde{B}_{l_1 k B}^{R,1} \tilde{B}_{l_2 m B}^{R,1*} + \tilde{B}_{l_1 k B}^{R,2} \tilde{B}_{l_2 m B}^{R,2*})(\tilde{B}_{l' m A}^{R,1} \tilde{B}_{l k A}^{R,1*} + \tilde{B}_{l' m A}^{R,2} \tilde{B}_{l k A}^{R,2*}) \\ &\quad \cdot J_{1111}^1(\lambda_{\tilde{\chi}_k}, \lambda_{\tilde{\chi}_m}, \lambda_{\tilde{N}_A}, \lambda_{\tilde{N}_B}), \end{aligned}$$

$$\begin{aligned}
B_{\ell V,F}^{RL,\tilde{N}} &= (\tilde{B}_{l_1 k B}^{L,1} \tilde{B}_{l_2 m B}^{R,1*} + \tilde{B}_{l_1 k B}^{L,2} \tilde{B}_{l_2 m B}^{R,2*}) (\tilde{B}_{l' m A}^{R,1} \tilde{B}_{lkA}^{L,1*} + \tilde{B}_{l' m A}^{R,2} \tilde{B}_{lkA}^{L,2*}) \\
&\quad \cdot \frac{m_{l'} m_l}{2 c_\beta^2 M_W^2} J_{1111}^1(\lambda_{\tilde{\chi}_k}, \lambda_{\tilde{\chi}_m}, \lambda_{\tilde{N}_A}, \lambda_{\tilde{N}_B}), \\
B_{\ell S,F}^{RR,\tilde{N}} &= (\tilde{B}_{l_1 k B}^{R,1} \tilde{B}_{l_2 m B}^{L,1*} + \tilde{B}_{l_1 k B}^{R,2} \tilde{B}_{l_2 m B}^{L,2*}) (\tilde{B}_{l' m A}^{R,1} \tilde{B}_{lkA}^{L,1*} + \tilde{B}_{l' m A}^{R,2} \tilde{B}_{lkA}^{L,2*}) \\
&\quad \cdot \frac{2 m_{l_2} m_l}{c_\beta^2 M_W^2} \sqrt{\lambda_{\tilde{\chi}_k} \lambda_{\tilde{\chi}_m}} J_{1111}^0(\lambda_{\tilde{\chi}_k}, \lambda_{\tilde{\chi}_m}, \lambda_{\tilde{N}_A}, \lambda_{\tilde{N}_B}), \\
B_{\ell S,F}^{RL,\tilde{N}} &= (\tilde{B}_{l_1 k B}^{R,1} \tilde{B}_{l_2 m B}^{R,1*} + \tilde{B}_{l_1 k B}^{R,2} \tilde{B}_{l_2 m B}^{R,2*}) (\tilde{B}_{l' m A}^{L,1} \tilde{B}_{lkA}^{L,1*} + \tilde{B}_{l' m A}^{L,2} \tilde{B}_{lkA}^{L,2*}) \\
&\quad \cdot \frac{2 m_{l_1} m_l}{c_\beta^2 M_W^2} \sqrt{\lambda_{\tilde{\chi}_k} \lambda_{\tilde{\chi}_m}} J_{1111}^0(\lambda_{\tilde{\chi}_k}, \lambda_{\tilde{\chi}_m}, \lambda_{\tilde{N}_A}, \lambda_{\tilde{N}_B}),
\end{aligned} \tag{C.13}$$

$$\begin{aligned}
& + 2\tilde{V}_{l_2mb}^{0\ell R}\tilde{V}_{lma}^{0\ell R*}\tilde{V}_{l'na}^{0\ell L}\tilde{V}_{l_1nb}^{0\ell L*}\sqrt{\lambda_{\tilde{\chi}_m^0}\lambda_{\tilde{\chi}_k^0}}J_{1111}^0(\lambda_{\tilde{\chi}_m^0}, \lambda_{\tilde{\chi}_n^0}, \lambda_{\tilde{e}_a}, \lambda_{\tilde{e}_b}), \\
B_{\ell T,D}^{RR,\text{SB}} & = -2\tilde{V}_{l_1mb}^{0\ell R}\tilde{V}_{lma}^{0\ell L*}\tilde{V}_{l'na}^{0\ell R}\tilde{V}_{l_2nb}^{0\ell L*}\sqrt{\lambda_{\tilde{\chi}_m^0}\lambda_{\tilde{\chi}_k^0}}J_{1111}^0(\lambda_{\tilde{\chi}_m^0}, \lambda_{\tilde{\chi}_n^0}, \lambda_{\tilde{e}_a}, \lambda_{\tilde{e}_b}) \\
& + 2\tilde{V}_{l_2mb}^{0\ell L}\tilde{V}_{lma}^{0\ell L*}\tilde{V}_{l'na}^{0\ell R}\tilde{V}_{l_1nb}^{0\ell R*}\sqrt{\lambda_{\tilde{\chi}_m^0}\lambda_{\tilde{\chi}_k^0}}J_{1111}^0(\lambda_{\tilde{\chi}_m^0}, \lambda_{\tilde{\chi}_n^0}, \lambda_{\tilde{e}_a}, \lambda_{\tilde{e}_b}). \quad (\text{C.14})
\end{aligned}$$

§ C.4 Semileptonic Box Form factors

Semileptonic form factors have only *direct* contributions, with the following N , \tilde{N} and SB content:

$$\begin{aligned}
B_{dV}^{LL} & = B_{dV}^{LL,N} + B_{dV}^{LL,\tilde{N}} + B_{dV}^{LL,\text{SB}}, \\
B_{uV}^{LL} & = B_{uV}^{LL,N} + B_{uV}^{LL,\tilde{N}} + B_{uV}^{LL,\text{SB}}, \quad (\text{C.15})
\end{aligned}$$

and

$$B_{dA}^{XY} = B_{dA}^{XY,\text{SB}}, \quad B_{uA}^{XY} = B_{uA}^{XY,\text{SB}}, \quad (\text{C.16})$$

for $(X, Y, A) \neq (L, L, V)$. The N and \tilde{N} contributions are given by

$$\begin{aligned}
B_{dV}^{LL,N} & = B_{l'a}B_{la}^*(V^*)_{bd_1}(V)_{bd_2}\left[-\left(1+\frac{\lambda_{n_a}\lambda_{u_b}}{4}\right)J_{211}^1(1, \lambda_{n_a}, \lambda_{u_b})\right. \\
& + 2\lambda_{n_a}\lambda_{u_b}J_{211}^0(1, \lambda_{n_a}, \lambda_{u_b}) + \frac{1}{2t_\beta^2}\lambda_{n_a}\lambda_{u_b}J_{1111}^0(1, \lambda_{H^+}, \lambda_{n_a}, \lambda_{u_b}) \\
& \left.-\frac{1}{2t_\beta^2}\lambda_{n_a}\lambda_{u_b}J_{1111}^1(1, \lambda_{H^+}, \lambda_{n_a}, \lambda_{u_b}) - \frac{1}{4t_\beta^4}\lambda_{n_a}\lambda_{u_b}J_{211}^1(\lambda_{H^+}, \lambda_{n_a}, \lambda_{u_b})\right], \\
B_{uV}^{LL,N} & = B_{l'a}B_{la}^*(V^*)_{d_2b}(V)_{d_1b}\left[\left(4+\frac{\lambda_{n_a}\lambda_{d_b}}{4}\right)J_{211}^1(1, \lambda_{n_a}, \lambda_{d_b})\right. \\
& - 2\lambda_{n_a}\lambda_{d_b}J_{211}^0(1, \lambda_{n_a}, \lambda_{d_b}) + \frac{1}{2}\lambda_{n_a}\lambda_{d_b}J_{1111}^0(1, \lambda_{H^+}, \lambda_{n_a}, \lambda_{d_b}) \\
& \left.-\frac{1}{2}\lambda_{n_a}\lambda_{d_b}J_{1111}^1(1, \lambda_{H^+}, \lambda_{n_a}, \lambda_{d_b}) + \frac{1}{4}\lambda_{n_a}\lambda_{d_b}J_{211}^1(\lambda_{H^+}, \lambda_{n_a}, \lambda_{d_b})\right], \\
& \quad (\text{C.17})
\end{aligned}$$

$$\begin{aligned}
B_{dV}^{LL,\tilde{N}} & = -\frac{1}{2}\tilde{V}_{d_1ka}^{-dR}\tilde{V}_{d_2ma}^{-dR*}(\tilde{V}_{lkA}^{-\ell R,1*}\tilde{V}_{l'mA}^{-\ell R,1} + \tilde{V}_{lkA}^{-\ell R,2*}\tilde{V}_{l'mA}^{-\ell R,2}) \\
& \cdot J_{1111}^1(\lambda_{\tilde{\chi}_k}, \lambda_{\tilde{\chi}_m}, \lambda_{\tilde{N}_A}, \lambda_{\tilde{u}_a}),
\end{aligned}$$

$$B_{uV}^{LL,\tilde{N}} = -\tilde{V}_{u_1 ka}^{-uR} \tilde{V}_{u_2 ma}^{-uR*} (\tilde{V}_{lkA}^{-\ell R,1*} \tilde{V}_{l'mA}^{-\ell R,1} + \tilde{V}_{lkA}^{-\ell R,2*} \tilde{V}_{l'mA}^{-\ell R,2}) \sqrt{\lambda_{\tilde{\chi}_k} \lambda_{\tilde{\chi}_m}} \\ \cdot J_{1111}^0(\lambda_{\lambda_{\tilde{\chi}_k}}, \lambda_{\tilde{\chi}_m}, \lambda_{\tilde{N}_A}, \lambda_{\tilde{d}_a}) . \quad (C.18)$$

The SB form factors $B_{dA}^{XY,SB}$ and $B_{uA}^{XY,SB}$, with $X = L, R$, $Y = L, R$ and $A = V, S, T$, are obtained from the *direct* leptonic form factors $B_{\ell A}^{XY,SB}$, by making the replacements: $\ell \rightarrow d$, $l_1 \rightarrow d$, $l_2 \rightarrow d$, $\tilde{e} \rightarrow \tilde{d}$ and $\ell \rightarrow u$, $l_1 \rightarrow u$, $l_2 \rightarrow u$, $\tilde{e} \rightarrow \tilde{u}$, in both the interaction vertices and the arguments of the J -loop functions that carry the index b in Eq (C.14).

Appendix D

Form factor analysis

In order to calculate three-body decays given by Eqs (3.10) and (3.11), we have developed the *model independent* procedure for calculation of CLFV three-body decay rates. The analytical calculus is for the most part performed using *Wolfram Mathematica*, with the aid of *FeynCalc* package [169] which was found to be very useful in dealing with the Dirac algebra (traces of γ matrices, kinematics, etc.).

The starting point of the calculation are the most general photon mediated, Z -boson mediated and box-diagram effective operators inducing $l \rightarrow l' l_1 l_2^c$ LFV transitions,

$$\begin{aligned} \mathcal{T}_\gamma^{l \rightarrow l' l_1 l_2} = & \frac{\alpha_w^2}{M_W^2} \cdot \left\{ \bar{l}' \gamma_\alpha P_L l \bar{l}_1 \gamma^\alpha P_L l_2 \cdot P_1 + \bar{l}' \gamma_\alpha P_R l \bar{l}_1 \gamma^\alpha P_R l_2 \cdot P_2 \right. \\ & + \bar{l}' \gamma_\alpha P_L l \bar{l}_1 \gamma^\alpha P_R l_2 \cdot P_3 + \bar{l}' \gamma_\alpha P_R l \bar{l}_1 \gamma^\alpha P_L l_2 \cdot P_4 \\ & + \bar{l}' i \sigma_{\alpha\beta} q^\beta P_L l \bar{l}_1 \gamma^\alpha P_L l_2 \cdot \frac{P_{11}}{q^2} + \bar{l}' i \sigma_{\alpha\beta} q^\beta P_R l \bar{l}_1 \gamma^\alpha P_R l_2 \cdot \frac{P_{12}}{q^2} \\ & \left. + \bar{l}' i \sigma_{\alpha\beta} q^\beta P_L l \bar{l}_1 \gamma^\alpha P_R l_2 \cdot \frac{P_{13}}{q^2} + \bar{l}' i \sigma_{\alpha\beta} q^\beta P_R l \bar{l}_1 \gamma^\alpha P_L l_2 \cdot \frac{P_{14}}{q^2} \right\}, \end{aligned} \quad (\text{D.1})$$

$$\begin{aligned} \mathcal{T}_Z^{l \rightarrow l' l_1 l_2} = & \frac{\alpha_w^2}{M_W^2} \cdot \left\{ \bar{l}' \gamma_\alpha P_{Ll} \bar{l}_1 \gamma^\alpha P_{Ll_2} \cdot Z_1 + \bar{l}' \gamma_\alpha P_{Rl} \bar{l}_1 \gamma^\alpha P_{Rl_2} \cdot Z_2 \right. \\ & \left. + \bar{l}' \gamma_\alpha P_{Ll} \bar{l}_1 \gamma^\alpha P_{Rl_2} \cdot Z_3 + \bar{l}' \gamma_\alpha P_{Rl} \bar{l}_1 \gamma^\alpha P_{Ll_2} \cdot Z_4 \right\}, \end{aligned} \quad (\text{D.2})$$

$$\begin{aligned} \mathcal{T}_{box}^{l \rightarrow l' l_1 l_2} = & \frac{\alpha_w^2}{M_W^2} \cdot \left\{ \bar{l}' \gamma_\alpha P_{Ll} \bar{l}_1 \gamma^\alpha P_{Ll_2} \cdot B_1 + \bar{l}' \gamma_\alpha P_{Rl} \bar{l}_1 \gamma^\alpha P_{Rl_2} \cdot B_2 \right. \\ & + \bar{l}' \gamma_\alpha P_{Ll} \bar{l}_1 \gamma^\alpha P_{Rl_2} \cdot B_3 + \bar{l}' \gamma_\alpha P_{Rl} \bar{l}_1 \gamma^\alpha P_{Ll_2} \cdot B_4 \\ & + \bar{l}' P_{Ll} \bar{l}_1 P_{Ll_2} \cdot B_5 + \bar{l}' P_{Rl} \bar{l}_1 P_{Rl_2} \cdot B_6 \\ & + \bar{l}' P_{Ll} \bar{l}_1 P_{Rl_2} \cdot B_7 + \bar{l}' P_{Rl} \bar{l}_1 P_{Ll_2} \cdot B_8 \\ & \left. + \bar{l}' \sigma_{\alpha\beta} P_{Ll} \bar{l}_1 \sigma^{\alpha\beta} P_{Ll_2} \cdot B_9 + \bar{l}' \sigma_{\alpha\beta} P_{Rl} \bar{l}_1 \sigma^{\alpha\beta} P_{Rl_2} \cdot B_{10} \right\}, \end{aligned} \quad (\text{D.3})$$

expressed in terms of the form factors P_i , Z_i and B_i multiplied by the corresponding four-lepton operators. The Higgs mediated contributions were not included since we assured their smallness assuming small $\tan \beta$ ($\tan \beta \lesssim 20$).

Note that the four-lepton operators are all written in the form $\bar{l}' \cdots l \bar{l}_1 \cdots l_2$. This is achieved by applying the Fiertz transformations

$$\begin{aligned} (\gamma^\mu P_L \times \gamma_\mu P_L)_{1234} &= (\gamma^\mu P_L \times \gamma_\mu P_L)_{1432}, \\ (\gamma^\mu P_R \times \gamma_\mu P_R)_{1234} &= (\gamma^\mu P_R \times \gamma_\mu P_R)_{1432}, \\ (\gamma^\mu P_L \times \gamma^\mu P_R)_{1234} &= -2(P_R \times P_L)_{1432}, \\ (\gamma^\mu P_R \times \gamma_\mu P_L)_{1234} &= -2(P_L \times P_R)_{1432}, \\ (P_R \times P_L)_{1234} &= -\frac{1}{2}(\gamma_\mu P_L \times \gamma^\mu P_R)_{1432}, \\ (P_L \times P_R)_{1234} &= -\frac{1}{2}(\gamma_\mu P_R \times \gamma^\mu P_L)_{1432}, \\ (P_R \times P_R)_{1234} &= \left[-\frac{1}{2}(P_R \times P_R) + \frac{1}{8}\sigma_{\mu\nu} P_R \times \sigma^{\mu\nu} P_R \right]_{1432}, \\ (P_L \times P_L)_{1234} &= \left[-\frac{1}{2}(P_L \times P_L) + \frac{1}{8}\sigma_{\mu\nu} P_L \times \sigma^{\mu\nu} P_L \right]_{1432}. \end{aligned} \quad (\text{D.4})$$

to the terms with different ordering of the lepton fields.

The total effective operator is a sum of the photon-mediated, Z -boson me-

diated and box contributions,

$$\begin{aligned}
\mathcal{T}_{TOT}^{l \rightarrow l' l_1 l_2} = & \frac{\alpha_w^2}{M_W^2} \cdot \left\{ \bar{l}' \gamma_\alpha P_L l \bar{l}_1 \gamma^\alpha P_L l_2 \cdot [P_1 + Z_1 + B_1] \right. \\
& + \bar{l}' \gamma_\alpha P_R l \bar{l}_1 \gamma^\alpha P_R l_2 \cdot [P_2 + B_2 + Z_2] \\
& + \bar{l}' \gamma_\alpha P_L l \bar{l}_1 \gamma^\alpha P_R l_2 \cdot [P_3 + Z_3 + B_3] \\
& + \bar{l}' \gamma_\alpha P_R l \bar{l}_1 \gamma^\alpha P_L l_2 \cdot [P_4 + Z_4 + B_4] \\
& + \bar{l}' P_L l \bar{l}_1 P_L l_2 \cdot B_5 + \bar{l}' P_R l \bar{l}_1 P_R l_2 \cdot B_6 \\
& + \bar{l}' P_L l \bar{l}_1 P_R l_2 \cdot B_7 + \bar{l}' P_R l \bar{l}_1 P_L l_2 \cdot B_8 \\
& + \bar{l}' \sigma_{\alpha\beta} P_L l \bar{l}_1 \sigma^{\alpha\beta} P_L l_2 \cdot B_9 + \bar{l}' \sigma_{\alpha\beta} P_R l \bar{l}_1 \sigma^{\alpha\beta} P_R l_2 \cdot B_{10} \\
& + \bar{l}' i \sigma_{\alpha\beta} q^\beta P_L l \bar{l}_1 \gamma^\alpha P_L l_2 \cdot \frac{P_{11}}{q^2} + \bar{l}' i \sigma_{\alpha\beta} q^\beta P_R l \bar{l}_1 \gamma^\alpha P_R l_2 \cdot \frac{P_{12}}{q^2} \\
& \left. + \bar{l}' i \sigma_{\alpha\beta} q^\beta P_L l \bar{l}_1 \gamma^\alpha P_R l_2 \cdot \frac{P_{13}}{q^2} + \bar{l}' i \sigma_{\alpha\beta} q^\beta P_R l \bar{l}_1 \gamma^\alpha P_L l_2 \cdot \frac{P_{14}}{q^2} \right\}. \tag{D.5}
\end{aligned}$$

This is the most general form factor CLFV $l \rightarrow l' l_1 l_2^c$ structure valid in any model. The four-lepton operators with the Lorentz structure $P_L \times P_R$ and $P_R \times P_L$ are novelty, since they have not been considered in the previous publications [114, 141].

The total amplitude can be written down in the more compact form,

$$\mathcal{T}_{TOT}^{l \rightarrow l' l_1 l_2} = \frac{\alpha_w^2}{M_W^2} \cdot \sum_{i=1}^{14} \bar{l}' \Gamma_{1i} l \bar{l}_1 \Gamma_{2i} l_2 \cdot \mathcal{F}_i, \tag{D.6}$$

where Γ_1 , Γ_2 and \mathcal{F}_i are given by

$$\Gamma_{1i} = \left\{ \gamma_\alpha P_L, \gamma_\alpha P_R, \gamma_\alpha P_L, \gamma_\alpha P_R, P_L, P_R, P_L, P_R, \sigma_{\alpha\beta} P_L, \sigma_{\alpha\beta} P_R, \right. \tag{D.7}$$

$$\left. i \sigma_{\alpha\beta} q^\beta P_L, i \sigma_{\alpha\beta} q^\beta P_R, i \sigma_{\alpha\beta} q^\beta P_L, i \sigma_{\alpha\beta} q^\beta P_R \right\}, \tag{D.8}$$

$$\Gamma_{2i} = \left\{ \gamma_\alpha P_L, \gamma_\alpha P_R, \gamma_\alpha P_R, \gamma_\alpha P_L, P_L, P_R, P_R, P_L, \sigma_{\alpha\beta} P_L, \sigma_{\alpha\beta} P_R, \right. \tag{D.9}$$

$$\left. \gamma^\alpha P_L, \gamma_\alpha P_R, \gamma_\alpha P_R, \gamma_\alpha P_L \right\}, \tag{D.10}$$

$$\mathcal{F}_i = \left\{ F_1, F_2, F_3, F_4, F_5, F_6, F_7, F_8, F_9, F_{10}, \frac{F_{11}}{q^2}, \frac{F_{12}}{q^2}, \frac{F_{13}}{q^2}, \frac{F_{14}}{q^2} \right\}. \quad (\text{D.11})$$

Evaluating the operator (D.6) between initial and final lepton states of the $l \rightarrow l' l_1 l_2^c$ transition, one arrives at the amplitude written in the terms of spinors,

$$\begin{aligned} \mathcal{T}_{TOT}^{e_1 \rightarrow e_2 e_3 e_4^c} &= \frac{\alpha_w^2}{M_W^2} \cdot \left\{ \sum_{i=1}^{14} \bar{u}_2 \Gamma_{1i}^A u_1 \bar{u}_3 \Gamma_{2i}^A v_4 \cdot \mathcal{F}_i^A \right. \\ &\quad \left. - \sum_{i=1}^{14} \bar{u}_3 \Gamma_{1i}^B u_1 \bar{u}_2 \Gamma_{2i}^B v_4 \cdot \mathcal{F}_i^B \right\}. \end{aligned} \quad (\text{D.12})$$

The contents of the arrays denoted by \mathcal{F}_i^A and \mathcal{F}_i^B depends on the leptons in the final state. There are three possible cases:

1) $l' = l_1 = l_2$ ($\tau^- \rightarrow \mu^- \mu^- \mu^+$; $\tau^- \rightarrow e^- e^- \mu^+$; $\mu^- \rightarrow e^- e^- e^+$):

$$\mathcal{F}_i^A = \left\{ F_1^A, F_2^A, F_3^A, F_4^A, F_5^A, F_6^A, F_7^A, F_8^A, F_9^A, F_{10}^A, \frac{F_{11}^A}{s_{12}}, \frac{F_{12}^A}{s_{12}}, \frac{F_{13}^A}{s_{12}}, \frac{F_{14}^A}{s_{12}} \right\},$$

$$\mathcal{F}_i^B = \left\{ F_1^B, F_2^B, F_3^B, F_4^B, F_5^B, F_6^B, F_7^B, F_8^B, F_9^B, F_{10}^B, \frac{F_{11}^B}{s_{13}}, \frac{F_{12}^B}{s_{13}}, \frac{F_{13}^B}{s_{13}}, \frac{F_{14}^B}{s_{13}} \right\}.$$

2) $l' \neq l_2, l_1 = l_2$ ($\tau^- \rightarrow e^- \mu^- \mu^+$; $\tau^- \rightarrow e^- \mu^- e^+$):

$$\mathcal{F}_i^A = \left\{ F_1^A, F_2^A, F_3^A, F_4^A, F_5^A, F_6^A, F_7^A, F_8^A, F_9^A, F_{10}^A, \frac{F_{11}^A}{s_{12}}, \frac{F_{12}^A}{s_{12}}, \frac{F_{13}^A}{s_{12}}, \frac{F_{14}^A}{s_{12}} \right\},$$

$$\mathcal{F}_i^B = \left\{ F_1^B, F_2^B, F_3^B, F_4^B, F_5^B, F_6^B, F_7^B, F_8^B, F_9^B, F_{10}^B, 0, 0, 0, 0 \right\}.$$

3) $l' \neq l_2, l_1 \neq l_2$ ($\tau^- \rightarrow \mu^- \mu^- e^+$; $\tau^- \rightarrow e^- e^- \mu^+$):

$$\mathcal{F}_i^A = \left\{ F_1^A, F_2^A, F_3^A, F_4^A, F_5^A, F_6^A, F_7^A, F_8^A, F_9^A, F_{10}^A, 0, 0, 0, 0 \right\},$$

$$\mathcal{F}_i^B = \left\{ F_1^B, F_2^B, F_3^B, F_4^B, F_5^B, F_6^B, F_7^B, F_8^B, F_9^B, F_{10}^B, 0, 0, 0, 0 \right\}.$$

Here, s_{12} and s_{13} are Mandelstem variables defined in (D.15).

Absolute square of the amplitude (D.12) reads

$$\begin{aligned}
& \left| \mathcal{T}_{TOT}^{e_1 \rightarrow e_2 e_3 e_4^c} \right|^2 = \frac{\alpha_w^4}{M_W^4} \cdot \left\{ \right. \\
& \sum_{i,j} \text{Tr} [(\not{p}_2 + m_2) \Gamma_{1i}^A (\not{p}_1 + m) \bar{\Gamma}_{1j}^A] \cdot \text{Tr} [(\not{p}_3 + m_3) \Gamma_{2i}^A (\not{p}_4 - m_4) \bar{\Gamma}_{2j}^A] \cdot \mathcal{F}_i^A \mathcal{F}_j^{A*} \\
& + \sum_{i,j} \text{Tr} [(\not{p}_3 + m_3) \Gamma_{1i}^B (\not{p}_1 + m) \bar{\Gamma}_{1j}^B] \cdot \text{Tr} [(\not{p}_2 + m_2) \Gamma_{2i}^B (\not{p}_4 - m_4) \bar{\Gamma}_{2j}^B] \cdot \mathcal{F}_i^B \mathcal{F}_j^{B*} \\
& - \sum_{i,j} \text{Tr} [(\not{p}_2 + m_2) \Gamma_{1i}^A (\not{p}_1 + m) \bar{\Gamma}_{1j}^B (\not{p}_3 + m_3) \Gamma_{2i}^A (\not{p}_4 - m_4) \bar{\Gamma}_{2j}^B] \cdot \mathcal{F}_i^A \mathcal{F}_j^{B*} \\
& \left. - \sum_{i,j} \text{Tr} [(\not{p}_3 + m_3) \Gamma_{1i}^B (\not{p}_1 + m) \bar{\Gamma}_{1j}^A (\not{p}_2 + m_2) \Gamma_{2i}^B (\not{p}_4 - m_4) \bar{\Gamma}_{2j}^A] \cdot \mathcal{F}_i^{A*} \mathcal{F}_j^B \right\}. \tag{D.13}
\end{aligned}$$

After evaluating the traces in Eq (D.13), one imposes the kinematics of the three-body process:

$$\begin{aligned}
p_1 \cdot p_2 &= \frac{1}{2} (m^2 + m_2^2 - s_{12}) , \\
p_1 \cdot p_3 &= \frac{1}{2} (m^2 + m_3^2 - s_{13}) , \\
p_3 \cdot p_4 &= \frac{1}{2} (s_{12} - m_3^2 - m_4^2) , \\
p_2 \cdot p_4 &= \frac{1}{2} (s_{13} - m_2^2 - m_4^2) , \\
p_1 \cdot p_4 &= \frac{1}{2} (m^2 + m_4^2 - s_{14}) = \frac{1}{2} (s_{12} + s_{13} - m_2^2 - m_3^2) , \\
p_2 \cdot p_3 &= \frac{1}{2} (s_{14} - m_2^2 - m_3^2) = \frac{1}{2} (m^2 + m_4^2 - s_{12} - s_{13}) , \tag{D.14}
\end{aligned}$$

where s_{12} , s_{13} and s_{14} are well-known Mandelstam variables,

$$\begin{aligned}
s_{12} &\equiv (p_1 - p_2)^2 = s_{34} , \\
s_{13} &\equiv (p_1 - p_3)^2 = s_{24} , \\
s_{14} &\equiv (p_1 - p_4)^2 = s_{23} , \tag{D.15}
\end{aligned}$$

satisfying $s_{12} + s_{13} + s_{14} = m^2 + m_2^2 + m_3^2 + m_4^2$.

The last step in the evaluation of the branching ratios is an evaluation of the three-body phase-space integral [37]

$$\Gamma(e_1 \rightarrow e_2 e_3 e_4^c) = \frac{1}{(2\pi)^3} \frac{1}{32m^3} \int_{4\varepsilon^2}^{m^2} ds_{12} \int_{s_{13}^-}^{s_{13}^+} ds_{13} \left| \mathcal{T}_{TOT}^{e_1 \rightarrow e_2 e_3 e_4^c} \right|^2, \quad (\text{D.16})$$

where

$$s_{13}^\pm = \varepsilon^2 + \frac{m^2 - s_{12}}{2} \left[1 \pm \left(1 - \frac{4\varepsilon^2}{s_{12}} \right)^{1/2} \right], \quad (\text{D.17})$$

and ε is equal to the external masses ($\varepsilon = m_2 = m_3 = m_4$ for $l' = l_1 = l_2$ and $\varepsilon = m_3 = m_4$ for $l' \neq l_1, l_1 = l_2$). Since the decaying particle is much more massive than the resulting particles, we take $\varepsilon \rightarrow 0$ whenever possible.

In Eq (D.16) there are seven types of integrals which are divergent in the $\varepsilon \rightarrow 0$ limit. These integrals were evaluated partly by hand and partly using *Mathematica*, keeping the leading terms in ε expansion,

$$\begin{aligned} \mathcal{I}_1 &= \int_{4\varepsilon^2}^{m^2} \frac{ds_{12}}{s_{12}} \int_{s_{13}^-}^{s_{13}^+} ds_{13} \simeq m^2 \left(\ln \frac{m^2}{\varepsilon^2} - 3 \right), \\ \mathcal{I}_2 &= \int_{4\varepsilon^2}^{m^2} \frac{ds_{12}}{s_{12}} \int_{s_{13}^-}^{s_{13}^+} s_{13} ds_{13} \simeq m^4 \left(\frac{1}{2} \ln \frac{m^2}{\varepsilon^2} - \frac{7}{4} \right), \\ \mathcal{I}_3 &= \int_{4\varepsilon^2}^{m^2} \frac{ds_{12}}{s_{12}} \int_{s_{13}^-}^{s_{13}^+} s_{13}^2 ds_{13} \simeq m^6 \left(\frac{1}{3} \ln \frac{m^2}{\varepsilon^2} - \frac{4}{3} \right), \\ \mathcal{I}_4 &= \int_{4\varepsilon^2}^{m^2} \frac{ds_{12}}{s_{12}} \int_{s_{13}^-}^{s_{13}^+} \frac{ds_{13}}{s_{13}} \simeq -\frac{\pi^2}{6} + \frac{1}{2} \ln^2 \frac{m^2}{\varepsilon^2}, \\ \mathcal{I}_5 &= \int_{4\varepsilon^2}^{m^2} \frac{ds_{12}}{s_{12}^2} \int_{s_{13}^-}^{s_{13}^+} ds_{13} \simeq \frac{m^6}{6\varepsilon^2} - \ln \frac{m^2}{\varepsilon^2} + 1, \\ \mathcal{I}_6 &= \int_{4\varepsilon^2}^{m^2} \frac{ds_{12}}{s_{12}^2} \int_{s_{13}^-}^{s_{13}^+} s_{13}^2 ds_{13} \simeq m^4 \left(\frac{m^2}{20\varepsilon^2} + \frac{17}{6} - \ln \frac{m^2}{\varepsilon^2} \right), \\ \mathcal{I}_7 &= \int_{4\varepsilon^2}^{m^2} \frac{ds_{12}}{s_{12}^2} \int_{s_{13}^-}^{s_{13}^+} s_{13} ds_{13} \simeq m^2 \left(\frac{m^2}{12\varepsilon^2} + \frac{13}{3} - \ln \frac{m^2}{\varepsilon^2} \right). \end{aligned}$$

The leading order divergences in the integrals \mathcal{I}_4 , \mathcal{I}_5 , \mathcal{I}_6 and \mathcal{I}_7 cancel out in the final expression, leaving only ε -divergent terms which comprise $\ln \frac{m^2}{\varepsilon^2}$.

The final result again depends on the lepton content of the final state:

1) $l' = l_1 = l_2$

$$\begin{aligned} \left| \mathcal{T}_{TOT}^{e_1 \rightarrow e_2 e_2 e_2^c} \right|^2 &= \frac{m_l^6}{12} \cdot \left\{ \right. \\ &(|B_5| + |B_6|^2) m_l^2 + 2(|B_7|^2 + |B_8|^2) m_l^2 + 144(|B_9|^2 + |B_{10}|^2) m_l^2 \\ &- 4[(B_3 + P_3 + Z_3)^* B_7 + (B_4 + P_4 + Z_4)^* B_8 + \text{c.c.}] m_l^2 \\ &+ 8(|B_3 + P_3 + Z_3| + |B_4 + P_4 + Z_4|) m_l^2 \\ &- 12(B_9^* B_5 + B_{10}^* B_6 + \text{c.c.}) m_l^2 \\ &+ 16(|B_1 + P_1 + Z_1| + |B_2 + P_2 + Z_2|) m_l^2 \\ &+ 8(P_{12}^* B_7 + P_{11}^* B_8 + \text{c.c.}) m_l \\ &- 16[(B_4 + P_4 + Z_4)^* P_{11} + (B_3 + P_3 + Z_3)^* P_{12} + \text{c.c.}] m_l \\ &- 32[(B_1 + P_1 + Z_1)^* P_{12} + (B_2 + P_2 + Z_2)^* P_{11} + \text{c.c.}] m_l \\ &\left. + 64(|P_{11}|^2 + |P_{12}|^2) \left(\ln \frac{m^2}{\varepsilon^2} - \frac{11}{4} \right) \right\}. \end{aligned} \quad (\text{D.18})$$

2) $l' \neq l_2, l_1 = l_2$

$$\begin{aligned} \left| \mathcal{T}_{TOT}^{e_1 \rightarrow e_2 e_3 e_3^c} \right|^2 &= \frac{m_l^6}{12} \cdot \left\{ \right. \\ &(|B_5| + |B_6|^2) m_l^2 + 2(|B_7|^2 + |B_8|^2) m_l^2 + 4(|B_3|^2 + |B_4|^2) m_l^2 \\ &+ 8(|B_1|^2 + |B_2|^2) m_l^2 + 144(|B_9|^2 + |B_{10}|^2) m_l^2 \\ &+ 8(B_1 + P_1 + Z_1)^* B_1 m_l^2 + 8(B_2 + P_2 + Z_2)^* B_2 m_l^2 - 4B_7^* B_3 m_l^2 \\ &+ 4(B_3 + P_3 + Z_3)^* B_3 m_l^2 - 4B_8^* B_4 m_l^2 + 4(B_4 + P_4 + Z_4)^* B_4 m_l^2 \\ &- 12B_9^* B_5 m_l^2 - 12B_{10}^* B_5 m_l^2 - 2B_3^* B_7 m_l^2 \\ &- 2(B_3 + P_3 + Z_3)^* B_7 m_l^2 - 2B_4^* B_8 m_l^2 + 2(B_4 + P_4 + Z_4)^* B_8 m_l^2 \\ &- 12B_5^* B_9 m_l^2 - 12B_6^* B_{10} m_l^2 + 4B_1^* P_1 m_l^2 \\ &+ 4(B_1 + P_1 + Z_1)^* P_1 m_l^2 + 4B_2^* P_2 m_l^2 + 4(B_2 + P_2 + Z_2)^* P_2 m_l^2 \\ &\left. - 2B_7^* P_3 m_l^2 + 4(B_3 + P_3 + Z_3)^* P_3 m_l^2 - 2B_8^* P_4 m_l^2 \right\} \end{aligned}$$

$$\begin{aligned}
& + 4(B_4 + P_4 + Z_4)^*P_4m_l^2 + 4B_1^*Z_1m_l^2 + 4(B_1 + P_1 + Z_1)^*Z_1m_l^2 \\
& + 4B_2^*Z_2m_l^2 + 4(B_2 + P_2 + Z_2)^*Z_2m_l^2 - 2B_7^*Z_3m_l^2 \\
& + 4(B_3 + P_3 + Z_3)^*Z_3m_l^2 - 2B_8^*Z_4m_l^2 + 4(B_4 + P_4 + Z_4)^*Z_4m_l^2 \\
& - 16P_{12}^*B_1m_l - 16P_{11}^*B_2m_l - 8P_{12}^*B_3m_l \\
& - 8P_{11}^*B_4m_l + 4P_{12}^*B_7m_l + 4P_{11}^*B_8m_l \\
& - 8P_{12}^*P_1m_l - 8P_{11}^*P_2m_l - 8P_{12}^*P_3m_l \\
& - 8P_{11}^*P_4m_l - 8B_2^*P_{11}m_l + 4B_8^*P_{11}m_l \\
& - 8(B_2 + P_2 + Z_2)^*P_{11}m_l - 8(B_4 + P_4 + Z_4)^*P_{11}m_l - 8B_1^*P_{12}m_l \\
& + 4B_7^*P_{12}m_l - 8(B_1 + P_1 + Z_1)^*P_{12}m_l - 8(B_3 + P_3 + Z_3)^*P_{12}m_l \\
& - 8P_{12}^*Z_1m_l - 8P_{11}^*Z_2m_l - 8P_{12}^*Z_3m_l - 8P_{11}^*Z_4m_l \\
& + 32(|P_{11}|^2|P_{12}|^2) \left(\ln \frac{m^2}{\varepsilon^2} - 3 \right) \}. \tag{D.19}
\end{aligned}$$

3) $l' \neq l_2, l_1 \neq l_2$

$$\begin{aligned}
\left| \mathcal{T}_{TOT}^{e_1 \rightarrow e_2 e_3 e_3^c} \right|^2 = \frac{m_l^8}{12} \cdot \left\{ \right. & \\
& 16(|B_1|^2 + |B_2|^2) + 8(|B_3|^2 + |B_4|^2)(|B_5|^2 + |B_6|^2) \\
& + 2(|B_7|^2 + |B_8|^2) + 144(|B_9|^2 + |B_{10}|^2) \\
& \left. + 4[B_7^*B_3 + B_8^*B_4 + 3B_9^*B_5 + 3B_{10}^*B_6 + \text{c.c.}] \right\}. \tag{D.20}
\end{aligned}$$

The results (D.18), (D.19) and (D.20) were tested in several different manners. One of the main tests was to reproduce the result from Ref [110], which was performed with success.

Prošireni sažetak

Ova disertacija izlaže minimalni supersimetrični standardni model sa modelom njihalice na niskoj skali. U okviru tog modela napravljena je detaljna studija narušenja leptonskog okusa u nabijenom leptonskom sektoru. Izveden je cjelovit skup kiralnih amplituda i pridruženih im form-faktora povezanih sa tročestičnim CLFV raspadima miona i tau-leptona bez neutrina, kao što su $\mu \rightarrow eee$, $\tau \rightarrow \mu\mu\mu$, $\tau \rightarrow \mu ee$ i $\tau \rightarrow ee\mu$ te $\mu \rightarrow e$ prijelazi na atomskim jezgrama. Dobiveni analitički rezultati su općeniti i mogu se primijeniti na većinu modela nove fizike koji uključuju narušenje nabijenog leptonskog broja.

Osim toga, u istom su modelu sustavno izučeni doprinosi na razini jedne petlje anomalnom magnetskom dipolnom momentu miona a_μ i električnom dipolnom momentu elektrona d_e .

Pregled tekućih i budućih eksperimenata

Kada neutrino nastane u nekom slabo-interakcijskom procesu i propagira se putem neke konačne udaljenosti, postoji konačna vjerojatnost da će promjeniti okus. Ova opažena i dobro utvrđena činjenica poznata je pod nazivom *neutrinske oscilacije* [1–3], poradi oscilatorne ovisnosti vjerojatnosti promjene okusa u odnosu na energiju neutrina i udaljenost propagacije.

Nebrojeni eksperimenti s neutrinima izvještavaju o narušenju leptonskog okusa u neutrinskom sektoru, bilo da je riječ o nestanku ili nastanku pojedinog okusa [4–25].

Ti su eksperimenti pružili nedvojbeni dokaz postojanja neutrinskih oscilacija uzrokovane konačnim neutrinskim masama i, posljedično, parametrima miješanja neutrina. Budući su neutrini masivni, prijelaz između neutrinskih polja napisanih u bazi okusa (ν_e , ν_μ , ν_τ) u neutrinska polja napisanih u masenoj bazi (ν_1 , ν_2 , ν_3) postaje netrivijalan,

$$\nu_l(x) = \sum_{i=1}^3 U_{li} \nu_i(x), \quad l = e, \mu, \tau. \quad (1)$$

Unitarna matrica U poznata je kao Pontecorvo-Maki-Nakagawa-Sakata matrica [1–3] i obično se parametrizira na sljedeći način:

$$U_{PMNS} = \begin{pmatrix} c_{12}c_{13} & s_{12}c_{13} & s_{13}e^{-i\delta} \\ -s_{12}c_{23} - c_{12}s_{23}s_{13}e^{i\delta} & c_{12}c_{23} - s_{12}s_{23}s_{13}e^{i\delta} & s_{23}c_{13} \\ s_{12}s_{23} - c_{12}c_{23}s_{13}e^{i\delta} & -c_{12}s_{23} - s_{12}c_{23}s_{13}e^{i\delta} & c_{23}c_{13} \end{pmatrix} \cdot P, \quad (2)$$

gdje su $P = \text{diag}(1, e^{i\alpha}, e^{i\beta})$, $c_{ij} \equiv \cos \theta_{ij}$ i $s_{ij} \equiv \sin \theta_{ij}$. θ_{12} označava solarni kut miješanja, θ_{23} atmosferski kut miješanja, a θ_{13} reaktorski kut miješanja. Faze δ , α i β označavaju Diracovu, odnosno dvije Majoranine faze koje narušavaju CP simetriju.

Nedavno izviješće reaktorskih neutrinskih eksperimenata [17, 21, 23] o konačnoj vrijednosti parametra θ_{13} , snažno upućuje na netrivijalnu okusnu

strukturu neutrinskog sektora, kao i mogućnost postojanja CP narušenja.

Narušenje leptonskog okusa (LFV) u neutrinskom sektoru može implicirati mogućnost postojanja LFV-a i nabijenom sektorom. Međutim, unatoč intenzivnoj eksperimentalnoj potrazi [26–37] još uvijek nije pronađen dokaz narušenja leptonskog okusa u nabijenom leptonskom sektoru standardnog modela (SM). Tekući i budući eksperimenti usmjereni na detekciju narušenja leptonskog okusa u nabijenom sektoru (CLFV) uspjeli su odrediti neke gornje granice na pripadajuće opservable. U donjoj tablici navedene su neke trenutne gornje granice, kao i one koje se očekuju u budućnosti, tokom iduće dvije dekade.

Br.	Opservabla	Gornja granica	Očekivana buduća osjetljivost
1.	$B(\mu \rightarrow e\gamma)$	2.4×10^{-12} [26]	$1-2 \times 10^{-13}$ [38,39], 10^{-14} [40]
2.	$B(\mu \rightarrow eee)$	10^{-12} [27]	10^{-16} [41], 10^{-17} [40]
3.	$R_{\mu e}^{\text{Ti}}$	4.3×10^{-12} [28]	$3-7 \times 10^{-17}$ [42–45], 10^{-18} [40,46,47]
4.	$R_{\mu e}^{\text{Au}}$	7×10^{-13} [29]	$3-7 \times 10^{-17}$ [42–45], 10^{-18} [40,46,47]
5.	$B(\tau \rightarrow e\gamma)$	3.3×10^{-8} [30–37]	$1-2 \times 10^{-9}$ [48,49]
6.	$B(\tau \rightarrow \mu\gamma)$	4.4×10^{-8} [30–37]	2×10^{-9} [48,49]
7.	$B(\tau \rightarrow eee)$	2.7×10^{-8} [30–37]	2×10^{-10} [48,49]
8.	$B(\tau \rightarrow e\mu\mu)$	2.7×10^{-8} [30–37]	10^{-10} [48]
9.	$B(\tau \rightarrow \mu\mu\mu)$	2.1×10^{-8} [30–37]	2×10^{-10} [48,49]
10.	$B(\tau \rightarrow \mu ee)$	1.8×10^{-8} [30–37]	10^{-10} [48]

Budući da je CLFV zabranjen u okviru standardnog modela, opažanje takve pojave bio bi jasan signal postojanja nove fizike, što ovo područje istraživanja čini posebno zanimljivim.

Uz opservable koje uključuju CLFV, korisno je i osvrnuti se na leptonske dipolne momente, posebno anomalni magnetski dipolni moment (MDM) miona i električni dipolni moment (EDM) elektrona.

Trenutna eksperimentalna vrijednost MDM-a miona a_μ , prema podacima navedenim u *Particle Data Group* [37] iznosi

$$a_\mu^{\text{exp}} = (116592089 \pm 63) \times 10^{-11}. \quad (3)$$

S druge strane, teorijska vrijednost koja proizlazi iz standardnog modela glasi

$$a_\mu^{\text{SM}} = (116591820 \pm 49) \times 10^{-11}. \quad (4)$$

Razlike između izmjerene i predviđene vrijednosti,

$$\Delta a_\mu \equiv a_\mu^{\text{exp}} - a_\mu^{\text{SM}} = (287 \pm 80) \times 10^{-11} \quad (5)$$

nalazi se na nivou pouzdanosti od 3.6σ pa se stoga naziva *mionska anomalijsa*. Ova vrijednost ograničava dozvoljene doprinose nove fizike, pa se kao takva često upotrebljava kao ograničavajući faktor u građenju novih modela, a ponekad čak i kao argument za eliminaciju nekih od predloženih modela nove fizike.

U skoroj budućnosti očekujemo znatno preciznija mjerena ove opservable. Tako Fermilab eksperiment E989 najavljuje povećanje preciznosti mjerena za faktor 4 [61–65].

Slično tomu, EDM elektrona d_e može služiti kao iznimno precizan test postojanja narušenja CP simetrije inducirano novim CP fazama koje mogu biti prisutne u fizici izvan standardnog modela. Trenutna gornja granica na d_e [37, 51, 52] iznosi

$$d_e < 10.5 \times 10^{-28} \text{ e cm}. \quad (6)$$

Neki budući eksperimenti mogli bi znatno povećati ovu osjetljivost, čak do reda veličine $10^{-29} - 10^{-31}$ e cm [52–59]. S druge strane, predviđanja standardnog modela za d_e kreću se između 10^{-38} e cm i 10^{-33} e cm, ovisno o tome jesu li Diracove CP faze u matricama koje opisuju miješanje lakih neutrina različite od nule ili ne (za detalje vidi ref. [60]). Prema tome, svako opažanje EDM-a različitog od nule, tj. opažanje vrijednosti veće od 10^{-33} e cm, značilo bi postojanje fizike izvan standardnog modela koja u sebi sadrži narušenje CP simetrije.

Iz svega navedenog, vidimo da su ove opservable od velikog interesa za istraživanje mogućih scenarija u okvirima nove fizike. Za više detalja, preporučamo konzultirati neke od izvrsnih preglednih radova navedenih u refer-

encama [59, 66, 67].

Teorijski okvir

Osnovna ideja iza svih supersimetričnih modela jest postojanje simetrije (prikladno nazvane *supersimetrija*) koja transformira fermion u bozon i obratno. *Minimalni supersimetrični standardni model* (MSSM) supersimetrizira standardni model (SM) uz minimalno proširenje standardnomodelskog čestičnog spektra: svakoj čestici iz SM-a pridružena je jedna *superčestica* ili *superpartner*. Superpartneri fermiona materije su čestice spina nula, nazvani *sfermioni*. Oni se dalje mogu klasificirati u skalarne leptone ili *sleptone* i skalarne kvarkove ili *skvarkove*. Fermioni materije i njihovi superpartneri opisani su *kiralnim superpoljima*. Superparneri baždarnih bozona SM-a čestice su spina $1/2$ i zovemo ih *gejdžini* (engl. *gauginos*). Oni se dalje mogu klasificirati u jako interagirajući *gluino* i elektroslabe interagirajući *zino* i *vino* (engl. *wino*) (superpartneri Z odnosno W bozona). Zajedno sa baždarnim bozonima SM-a, oni su opisani *vektorskim superpoljima*. Superpartneri Higgsovih bozona čestice su spina $1/2$ nazvani *higgsini* i skupa s njima opisani su kiralnim superpoljima. Lom elektroslabe simetrije mijesha elektroslabe gejdžine sa higgsinima, što rezultira fizikalnim česticama koje nazivamo *čardžini* (engl. *charginos*) i *neutralini*. Donja tablica prikazuje sadržaj čestica i polja MSSM-a, zajedno sa pripadajućim kvantnim brojevima.

Sadržaj čestica MSSM-a							
Superpolje	Bozoni		Fermioni		$SU_c(3)$	$SU_L(2)$	$U_Y(1)$
baždarno							
G^a	gluon	g^a	gluino	\tilde{g}^a	8	0	0
V^k	slabi	$W^k (W^\pm, Z)$	vino, zino	$\tilde{w}^k (\tilde{w}^\pm, \tilde{z})$	1	3	0
V'	hipernabojni	$B (\gamma)$	bino	$\tilde{b} (\tilde{\gamma})$	1	1	0
materije							
L_i	sleptoni	$\tilde{L}_i = (\tilde{\nu}, \tilde{e})_L$	leptoni	$L_i = (\nu, e)_L$	1	2	-1
E_i		$\tilde{E}_i = \tilde{e}_R$		$E_i = e_R$	1	1	2
Q_i		$\tilde{Q}_i = (\tilde{u}, \tilde{d})_L$		$Q_i = (u, d)_L$	3	2	1/3
U_i	skvarkovi	$\tilde{U}_i = \tilde{u}_R$	kvarkovi	$U_i = u_R^c$	3*	1	-4/3
D_i		$\tilde{D}_i = \tilde{d}_R$		$D_i = d_R^c$	3*	1	2/3
Higgs							
H₁	Higgsovi	H_1		\tilde{H}_1	1	2	-1
H₂		H_2	higgsini	\tilde{H}_2	1	2	1

Kao što se vidi iz tablice, u MSSM-u postoje dva Higgsova superpolja, koja se mogu napisati kao

$$H_1 = \begin{pmatrix} H_1^1 \\ H_1^2 \end{pmatrix}, \quad H_2 = \begin{pmatrix} H_2^1 \\ H_2^2 \end{pmatrix}. \quad (7)$$

Polje H_1 ponekad se naziva donje Higgsovo superpolje ($Y = -1$), a sastoji se od polja h_1 and \tilde{h}_{1L} . Polje H_2 također se naziva gornje Higgsovo superpolje, a sastoji se od polja h_2 and \tilde{h}_{2L} . Komponentna polja označena malim tiskanim slovima mogu se dalje napisati kao

$$h_1 \equiv \begin{pmatrix} h_1^1 \\ h_1^2 \end{pmatrix} = \begin{pmatrix} h_1^0 \\ h_1^- \end{pmatrix}; \quad h_2 \equiv \begin{pmatrix} h_2^1 \\ h_2^2 \end{pmatrix} = \begin{pmatrix} h_2^+ \\ h_2^0 \end{pmatrix}, \quad (8)$$

$$\tilde{h}_{1L} \equiv \begin{pmatrix} \tilde{h}_1^1 \\ \tilde{h}_1^2 \end{pmatrix} = \begin{pmatrix} \tilde{h}_1^0 \\ \tilde{h}_1^- \end{pmatrix}_L; \quad \tilde{h}_{2L} \equiv \begin{pmatrix} \tilde{h}_2^1 \\ \tilde{h}_2^2 \end{pmatrix} = \begin{pmatrix} \tilde{h}_2^+ \\ \tilde{h}_2^0 \end{pmatrix}_L. \quad (9)$$

Nakon spontanog loma elektroslabe simetrije, vakuumске očekivane vrijednosti dane su realnim i pozitivnim vrijednostima v_1 i v_2 ,

$$\langle h_1 \rangle = \frac{1}{\sqrt{2}} \begin{pmatrix} v_1 \\ 0 \end{pmatrix}; \quad \langle h_2 \rangle = \frac{1}{\sqrt{2}} \begin{pmatrix} 0 \\ v_2 \end{pmatrix}, \quad (10)$$

koji dolaze od minimalizacije Higgsovog potencijala. Omjer ovih vrijednosti,

$$\frac{v_2}{v_1} \equiv \tan \beta, \quad (11)$$

smatra se slobodnim parametrom teorije, barem što se tiče fermionskih masa.

Lagranđian MSSM-a može se napisati kao zbroj dvaju dijelova: prvi koji dolazi od egzaktne supersimetrisacije standardnog modela, i drugi koji eksplikite lomi supersimetriju,

$$\mathcal{L}_{\text{MSSM}} = \mathcal{L}_{\text{SUSY}} + \mathcal{L}_{\text{SSB}}. \quad (12)$$

Prvi član možemo dalje pisati po komponentama,

$$\mathcal{L}_{\text{SUSY}} = \mathcal{L}_g + \mathcal{L}_M + \mathcal{L}_H, \quad (13)$$

gdje su \mathcal{L}_g , \mathcal{L}_M i \mathcal{L}_H lagranžijani koji sadrže baždarna polja, polja materije te Higgsova polja. Detaljan prikaz ovih komponenti može se naći u literaturi [68, str. 171-172]. U kontekstu ove disertacije najviše će nas zanimati tzv. *superpotencijal*, koji čini važan dio lagranžijana \mathcal{L}_H i glasi

$$\mathcal{W}_{\text{MSSM}} = \mu H_1 \cdot H_2 + \bar{E}_i \mathbf{h}_{ij}^e H_1 \cdot L_j + \bar{D}_i \mathbf{h}_{ij}^d H_1 \cdot Q_j + \bar{U}_i \mathbf{h}_{ij}^u H_2 \cdot Q_j. \quad (14)$$

Matrice \mathbf{h} dane su sa

$$\mathbf{h}_{ij}^{e\dagger} = \frac{g_2}{\sqrt{2}M_W \cos \beta} (\mathbf{m}_e)_{ij}, \quad (15)$$

$$\mathbf{h}_{ij}^{d\dagger} = \frac{g_2}{\sqrt{2}M_W \cos \beta} (\mathbf{m}_d)_{ij}, \quad (16)$$

$$\mathbf{h}_{ij}^{u\dagger} = \frac{g_2}{\sqrt{2}M_W \cos \beta} (\mathbf{m}_u)_{ij}. \quad (17)$$

Matrice \mathbf{m}_e , \mathbf{m}_d i \mathbf{m}_u su dimenzije 3×3 , a predstavljaju leptonsku masenu matricu, te masene matrice donjih odnosno gornjih kvarkova. Skalarni proizvodi definirani su u dvokomponentnoj notaciji [72, 74] kao $A \cdot B \equiv \epsilon_{\alpha\beta} A^\alpha B^\beta$ ($\epsilon_{12} \equiv +1$). Drugi, treći i četvrti član na desnoj strani izraza za superpotencijal samo su supersimetrično popoćenje Yukawinih vezanja u lagranžijanu standardnog modela [75]. Prvi član međutim predstavlja novost te o njemu možemo razmišljati kao o supersimetričnom poopćenju masenih članova Higgsovog polja. Može se pokazati da konzistentno provođenje loma elektroslabe simetrije zahtjeva da parametar μ bude reda veličine mase W bozona.

Ovdje je još potrebno reći da je u cijelom ovom razmatranju implicitno pretpostavljeno sačuvanje R -pariteta, definiranog kvantnim brojem R_p ,

$$R_p = (-1)^{3(B-L)+2S}, \quad (18)$$

pri čemu su B , L i S barionski i leptonski broj, odnosno spin dane čestice. Sačuvanje ovog kvantnog broja u MSSM-u može se smatrati prirodnom pretpostavkom u minimalnom supersimetričnom proširenju standardnog modela, s obzirom na činjenicu da su barionski i leptonski broj sačuvani u lagranžijanu SM-a.

Pogledajmo sada sadržaj drugog dijela lagranžijana MSSM-a, onog koji eksplicitno lomi supersimetriju (\mathcal{L}_{SSB}). Koristeći Symanzikovo pravilo [76, str. 107-8], može se pokazati da, ukoliko želimo zadržati poželjno konvergentno ponašanje supersimetrične teorije, članovi u \mathcal{L}_{SSB} moraju biti *mekani* [77–80], što znači da operatori polja u tom lagranžijanu moraju biti dimenzije strogo manje od četiri. Osim toga, očekujemo da ti članovi budu mali u odnosu na članove u \mathcal{L}_{SUSY} .

Kada to uzmemo u obzir, možemo pisati [68, str. 185]

$$\begin{aligned}
-\mathcal{L}_{SOFT} = & \tilde{q}_{iL}^*(\mathcal{M}_{\tilde{q}}^2)_{ij}\tilde{q}_{jL} + \tilde{u}_{iR}^*(\mathcal{M}_{\tilde{u}}^2)_{ij}\tilde{u}_{jR} + \tilde{d}_{iR}^*(\mathcal{M}_{\tilde{d}}^2)_{ij}\tilde{d}_{jR} \\
& + \tilde{l}_{iL}^*(\mathcal{M}_{\tilde{l}}^2)_{ij}\tilde{l}_{jL} + \tilde{e}_{iR}^*(\mathcal{M}_{\tilde{e}}^2)_{ij}\tilde{e}_{jR} \\
& + \left[h_1 \cdot \tilde{l}_{iL}(A^e)_{ij}^T \tilde{e}_{jR}^* + h_1 \cdot \tilde{q}_{iL}(A^d)_{ij}^T \tilde{d}_{jR}^* \right. \\
& \quad \left. + \tilde{q}_{iL} \cdot h_2(A^u)_{ij}^T \tilde{u}_{jR}^* + \text{h.c.} \right] \\
& + m_1^2|h_1|^2 + m_2^2|h_2|^2 + (B\mu h_1 \cdot h_2 + \text{h.c.}) \\
& + \frac{1}{2}(M_1\bar{\tilde{\lambda}}_0P_L\tilde{\lambda}_0 + M_1^*\bar{\tilde{\lambda}}_0P_R\tilde{\lambda}_0) \\
& + \frac{1}{2}(M_2\bar{\tilde{\lambda}}_0P_L\tilde{\lambda}_0 + M_2^*\bar{\tilde{\lambda}}_0P_R\tilde{\lambda}_0) \\
& + \frac{1}{2}(M_3\bar{\tilde{g}}^aP_L\tilde{g}^a + M_3^*\bar{\tilde{g}}^aP_R\tilde{g}^a)
\end{aligned} \tag{19}$$

Praktični izračuni unutar MSSM-a obično uključuju nekoliko pojednostavljujućih pretpostavki, kako bi se smanji veliki broj parametara koje smo morali dodati u teoriju. Takve pretpostavke rezultiraju različitim inačicama ograničenog minimalnog supersimetričnog standardnog modela ili CMSSM-a.

U ovoj disertaciji usvojiti ćemo jednu takovu inačicu, tzv. minimalni supergravitacijski model, skraćeno mSUGRA. Budući da polja MSSM-a ne mogu sama spontano slomiti supersimetriju na skalama karakteriziranim masom

W bozona, spontani lom supersimetrije mora se odviti u sektoru polja koji su singleti u odnosu na baždarnu grupu standardnog modela. Jedan od najekonomičnijih mehanizama ove vrste koristi gravitacijsku interakciju koja se temelji na lokalnoj supersimetriji poznatoj kao *supergravitacija* [70, 81].

Velika korist od ovog modela sastoji se u tome da dodatnih 105 parametara uspjeva svesti na samo pet parametara,

$$\{p\} = \{\text{sign}(\mu), m_0, M_{1/2}, A_0, \tan \beta\}. \quad (20)$$

Ovdje $\text{sign}(\mu)$ označava predznak parametra μ koji se nalazi u superpotencijalu, m_0 označava mase skalara ($m_{ij} = m_0 \delta_{ij}$), $M_{1/2}$ zajedničku masu svih MSSM gejdžina, A_0 zajedničku konstantu trilinearnog vezanja (higgs-sfermion-sfermion), a $\tan \beta$ omjer vakuumskih očekivanih vrijednosti kojeg smo definirali ranije. Ove parametre nazivamo *parametrima loma supersimetrije*. Njihove vrijednosti obično se postavljaju na skali velikog ujedinjenja (GUT), te se putem renormalizacijskih grupnih jednadžbi [69] prenose do skale karakterizirane masom W bozona.

Recimo i to da postoji više teorijskih motivacija za rad unutar MSSM-a. MSSM nudi stabilno kvantnomehaničko rješenje problema hijerarhije u baždarnom sektoru i daje prilično preciznu predikciju ujedinjenja baždarnih vezanja SM-a na skali bliskoj GUT skali. Najlakša supersimetrična čestica je stabilna i, ako bi bila neutralna poput neutralina, može predstavljati dobrog kandidata za konstituenta tamne tvari u svemiru. Osim toga, MSSM tipično predviđa da je masa standardnomodelskog Higgsa manja od 135 GeV, što je u skladu s nedavnim opažanjima od strane kolaboracija ATLAS [82] i CMS [83, 84].

U minimalnom supersimetričnom standardnom modelu sa sadržajem polja kakav je dan u gornjoj tablici ne dolazi do narušenja leptonskog okusa u nabijenom leptonskom sektoru (CLFV). To je posljedica odsustva desnih neutrina, što rezultira trivijalnom okusnom strukturu. Jedan od načina da unutar MSSM-a omogućimo procese koji uključuju CLFV jest da navedeni čestični spektar proširimo s desnim neutrinima čija je masa reda veličine

1 TeV. Takav model označit ćemo sa ν_R MSSM.

Proširenje čestičnog spektra vrši se putem mehanizma njihalice (engl. *seesaw mechanism*) na niskoj skali. Za razliku od uobičajenog mehanizma njihalice u kojem teški neutrinski singleti poprimaju mase $m_N \sim 10^{12-14}$ GeV, mehanizam njihalice na niskoj skali omogućava da desni neutrini imaju znatno niže mase, već od 100 GeV. Dok je u običajenom mehanizmu njihalice vezanje između teških i lakih neutrina reda veličine $\xi_{\nu N} \sim \sqrt{m_\nu/m_N} \sim 10^{-12}$ (za $m_\nu \sim 10^{-1}$ GeV), u mehanizmu njihalice na niskoj skali $\xi_{\nu N}$ postaje slobodan parametar. Sve te pogodnosti omogućavaju nam da masu desnih neutrina postavimo na skalu eksperimentalne dohvatljivosti, kao i da povećamo učinak CLFV-a uslijed nezanemarive jakosti vezanja lakih i teških neutrina.

Realizacija mehanizma njihalice na niskoj skali postiže se uvođenjem dodatnih leptonskih simetrija [99–105] u teoriju koje razultiraju time da laki neutrini postaju bezmaseni, dok teški neutrini mogu biti na skali ~ 1 TeV. Ukoliko bismo željeli reproducirati niskoenergetski maseni spektar lakih neutrina, te simetrije se mogu blago narušiti pa u tom slučaju govorimo o *aproksimativnim leptonskim simetrijama*.

Ovakav model može biti zanimljiv iz više razloga. Novo uvedeni singletni neutrini mogu biti kandidati za hladnu tamnu tvar [120–124]. Uz to, mehanizam rezonantne leptogeneze na niskoj skali [125–129] može ponuditi objašnjenje za opaženu barionsku asimetriju u svemiru, što je posebno aktualno u svjetlu činjenice da se parametarski prostor za elektroslabu bariogenezu svakoga dana sve više sužava novim podacima koji pristižu sa LHC-a [130, 131].

Leptonski dio superpotencijala u ν_R MSSM-u glasi

$$W_{\text{lepton}} = \widehat{E}^C \mathbf{h}_e \widehat{H}_d \widehat{L} + \widehat{N}^C \mathbf{h}_\nu \widehat{L} \widehat{H}_u + \frac{1}{2} \widehat{N}^C \mathbf{m}_M \widehat{N}^C, \quad (21)$$

gdje $\widehat{H}_{u,d}$, \widehat{L} , \widehat{E} i \widehat{N}^C označavaju dva superpolja Higgsovih dubleta, tri nabijena leptonska superpolja lijeve i desne kiralnosti te tri neutrinska superpolja desne kiralnosti, redom. Yukawina vezanja $\mathbf{h}_{e,\nu}$ i Majoranini maseni parametri \mathbf{m}_M čine kompleksnu 3×3 matricu. Za matricu \mathbf{m}_M uzeli smo da na skali m_N bude simetrična s obzirom na okusnu grupu SO(3),

tj. $\mathbf{m}_M = m_N \mathbf{1}_3$.

U ovoj disertaciji posebno ćemo razmatrati dva scenarija neutrinskih Yukawinih vezanja. Prvi realizira U(1) leptonsku simetriju [125–127] i dan je sa

$$\mathbf{h}_\nu = \begin{pmatrix} 0 & 0 & 0 \\ a e^{-\frac{i\pi}{4}} & b e^{-\frac{i\pi}{4}} & c e^{-\frac{i\pi}{4}} \\ a e^{\frac{i\pi}{4}} & b e^{\frac{i\pi}{4}} & c e^{\frac{i\pi}{4}} \end{pmatrix}. \quad (22)$$

U drugom scenariju, struktura neutrinske Yukawine matrice \mathbf{h}_ν motivirana je diskretnom grupom simetrija A_4 i poprima sljedeći oblik [137]:

$$\mathbf{h}_\nu = \begin{pmatrix} a & b & c \\ a e^{-\frac{2\pi i}{3}} & b e^{-\frac{2\pi i}{3}} & c e^{-\frac{2\pi i}{3}} \\ a e^{\frac{2\pi i}{3}} & b e^{\frac{2\pi i}{3}} & c e^{\frac{2\pi i}{3}} \end{pmatrix}. \quad (23)$$

U ovim izrazima pretpostavljamo da su Yukawini parametri a , b i c realni. Opervable koje uključuju CLFV ne ovise o niskoenergetskom masenom spektru lakih neutrina, pa ćemo iz praktičnih razloga uzeti da su mase lakih neutrina jednake nuli, tj. da su leptonske simetrije egzaktno realizirane.

Prema tome, u ν_R MSSM-u postoje tri relevantna doprinosa narušenju leptonskog okusa u nabijenom sektoru. Jedan dolazi od teških neutrina (N), drugi od sneutrina (\tilde{N}), a treći od sektora koji mekano lomi supersimetriju (SB). Svaki od tih doprinosa bit će zasebno analiziran.

CLFV opservable

Na razini jedne petlje, efektivna $\gamma l'l$ i $Z l'l$ vezanja generirana su Feynmanovim dijagramima prikazanim na slici 3.1 (str. 27). Opći oblici amplituda prijelaza povezan s ovim efektivnim vezanjima dani su sa

$$\mathcal{T}_\mu^{\gamma l'l} = \frac{e \alpha_w}{8\pi M_W^2} \bar{l}' \left[(F_\gamma^L)_{l'l} (q^2 \gamma_\mu - \not{q} q_\mu) P_L + (F_\gamma^R)_{l'l} (q^2 \gamma_\mu - \not{q} q_\mu) P_R \right]$$

$$+ (G_\gamma^L)_{l'l} i\sigma_{\mu\nu} q^\nu P_L + (G_\gamma^R)_{l'l} i\sigma_{\mu\nu} q^\nu P_R \Big] l, \quad (24)$$

$$\mathcal{T}_\mu^{Zl'l} = \frac{g_w \alpha_w}{8\pi \cos \theta_w} \bar{l}' \left[(F_Z^L)_{l'l} \gamma_\mu P_L + (F_Z^R)_{l'l} \gamma_\mu P_R \right] l, \quad (25)$$

gdje je $P_{L(R)} = \frac{1}{2} [1 - (+)\gamma_5]$, $\alpha_w = g_w^2/(4\pi)$, e je elektromagnetska konstanta vezanja, $M_W = g_w \sqrt{v_u^2 + v_d^2}/2$ masa W bozona, θ_w slabi kut vezanja, a $q = p_{l'} - p_l$ impuls fotona. Form-faktori $(F_\gamma^L)_{l'l}$, $(F_\gamma^R)_{l'l}$, $(G_\gamma^L)_{l'l}$, $(G_\gamma^R)_{l'l}$, $(F_Z^L)_{l'l}$ i $(F_Z^R)_{l'l}$ dobijaju doprinose od teških neutrina $N_{1,2,3}$, teških sneutrina $\tilde{N}_{1,2,3}$ i članova koji mekano lome supersimetriju induciranih putem renormalizacijskih grupnih jednadžbi (RGE). Analitički izrazi za svaki od ovih doprinosa mogu se naći u Dodatku C.

Iz amplitude možemo izračunati i pripadajuće omjere grananja,

$$B(l \rightarrow l'\gamma) = \frac{\alpha_w^3 s_w^2}{256\pi^2} \frac{m_l^3}{M_W^4 \Gamma_l} \left(|(G_\gamma^L)_{l'l}|^2 + |(G_\gamma^R)_{l'l}|^2 \right), \quad (26)$$

$$B(Z \rightarrow l'l^C + l'^C l) = \frac{\alpha_w^3 M_W}{768\pi^2 c_w^3 \Gamma_Z} \left(|(F_Z^L)_{l'l}|^2 + |(F_Z^R)_{l'l}|^2 \right). \quad (27)$$

Svi ovi izrazi napisani su u aproksimaciji razvoja do vodećeg reda u vanjskim masama i impulsima, kao i prepostavci da je masa Z bozona M_Z znatno ispod supersimetrične skale M_{SUSY} i mase teškog neutrina m_N .

U idućem koraku prelazimo na tročestične CLFV raspade $l \rightarrow l'l_1 l_2^C$, pri čemu l može biti mion ili tau-lepton, a l' , l_1 , l_2 označavaju drugi nabijeni lepton u kojeg se lepton l može raspasti s obzirom na kinematiku.

Prijelazna amplituda za $l \rightarrow l'l_1 l_2^C$ sadrži doprinose od fotonskih i Z -bozonskih dijagrama prikazanih na slici 3.1 (str. 27), ali i od pravokutnih dijagrama prikazanih na slici 3.2 (str. 29). Amplitude za ova tri doprinosa glase:

$$\begin{aligned} \mathcal{T}_\gamma^{ll'l_1 l_2} &= \frac{\alpha_w^2 s_w^2}{2M_W^2} \left\{ \delta_{l_1 l_2} \bar{l}' \left[(F_\gamma^L)_{l'l} \gamma_\mu P_L + (F_\gamma^R)_{l'l} \gamma_\mu P_R + \frac{(\not{p} - \not{p}')}{(p - p')^2} \right. \right. \\ &\quad \cdot \left. \left. \left((G_\gamma^L)_{l'l} \gamma_\mu P_L + (G_\gamma^R)_{l'l} \gamma_\mu P_R \right) \right] l \bar{l}_1 \gamma^\mu l_2^C - [l' \leftrightarrow l_1] \right\}, \quad (28) \end{aligned}$$

$$\mathcal{T}_Z^{ll'l_1 l_2} = \frac{\alpha_w^2}{2M_W^2} \left[\delta_{l_1 l_2} \bar{l}' \left((F_Z^L)_{l'l} \gamma_\mu P_L + (F_Z^R)_{l'l} \gamma_\mu P_R \right) l \right.$$

$$\cdot \bar{l}_1 \left(g_L^l \gamma^\mu P_L + g_R^l \gamma^\mu P_R \right) l_2^C - (l' \leftrightarrow l_1) \right], \quad (29)$$

$$\begin{aligned} \mathcal{T}_{\text{box}}^{ll'l_1l_2} = & -\frac{\alpha_w^2}{4M_W^2} \left(B_{\ell V}^{LL} \bar{l}' \gamma_\mu P_{Ll} \bar{l}_1 \gamma^\mu P_{Ll_2^C} + B_{\ell V}^{RR} \bar{l}' \gamma_\mu P_{Rl} \bar{l}_1 \gamma^\mu P_{Rl_2^C} \right. \\ & + B_{\ell V}^{LR} \bar{l}' \gamma_\mu P_{Ll} \bar{l}_1 \gamma^\mu P_{Rl_2^C} + B_{\ell V}^{RL} \bar{l}' \gamma_\mu P_{Rl} \bar{l}_1 \gamma^\mu P_{Ll_2^C} \\ & + B_{\ell S}^{LL} \bar{l}' P_{Ll} \bar{l}_1 P_{Ll_2^C} + B_{\ell S}^{RR} \bar{l}' P_{Rl} \bar{l}_1 P_{Rl_2^C} \\ & + B_{\ell S}^{LR} \bar{l}' P_{Ll} \bar{l}_1 P_{Rl_2^C} + B_{\ell S}^{RL} \bar{l}' P_{Rl} \bar{l}_1 P_{Ll_2^C} \\ & \left. + B_{\ell T}^{LL} \bar{l}' \sigma_{\mu\nu} P_{Ll} \bar{l}_1 \sigma^{\mu\nu} P_{Ll_2^C} + B_{\ell T}^{RR} \bar{l}' \sigma_{\mu\nu} P_{Rl} \bar{l}_1 \sigma^{\mu\nu} P_{Rl_2^C} \right). \quad (30) \end{aligned}$$

U gornjim izrazima, $g_L^l = -1/2 + s_w^2$ i $g_R^l = s_w^2$ su Z -bozonska leptonska vezanja, a $s_w = \sin \theta_w$. Kompozitni form-faktori pravokutnih dijagrama $B_{\ell A}^{XY}$ dani su u Dodatku C. Oznake V , S i T označavaju form-faktore vektorskih, skalarnih i tenzorskih kombinacija struja, dok L i R razlikuju lijeve i desne kiralnosti tih struja. Form-faktori iz pravokutnih dijagrama sadrže izravne i Fiertz-transformirane doprinose, što se može vidjeti u Dodatku D.

S obzirom na tri leptonske generacije, prijelazna amplituda za raspad $l \rightarrow l'l_1l_2^C$ može upasti u jednu od tri klase ili kategorije [110]: (i) $l' \neq l_1 = l_2$, (ii) $l' = l_1 = l_2$, (iii) $l' = l_1 \neq l_2$. Za prve dvije klase, ukupni leptonski broj je sačuvan, dok je u trećoj klasi ukupni leptonski broj na razini struja narušen za dvije jedinice. Budući da se za predikcije za opservable iz klase (iii) ispostavlja da su neopazivo malene u ν_R MSSM-u, ove procese ćemo ignorirati. Omjeri grananja za klase (i) i (ii) glase:

$$\begin{aligned} B(l \rightarrow l'l_1l_2^C) = & \frac{m_l^5 \alpha_w^4}{24576 \pi^3 M_W^4 \Gamma_l} \left\{ \left[\left| 2s_w^2 (F_\gamma^L + F_Z^L) - F_Z^L - B_{\ell V}^{LL} \right|^2 \right. \right. \\ & + \left| 2s_w^2 (F_\gamma^R + F_Z^R) - B_{\ell V}^{RR} \right|^2 + \left| 2s_w^2 (F_\gamma^L + F_Z^L) - B_{\ell V}^{LR} \right|^2 \\ & + \left. \left. \left| 2s_w^2 (F_\gamma^R + F_Z^R) - F_Z^R - B_{\ell V}^{RL} \right|^2 \right] \right. \\ & + \frac{1}{4} \left(|B_{\ell S}^{LL}|^2 + |B_{\ell S}^{RR}|^2 + |B_{\ell S}^{LR}|^2 + |B_{\ell S}^{RL}|^2 \right) \\ & + 12 \left(|B_{\ell T}^{LL}|^2 + |B_{\ell T}^{RR}|^2 \right) \\ & \left. + \frac{32 s_w^4}{m_l} \left[\text{Re} \left((F_\gamma^R + F_Z^R) G_\gamma^{L*} \right) + \text{Re} \left((F_\gamma^L + F_Z^L) G_\gamma^{R*} \right) \right] \right\} \end{aligned}$$

$$\begin{aligned}
& - \frac{8s_w^2}{m_l} \left[\text{Re} \left((F_Z^R + B_{\ell V}^{RR} + B_{\ell V}^{RL}) G_\gamma^{L*} \right) \right. \\
& + \text{Re} \left((F_Z^L + B_{\ell V}^{LL} + B_{\ell V}^{LR}) G_\gamma^{R*} \right) \left. \right] \\
& - \frac{32s_w^4}{m_l^2} \left(|G_\gamma^L|^2 + |G_\gamma^R|^2 \right) \left(\ln \frac{m_l^2}{m_{l'}^2} - 3 \right) \Bigg\}, \tag{31}
\end{aligned}$$

$$\begin{aligned}
B(l \rightarrow l' l' l'^C) = & \frac{m_l^5 \alpha_w^4}{24576 \pi^3 M_W^4 \Gamma_l} \left\{ 2 \left[\left| 2s_w^2 (F_\gamma^L + F_Z^L) - F_Z^L - \frac{1}{2} B_{\ell V}^{LL} \right|^2 \right. \right. \\
& + \left| 2s_w^2 (F_\gamma^R + F_Z^R) - \frac{1}{2} B_{\ell V}^{RR} \right|^2 \left. \right] + \left| 2s_w^2 (F_\gamma^L + F_Z^L) - B_{\ell V}^{LR} \right|^2 \\
& + \left| 2s_w^2 (F_\gamma^R + F_Z^R) - (F_Z^R + B_{\ell V}^{RL}) \right|^2 + \frac{1}{8} \left(|B_{\ell S}^{LL}|^2 + |B_{\ell S}^{RR}|^2 \right) \\
& + 6 \left(|B_{\ell T}^{LL}|^2 + |B_{\ell T}^{RR}|^2 \right) \\
& + \frac{48s_w^4}{m_l} \left[\text{Re} \left((F_\gamma^R + F_Z^R) G_\gamma^{L*} \right) + \text{Re} \left((F_\gamma^L + F_Z^L) G_\gamma^{R*} \right) \right] \\
& - \frac{8s_w^2}{m_l} \left[\text{Re} \left((F_Z^R + B_{\ell V}^{RR} + B_{\ell V}^{RL}) G_\gamma^{L*} \right) \right. \\
& + \text{Re} \left((2F_Z^L + B_{\ell V}^{LL} + B_{\ell V}^{LR}) G_\gamma^{R*} \right) \left. \right] \\
& + \frac{32s_w^4}{m_l^2} \left(|G_\gamma^L|^2 + |G_\gamma^R|^2 \right) \left(\ln \frac{m_l^2}{m_{l'}^2} - \frac{11}{4} \right) \Bigg\}, \tag{32}
\end{aligned}$$

gdje smo radi jednostavnosti izostavili univerzalne indekse $l'l$ koji se pojavljuju u fotonskim i Z -bozonskim form-faktorima. U gornjim izrazima, $m_{l'}$, m_{l_1} i m_{l_2} predstavljaju mase ulaznih i izlaznih nabijenih leptona, a Γ_l ukupnu širinu raspada nabijenog leptona l .

Prijelaz $\mu \rightarrow e$ na atomskim jezgrama odgovara procesu $J_\mu \rightarrow e^- J^+$, pri čemu je J_μ atom jezgre J u kojem je jedan orbitalni elektron zamjenjen mionom, a J^+ odgovarajući ion bez miona. Prijelazna amplituda za ovaj proces,

$$\mathcal{T}^{\mu e; J} = \langle J^+ e^- | \mathcal{T}^{d\mu \rightarrow de} | J_\mu \rangle + \langle J^+ e^- | \mathcal{T}^{u\mu \rightarrow ue} | J_\mu \rangle, \tag{33}$$

ovisi o dva efektivna operatora pravokutnih dijagrama:

$$\mathcal{T}_{\text{box}}^{d\mu \rightarrow de} = -\frac{\alpha_w^2}{2M_W^2} (d^\dagger d) \bar{e} (V_d^R P_R + V_d^L P_L) \mu , \quad (34)$$

$$\mathcal{T}_{\text{box}}^{u\mu \rightarrow ue} = -\frac{\alpha_w^2}{2M_W^2} (u^\dagger u) \bar{e} (V_u^R P_R + V_u^L P_L) \mu . \quad (35)$$

U gornjem izrazu, μ i e predstavljaju mionsku i elektronsku valnu funkciju, a d i u su operatori polja koji djeluju na J_μ odnosno J^+ stanja. Kompozitni form-faktori V_d^L , V_u^L , V_d^R i V_u^R mogu se napisati kao

$$\begin{aligned} V_d^L &= -\frac{1}{3}s_w^2 \left(F_\gamma^L - \frac{1}{m_\mu} G_\gamma^R \right) + \left(\frac{1}{4} - \frac{1}{3}s_w^2 \right) F_Z^L \\ &\quad + \frac{1}{4} \left(B_{dV}^{LL} + B_{dV}^{LR} + B_{dS}^{RR} + B_{dS}^{RL} \right), \end{aligned} \quad (36)$$

$$\begin{aligned} V_d^R &= -\frac{1}{3}s_w^2 \left(F_\gamma^R - \frac{1}{m_\mu} G_\gamma^L \right) + \left(\frac{1}{4} - \frac{1}{3}s_w^2 \right) F_Z^R \\ &\quad + \frac{1}{4} \left(B_{dV}^{RR} + B_{dV}^{RL} + B_{dS}^{LL} + B_{dS}^{LR} \right), \end{aligned} \quad (37)$$

$$\begin{aligned} V_u^L &= \frac{2}{3}s_w^2 \left(F_\gamma^L - \frac{1}{m_\mu} G_\gamma^R \right) + \left(-\frac{1}{4} + \frac{2}{3}s_w^2 \right) F_Z^L \\ &\quad + \frac{1}{4} \left(B_{uV}^{LL} + B_{uV}^{LR} + B_{uS}^{RR} + B_{uS}^{RL} \right), \end{aligned} \quad (38)$$

$$\begin{aligned} V_u^R &= \frac{2}{3}s_w^2 \left(F_\gamma^R - \frac{1}{m_\mu} G_\gamma^L \right) + \left(-\frac{1}{4} + \frac{2}{3}s_w^2 \right) F_Z^R \\ &\quad + \frac{1}{4} \left(B_{uV}^{RR} + B_{uV}^{RL} + B_{uS}^{LL} + B_{uS}^{LR} \right). \end{aligned} \quad (39)$$

Nukeonski matrični elementi operatora $u^\dagger u$ i $d^\dagger d$ glase

$$\begin{aligned} \langle J^+ e^- | u^\dagger u | J_\mu \rangle &= (2Z + N) F(-m_\mu^2), \\ \langle J^+ e^- | d^\dagger d | J_\mu \rangle &= (Z + 2N) F(-m_\mu^2), \end{aligned} \quad (40)$$

pri čemu $F(q^2)$ označava odboj iona J^+ [142], a faktori $2Z + N$ i $Z + 2N$ broj u odnosno d kvarkova u jezgri J . Matrični element za $J_\mu \rightarrow J^+ \mu^-$ se

prema tome može napisati kao:

$$T^{J_\mu \rightarrow J^+ e^-} = -\frac{\alpha_w^2}{2M_W^2} F(-m_\mu^2) \bar{e} (Q_W^L P_R + Q_W^R P_L) \mu, \quad (41)$$

uz

$$\begin{aligned} Q_W^L &= (2Z + N)V_u^L + (Z + 2N)V_d^L, \\ Q_W^R &= (2Z + N)V_u^R + (Z + 2N)V_d^R. \end{aligned} \quad (42)$$

Koristeći gore navedene izraze, dolazimo do izraza za brzinu prijelaza $J_\mu \rightarrow J^+ e^-$

$$R_{\mu e}^J = \frac{\alpha^3 \alpha_w^4 m_\mu^5}{16\pi^2 M_W^4 \Gamma_{\text{capture}}} \frac{Z_{\text{eff}}^4}{Z} |F(-m_\mu^2)|^2 \left(|Q_W^L|^2 + |Q_W^R|^2 \right), \quad (43)$$

gdje je Γ_{capture} brzina uhvata miona od jezgre, a Z_{eff} efektivni naboј koji uzima u obzir koherentne učinke koji se javljaju u jezgri J uslijed njegove konačne dimenzije. Vrijednosti za Z_{eff} uzete su iz ref. [143].

Na osnovi gore izloženih analitičkih rezultata napravljena je numerička analiza. mSUGRA parametri odabrani su tako da zadovoljavaju ograničenja koja je postavio LHC: $m_H = 125.5 \pm 2$ GeV [82, 84, 147], $m_{\tilde{g}} > 1500$ GeV i $m_{\tilde{t}} > 500$ GeV [146, 147], gdje je m_H masa standardnomodelskog Higgsa, a $m_{\tilde{g}}$ i $m_{\tilde{t}}$ mase gluina odnosno stop kvarka:

$$\begin{aligned} \tan \beta &= 10, & m_0 &= 1000 \text{ GeV}, \\ A_0 &= -3000 \text{ GeV}, & M_{1/2} &= 1000 \text{ GeV}. \end{aligned} \quad (44)$$

Korištenjem renormalizacijske grupne jednadžbe danih u referencama [69, 153], radimo evoluciju baždarnih vezanja te Yukawinih matrica za kvarkove i nabijene leptone od skale M_Z do GUT skale, dok neutrinska masena matrica (\mathbf{m}_M) i Yukawina matrica (\mathbf{h}_ν) matrica evoluiraju od skale određene masom teškog neutrina m_N , do GUT skale.

Analiza je provedena u dva različita scenarija. Prvi realizira U(1) simetriju

(22) i za njega uzimamo jednu od tri opcije: (i) $a = b$ i $c = 0$ za $\mu \rightarrow eX$, (ii) $a = c$ i $b = 0$ za $\tau \rightarrow eX$, (iii) $b = c$ i $a = 0$ za $\tau \rightarrow \mu X$, pri čemu je $X = \gamma, e^+e^-, \mu^+\mu^-, q\bar{q}$. Drugi scenarij realizira simetriju grupe A_4 (23) i tu smo uzeli $a = b = c$.

Rezultati numeričke analize prikazani su na slikama 3.3 – 3.11 na str. 37–45.

Dipolni momenti leptona

S obzirom na trenutno stanje eksperimenata, može se vidjeti da anomalni magnetski moment (MDM) miona i električni dipolni moment (EDM) elektrona zavrijedaju posebnu pažnju. Zbog toga se učinilo uputnim unutar modela s kojim smo izučavali procese s narušenjem leptonskog okusa u nabijenom sektoru izvrijedniti i ove observable.

Anomalni magnetski dipolni moment i električni dipolni moment leptona l može se iščitati iz lagranžijana [159]:

$$\mathcal{L} = \bar{l} \left[\gamma_\mu (i\partial^\mu + eA^\mu) - m_l - \frac{e}{2m_l} \sigma^{\mu\nu} (F_l + iG_l \gamma_5) \partial_\nu A_\mu \right] l. \quad (45)$$

U području u kojem se fotonsko polje A^μ nalazi na ljusci mase, form-faktor F_l definira magnetski dipolni moment leptona l , t.j. $a_l \equiv F_l$, dok form-faktor G_l definira njegov električni dipolni moment, t.j. $d_l \equiv eG_l/m_l$. Iz prethodnog analitičkog izraza za fotonsku amplitudu možemo napisati opću form-faktorsku dekompoziciju prijelazne amplitude,

$$i\mathcal{T}^{\gamma ll} = i \frac{e\alpha_w}{8\pi M_W^2} \left[(G_\gamma^L)_{ll} i\sigma_{\mu\nu} q^\nu P_L + (G_\gamma^R)_{ll} i\sigma_{\mu\nu} q^\nu P_R \right]. \quad (46)$$

Tako dolazimo do izraza za anomalni MDM (a_l) i EDM (d_l) leptona l ,

$$a_l = \frac{\alpha_w m_l}{8\pi M_W^2} \left[(G_\gamma^L)_{ll} + (G_\gamma^R)_{ll} \right], \quad (47)$$

$$d_l = \frac{e\alpha_w}{8\pi M_W^2} i \left[(G_\gamma^L)_{ll} - (G_\gamma^R)_{ll} \right], \quad (48)$$

gdje notacija za vezanja i form-faktore odgovara onoj koju smo koristili i ranije.

Kao što je pokazano u ref. [160], EDM leptona d_l iščezava u u MSSM-u sa univerzalnim rubnim uvjetima mekanog loma supersimetrije bez dodatno uvedenih CP faza. Ovaj rezultat vrijedi i u proširenjima MSSM-a teškim neutrinima, dok god sneutrinski sektor čuva CP simetriju.

Kao minimalno odstupanje od ovog scenarija, prepostavimo da samo sneutrinski sektor narušava CP simetriju i to putem mekanih CP faza u bilinearnim i trilinearnim parametrima u lagranžijanu mekanog loma CP simetrije,

$$\mathbf{b}_\nu \equiv \mathbf{B}_\nu \mathbf{m}_M = B_0 e^{i\theta} m_N \mathbf{1}_3, \quad (49)$$

$$\mathbf{A}_\nu = \mathbf{h}_\nu A_0 e^{i\phi}. \quad (50)$$

pri čemu su B_0 i A_0 realni parametri određeni na GUT skali, m_N realni parametar unesen na skali m_N , θ i ϕ fizikalne CP faze, a \mathbf{h}_ν neutrinska Yukawina 3×3 matrica dana sa (23). Ovi parametri nalaze se u sljedećim članovima lagranžijiana koji mekano lomi supersimetriju:

$$-(\mathbf{A}_\nu)^{ij} \tilde{\nu}_{iR}^c (h_{uL}^+ \tilde{e}_{jL} - h_{uL}^0 \tilde{\nu}_{jL}), \quad (51)$$

$$(\mathbf{b}_\nu \mathbf{m}_M)_{ii} \tilde{\nu}_{Ri} \tilde{\nu}_{Ri}. \quad (52)$$

Radi jednostavnosti prepostavljamo da je matrica \mathbf{b}_ν proporcionalna sa jediničnom matricom $\mathbf{1}_3$. U uobičajenim SUSY scenarijima sa mehanizmom njihalice uz ultra-teške neutrine mase m_N , doprinosi CP narušenja u sneutrinskom sektoru električnom dipolnom momentu d_l ponašaju se kao B_0/m_N i A_0/m_N na razini jedne petlje. A kako su mase m_N u tim scenarijima velike (blizu GUT skale), doprinos EDM-u praktički je zanemariv. Uočljivi doprinosi EDM-u mogu se dakle očekivati u scenarijima sa mehanizmom njihalice na niskoj skali, u kojem masa m_N može biti usporediva sa B_0 i A_0 .

Bilinearnu mekanu matricu \mathbf{b}_ν zanemarili smo kada smo izučavali procese s

narušenjem leptonskog okusa u nabijenom sektoru. Tada smo prešutno pretpostavili da je taj parametar malen u odnosu na druge parametre mekanog loma supersimetrije. Ovdje ćemo ga ipak uzeti u obzir, ali tako da senutrinske mase uvijek ostanu pozitivne, dakle i fizikalne.

U MSSM-u, vodeći doprinos anomalnom magnetskom momentu letona a_l ima sljedeće ponašanje [161–163]:

$$a_l^{\text{MSSM}} \propto \frac{m_l^2}{M_{\text{SUSY}}^2} \tan \beta \text{ sign}(\mu M_{1,2}) , \quad (53)$$

pri čemu je M_{SUSY} tipična masena skala mekanog loma supersimetrije, $\tan \beta = v_2/v_1$ omjer očekivanih vakuumskih vrijednosti Higgsovih dubleta, a $M_{1,2}$ mase gejdžina povezanih sa $U(1)_Y$ odnosno $SU(2)$ baždarnom grupom. Kao što ćemo vidjeti, doprinos MSSM-a anomalnom magnetskom momentu miona ostaje dominantan i u ν_R MSSM-u.

Uspoređujući izraze za d_l i a_l , možemo dati naivnu procjenu ponašanja električnog dipolnog momenta letona l na razini jedne petlje,

$$d_l^{\text{MSSM}} \propto \sin(\phi_{\text{CP}}) \frac{m_l}{M_{\text{SUSY}}^2} \tan \beta , \quad (54)$$

gdje je ϕ_{CP} generička CP faza iz sektora koji mekano lomi supersimetriju. Iako su u MSSM-u moguće i drugačije ovisnosti d_l -a o $\tan \beta$ [160, 164], pokazat će se da je u okviru ν_R MSSM-a ova ovisnost uvijek linearna na razini jedne petlje.

Numerička analiza napravljena je u ovisnosti o mSUGRA parametrima, i to u okolini točke određene parametrima

$$\begin{aligned} m_0 &= 1 \text{ TeV}, & M_{1/2} &= 1 \text{ TeV}, & A_0 &= -4 \text{ TeV}, & \tan \beta &= 20, \\ m_N &= 1 \text{ TeV}, & B_0 &= 0.1 \text{ TeV}, & a &= b = c = 0.05, \end{aligned} \quad (55)$$

Kao i ranije, parametri su odbrani tako da zadovoljavaju eksperimentalna ograničenja koja je postavio LHC ($m_H = 125.5 \pm 2$ GeV, $m_{\tilde{g}} > 1500$ GeV, $m_{\tilde{t}} > 500$ GeV).

Rezultati numeričke analize prikazani su na slikama 4.1 (str. 56), 4.2 (str. 58) i 4.3 (str. 59).

Zaključak

Narušenje leptonskog okusa (CLFV) izučavano je u okviru minimalnog supersimetričnog standardnog modela (MSSM) proširenog sa singletnim teškim neutrinima na niskoj skali, pri čemu je posebna pažnja posvećena pojedinim doprinosima petlji koji dolaze od teških neutrina $N_{1,2,3}$, sneutrina $\tilde{N}_{1,2,\dots,12}$ i članova koji mekano lome supersimetriju. U ovoj analizi, po prvi put smo uključili potpuni skup pravokutnih dijagrama, uz dijagrame sa fotonskim i Z -bozonskim doprinosima. Također smo izveli potpun skup kiralnih amplituda i pridruženih im form-faktora koji su povezani sa CLFV raspadima miona i tau-leptona bez neutrina, kao što su $\mu \rightarrow eee$, $\tau \rightarrow \mu\mu\mu$, $\tau \rightarrow e\mu\mu$ i $\tau \rightarrow ee\mu$, te $\mu \rightarrow e$ prijelazima na atomskim jezgrama. Dobiveni analitički rezultati su općeniti i mogu se primijeniti na većinu modela nove fizike koji uključuju CLFV. U tom kontekstu valja naglasiti da je sustavna analiza ovih procesa pokazala postojanje dvaju novih form faktora iz pravokutnih dijagrama, koji se ne navode u postojećoj literaturi koja se bavi teorijama sa CLFV-om.

Ova detaljna studija pokazala je da efekti mekanog loma supersimetrije u dijagramima sa Z bozonom dominira u CLFV opservablama, i to u velikom dijelu ν_R MSSM parametarskog prostora u okviru mSUGRA scenarija. Ipak, postoji značajno područje parametarskog prostora (za neutrinske mase $m_N \lesssim 1$ TeV) u kojima pravokutni dijagrami koji uključuju teške neutrine u petlji mogu biti usporedivi, pa čak i veći, od odgovarajućih doprinosa iz dijagrama sa Z bozonom u procesima $\mu \rightarrow eee$ i $\mu \rightarrow e$ prijelazima na atomskim jezgrama (v. sliku 3.11 na str. 45). U istom kinematičkom režimu, uslijed slučajnih numeričkih poništenja, opažamo i potisnuće omjera grananja za fotonske CLFV raspade $\mu \rightarrow e\gamma$, kao i za raspade $\tau \rightarrow e\gamma$ i $\tau \rightarrow \mu\gamma$. Kao što je već rečeno, takva potisnuća u mehanizmu njihalice na niskoj skali dolaze kao posljedica poništenja između čestičnih i s-čestičnih doprinosa uslijed aproksimativne realizacije supersimetričnog *no-go* teorema kojeg su postavili Ferrara

i Remiddi [132]. U mehanizmu njihalice na visokoj skali ova se poništenja mogu pojaviti samo za određeni izbor neutrinskih Yukawinih matrica i Majoraninih masenih matrica, kao što je pokazano u ref. [119, 141]. Stoga možemo reći da rezultati koje smo dobili unutar supersimetričnog modela njihalice na niskoj skali (uz $m_N \lesssim 10$ TeV), podržavaju izvorni rezultat iznesen u ref. [111], gdje uobičajena paradigma po kojoj fotonski operatori dipolnog momenta dominiraju CLFV opservablama u modelima njihalice na visokoj skali [114–118] doživljava radikalnu promjenu. Iz toga možemo zaključiti da raspadi $\mu \rightarrow eee$ i $\mu \rightarrow e$ prijelazi na jezgrama također mogu služiti kao precizan test narušenja leptonskog okusa u nabijenom sektoru.

Otkrili smo da CLFV efekti inducirani od strane sneutrina, za razliku od onih induciranih teškim neutrinima, ostaju potisnuti u cijelom prostoru mSUGRA parametarskog prostora. Uz to, perturbacijsko ograničenje na neutrinska Yukawina vezanja \mathbf{h}_ν do GUT skale čini kvadrične doprinose reda $(\mathbf{h}_\nu)^4$ malima. Ova studija usmjerena je na davanje numeričkih predikcija za male i umjerene vrijednosti parametra $\tan\beta$ ($\tan\beta \lesssim 20$), pri čemu se očekuje da neutralne interakcije s Higgsovim bozonima ograničene nedavnim opažanjima raspada $B_s \rightarrow \mu\mu$ ne daju značajan doprinos ovakvim procesima. Globalna analiza koja bi uključivala velike $\tan\beta$ na CLFV opservablama uz LHC ograničenja jedan je od ciljeva budućih istraživanja.

Uz navedeno, disertacija sadrži sustavnu studiju doprinosa jedne petlje mionskom anomalnom magnetskom momentu (MDM) a_μ te električnom dipolnom momentu (EDM) d_e u okviru ν_R MSSM modela. Posebna pažnja dana je učinku sneutrninskih parametara koji mekano lome supersimetriju, \mathbf{B}_ν i \mathbf{A}_ν , kao i njihovim univerzalnim CP fazama, θ i ϕ . Koliko znamo, leptonski dipolni momenti u prijašnjoj literaturi nisu detaljno analizirani u okviru supersimetričnih modela sa singletnim (s)neutrinima na niskoj skali.

Za anomalni MDM miona a_μ pokazali smo da su doprinosi teških neutrinskih i sneutrninskih singleta MDM-u maleni, tipično jedan ili dva reda veličine ispod mionske anomalije Δa_μ . S druge strane, sneutrini i sleptoni lijeve kiralnosti daju najveći efekt na Δa_μ , točno kao i u MSSM-u. Ovisnost MDM-a o mionu m_μ , $\tan\beta$ i masenoj skali mekanog loma supersimetrije M_{SUSY} pažljivo

su analizirani i potvrđeno je njihovo ponašanje u skladu s jednadžbom (53). Konačno smo utvrdili i to da ovisnost a_μ o univerzalnom mekom trilinearnom parameteru A_0 te neutrinskim Yukawinim vezanjima \mathbf{h}_ν , i masi teškog neutrina m_N zanemariva.

Nadalje, u okviru istog ν_R MSSM modela napravljena je analiza EDM-a elektrona d_e . Teški singletni neutrini ne doprinose EDM-u, a članovi koji mekano lome supersimetriju iz sneutrinskog sektora doprinose samo ako su faze ϕ i/ili θ različiti od nule. Numerički je pokazano da je mogući doprinos narušenju iz CP simetrije koji bi dolazili od relativno kompleksnih produkata vrhova (v. jednadžbu (4.9) na str. 52) jednak nuli. S druge strane, doprinos koji dolazi od konačnih vrijednosti faze ϕ najveći je i može rezultirati vrijednostima za EDM koji su usporedivi s trenutno postavljenom eksperimentalnom gornjom granicom. Efekt CP faze θ na d_e je od prilike jedan do dva reda veličine manji nego onaj koji dolazi od faze ϕ . EDM elektrona d_e linearno raste sa $\tan \beta$ i masom leptona m_l , približno je neovisan o parametrima A_0 i B_0 , ali općenito pada sa mSUGRA parametrima m_0 i $M_{1/2}$.

Na temelju ovih numeričkih rezultata, izvedeni su približni poluanalitički izrazi, koji se razlikuju od onih iz postojeće literature o supersimetričnim modelima s mehanizmom njihalice na visokoj skali. Specifično, dodavanje CP faza vodi na ponašanje EDM-a tipa $d_l \propto m_l \tan \beta / m_N^y$, gdje je $2/3 < y < 1$. Dok je istina da d_e općenito pada sa M_{SUSY} , ova ovisnost ne može se opisati jednostavnim potencijskim padom. Ovisnost o mSUGRA parametrima A_0 i B_0 su slabe u najvećem dijelu parametarskog prostora. Linearna ovisnost o $\tan \beta$ kao i ovisnost o masi teškog neutrina predstavljaju nove rezultate koji proizlaze iz ove studije.

Za usporedbu, ovisnost o $\tan \beta$ navedena u ref. [160] je, ovisno o veličini, ili kubična ili konstantna. Uvezši u obzir trenutne eksperimentalne granice na d_e značajan dio ν_R MSSM parametarskog prostora identificiran je maksimalnom vrijednošću CP faze $\phi = \pi/2$, pri čemu EDM elektrona d_e može poprimiti vrijednosti usporedive sa trenutnom i budućom eksperimentalnom osjetljivošću. Učinak CP narušenja iz sneutrinskog sektora na električne dipolne momente neutriona i žive trebao bi biti potisnut, pa ovakav tip studije može služiti kao

razlikovni kriterij za ν_R MSSM scenarije koje smo razmatrali u ovoj disertaciji.

U svom kratkom osvrtu o budućnosti fizike elementarnih čestica [165], dobitnik Nobelove nagrade Sheldon Lee Glashow iznio je šest točaka koje on osobno smatra najvažnijim za budućnost teorijskog istraživanja u fizici visokih energija. Između ostalog, ove točke uključuju procese s narušenjem leptonskog okusa u nabijenom sektoru, anomalni magnetski dipolni moment miona $a_\mu = g_\mu - 2$, kao i električni dipolni moment elektrona d_e . Autor ove disertacije rado bi se s time složio.

Bibliography

- [1] Pontecorvo B 1957 Mesonium and anti-mesonium *Sov. Phys. JETP* **6** 429
- [2] Pontecorvo B 1958 Inverse beta processes and nonconservation of lepton charge *Sov. Phys. JETP* **7** 172–173
- [3] Maki Z, Nakagawa M and Sakata S 1962 Remarks on the unified model of elementary particles *Prog. Theor. Phys.* **28** 870–880
- [4] Cleveland B, Daily T, Davis Raymond J, Distel J R, Lande K *et al.* 1998 Measurement of the solar electron neutrino flux with the Homestake chlorine detector *Astrophys. J.* **496** 505–526
- [5] Fukuda Y *et al.* (Kamiokande Collaboration) 1996 Solar neutrino data covering solar cycle 22 *Phys. Rev. Lett.* **77** 1683–1686
- [6] Abdurashitov J *et al.* (SAGE Collaboration) 2009 Measurement of the solar neutrino capture rate with gallium metal. III: Results for the 2002–2007 data-taking period *Phys. Rev. C* **80** 015807 (*Preprint arXiv:0901.2200*)
- [7] Anselmann P *et al.* (GALLEX Collaboration) 1992 Solar neutrinos observed by GALLEX at Gran Sasso. *Phys. Lett. B* **285** 376–389
- [8] Hampel W *et al.* (GALLEX Collaboration) 1999 GALLEX solar neutrino observations: Results for GALLEX IV *Phys. Lett. B* **447** 127–133

- [9] Altmann M *et al.* (GNO COLLABORATION) 2005 Complete results for five years of GNO solar neutrino observations *Phys. Lett. B* **616** 174–190 (*Preprint arXiv:hep-ex/0504037*)
- [10] Fukuda S *et al.* (Super-Kamiokande Collaboration) 2002 Determination of solar neutrino oscillation parameters using 1496 days of Super-Kamiokande I data *Phys. Lett. B* **539** 179–187 (*Preprint arXiv:hep-ex/0205075*)
- [11] Ahmad Q *et al.* (SNO Collaboration) 2001 Measurement of the rate of $\nu_e + d \rightarrow p + p + e^-$ interactions produced by B-8 solar neutrinos at the Sudbury Neutrino Observatory *Phys. Rev. Lett.* **87** 071301 (*Preprint arXiv:nucl-ex/0106015*)
- [12] Ahmad Q *et al.* (SNO Collaboration) 2002 Direct evidence for neutrino flavor transformation from neutral current interactions in the Sudbury Neutrino Observatory *Phys. Rev. Lett.* **89** 011301 (*Preprint arXiv:nucl-ex/0204008*)
- [13] Fukuda Y *et al.* (Super-Kamiokande Collaboration) 1998 Evidence for oscillation of atmospheric neutrinos *Phys. Rev. Lett.* **81** 1562–1567 (*Preprint arXiv:hep-ex/9807003*)
- [14] Ashie Y *et al.* (Super-Kamiokande Collaboration) 2004 Evidence for an oscillatory signature in atmospheric neutrino oscillation *Phys. Rev. Lett.* **93** 101801 (*Preprint arXiv:hep-ex/0404034*)
- [15] Eguchi K *et al.* (KamLAND Collaboration) 2003 First results from KamLAND: Evidence for reactor anti-neutrino disappearance *Phys. Rev. Lett.* **90** 021802 (*Preprint arXiv:hep-ex/0212021*)
- [16] Araki T *et al.* (KamLAND Collaboration) 2005 Measurement of neutrino oscillation with KamLAND: Evidence of spectral distortion *Phys. Rev. Lett.* **94** 081801 (*Preprint arXiv:hep-ex/0406035*)

- [17] Abe Y *et al.* (DOUBLE-CHOOZ Collaboration) 2012 Indication for the disappearance of reactor electron antineutrinos in the Double Chooz experiment *Phys. Rev. Lett.* **108** 131801 (*Preprint arXiv:1112.6353*)
- [18] Michael D *et al.* (MINOS Collaboration) 2006 Observation of muon neutrino disappearance with the MINOS detectors and the NuMI neutrino beam *Phys. Rev. Lett.* **97** 191801 (*Preprint arXiv:hep-ex/0607088*)
- [19] Adamson P *et al.* (MINOS Collaboration) 2008 Measurement of Neutrino Oscillations with the MINOS Detectors in the NuMI Beam *Phys. Rev. Lett.* **101** 131802 (*Preprint arXiv:0806.2237*)
- [20] Ahn M *et al.* (K2K Collaboration) 2006 Measurement of Neutrino Oscillation by the K2K Experiment *Phys. Rev. D* **74** 072003 (*Preprint arXiv:hep-ex/0606032*)
- [21] An F *et al.* (DAYA-BAY Collaboration) 2012 Observation of electron-antineutrino disappearance at Daya Bay *Phys. Rev. Lett.* **108** 171803 (*Preprint arXiv:1203.1669*)
- [22] An F *et al.* (Daya Bay Collaboration) 2013 Improved Measurement of Electron Antineutrino Disappearance at Daya Bay *Chin. Phys. C* **37** 011001 (*Preprint arXiv:1210.6327*)
- [23] Ahn J *et al.* (RENO collaboration) 2012 Observation of Reactor Electron Antineutrino Disappearance in the RENO Experiment *Phys. Rev. Lett.* **108** 191802 (*Preprint arXiv:1204.0626*)
- [24] Abe K *et al.* (T2K Collaboration) 2011 Indication of Electron Neutrino Appearance from an Accelerator-produced Off-axis Muon Neutrino Beam *Phys. Rev. Lett.* **107** 041801 (*Preprint arXiv:1106.2822*)
- [25] Adamson P *et al.* (MINOS Collaboration) 2011 Improved search for muon-neutrino to electron-neutrino oscillations in MINOS *Phys. Rev. Lett.* **107** 181802 (*Preprint arXiv:1108.0015*)

- [26] Adam J *et al.* (MEG collaboration) 2011 New limit on the lepton-flavour violating decay $\mu^+ \rightarrow e^+\gamma$ *Phys. Rev. Lett.* **107** 171801 (*Preprint arXiv:1107.5547*)
- [27] Bellgardt U *et al.* (SINDRUM Collaboration) 1988 Search for the Decay $\mu^+ \rightarrow e^+e^+e^-$ *Nucl. Phys. B* **299** 1
- [28] Dohmen C *et al.* (SINDRUM II Collaboration.) 1993 Test of lepton flavor conservation in $\mu \rightarrow e$ conversion on titanium *Phys. Lett. B* **317** 631–636
- [29] Bertl W H *et al.* (SINDRUM II Collaboration) 2006 A Search for muon to electron conversion in muonic gold *Eur. Phys. J. C* **47** 337–346
- [30] Miyazaki Y *et al.* (Belle Collaboration) 2011 Search for Lepton-Flavor-Violating tau Decays into a Lepton and a Vector Meson *Phys. Lett. B* **699** 251–257 (*Preprint arXiv:1101.0755*)
- [31] Miyazaki Y *et al.* (Belle Collaboration) 2013 Search for Lepton-Flavor-Violating and Lepton-Number-Violating $\tau \rightarrow \ell hh'$ Decay Modes *Phys. Lett. B* **719** 346–353 (*Preprint arXiv:1206.5595*)
- [32] Aubert B *et al.* (BaBar Collaboration) 2009 Improved limits on lepton flavor violating tau decays to l phi, l rho, l K* and l anti-K* *Phys. Rev. Lett.* **103** 021801 (*Preprint arXiv:0904.0339*)
- [33] Hayasaka K, Inami K, Miyazaki Y, Arinstein K, Aulchenko V *et al.* 2010 Search for Lepton Flavor Violating Tau Decays into Three Leptons with 719 Million Produced Tau+Tau- Pairs *Phys. Lett. B* **687** 139–143 (*Preprint arXiv:1001.3221*)
- [34] Lees J *et al.* (BaBar Collaboration) 2010 Limits on tau Lepton-Flavor Violating Decays in three charged leptons *Phys. Rev. D* **81** 111101 (*Preprint arXiv:1002.4550*)
- [35] Miyazaki Y *et al.* (Belle Collaboration) 2010 Search for Lepton Flavor Violating τ^- Decays into $\ell^-K_S^0$ and $\ell^-K_S^0\bar{K}_S^0$ *Phys. Lett. B* **692** 4–9 (*Preprint arXiv:1003.1183*)

- [36] Aubert B *et al.* (BaBar Collaboration) 2010 Searches for Lepton Flavor Violation in the Decays $\tau^\pm \rightarrow e^\pm\gamma$ and $\tau^\pm \rightarrow \mu^\pm\gamma$ *Phys. Rev. Lett.* **104** 021802 (*Preprint arXiv:0908.2381*)
- [37] Beringer J *et al.* (Particle Data Group) 2012 Review of Particle Physics (RPP) *Phys. Rev. D* **86** 010001
- [38] Golden B 2012 *In Pursuit of the Rare Decay $\mu^+ \rightarrow e^+\gamma$: A Window to the UV Completion of the Standard Model* Ph.D. thesis University of California, Irvine <http://meg.web.psi.ch/docs/theses/BenThesis.pdf>
- [39] Adam J 2012 *New Analysis Method to Confirm the Upper Limit of the Branching Ratio $B(\mu^+ \rightarrow e^+ + \gamma)$ from the MEG Experiment* Ph.D. thesis ETH Zurich URL http://meg.web.psi.ch/docs/theses/PhDThesis_Adam_2012.pdf
- [40] Hewett J, Weerts H, Brock R, Butler J, Casey B *et al.* 2012 Fundamental Physics at the Intensity Frontier (*Preprint arXiv:1205.2671*)
- [41] Berger N 2013 A Novel experiment searching for the lepton flavour violating decay $\mu \rightarrow eee$ *J. Phys. Conf. Ser.* **408** 012070 (*Preprint arXiv:1110.1504*)
- [42] Kurup A (COMET Collaboration) 2011 The COherent Muon to Electron Transition (COMET) experiment *Nucl. Phys. Proc. Suppl.* **218** 38–43
- [43] Abrams R *et al.* (Mu2e Collaboration) 2012 Mu2e Conceptual Design Report (*Preprint arXiv:1211.7019*)
- [44] Kutschke R K 2011 The Mu2e Experiment at Fermilab (*Preprint arXiv:1112.0242*)
- [45] Dukes E C (Mu2e Collaboration) 2011 Mu2e: A high-sensitivity search for charged lepton flavor violation at Fermilab *Nucl. Phys. Proc. Suppl.* **218** 32–37
- [46] Kuno Y 2005 PRISM/PRIME *Nucl. Phys. Proc. Suppl.* **149** 376–378

- [47] Barlow R 2011 The PRISM/PRIME project *Nucl. Phys. Proc. Suppl.* **218** 44–49
- [48] Hayasaka K 2009 Searches for LFV at B factories *J. Phys. Conf. Ser.* **171** 012079
- [49] Bona M *et al.* (SuperB Collaboration) 2007 SuperB: A High-Luminosity Asymmetric e^+e^- Super Flavor Factory. Conceptual Design Report Unfortunately, the information has been released that the SuperB project will be discontinued. (*Preprint arXiv:0709.0451*)
- [50] Bernstein R H and Cooper P S 2013 Charged Lepton Flavor Violation: An Experimenter’s Guide *Phys. Rept.* **532** 27–64 (*Preprint arXiv: 1307.5787*)
- [51] Hudson J, Kara D, Smallman I, Sauer B, Tarbutt M *et al.* 2011 Improved measurement of the shape of the electron *Nature* **473** 493–496
- [52] Jung M 2013 A robust limit for the electric dipole moment of the electron *JHEP* **1305** 168 (*Preprint arXiv:1301.1681*)
- [53] Amini J M, Munger Charles T J and Gould H 2008 Electron electric dipole moment experiment using electric-field quantized slow cesium atoms *Int. J. Mod. Phys. D* **16** 2337–2342 (*Preprint arXiv:0705.4428*)
- [54] Kittle M, Burton T, Feeney L and Heinzen D 2004 APS Division of Atomic, Molecular and Optical Physics Meeting Abstracts p 1059
- [55] Weiss D, Fang F and Chen J 2003 EDM searches at Storage Rings *Bull. Am. Phys. Soc.* **APR03** J1.008
- [56] Sakemi Y, Harada K, Hayamizu T, Itoh M, Kawamura H *et al.* 2011 Search for a permanent EDM using laser cooled radioactive atom *J. Phys. Conf. Ser.* **302** 012051

- [57] Wundt B, Munger C and Jentschura U 2012 Quantum dynamics in atomic-fountain experiments for measuring the electric dipole moment of the electron with improved sensitivity *Phys. Rev. X* **2** 041009 (*Preprint arXiv:1211.4057*)
- [58] Kara D, Smallman I, Hudson J, Sauer B, Tarbutt M *et al.* 2012 Measurement of the electron's electric dipole moment using YbF molecules: methods and data analysis *New J. Phys.* **14** 103051 (*Preprint arXiv:1208.4507*)
- [59] Raidal M, van der Schaaf A, Bigi I, Mangano M, Semertzidis Y K *et al.* 2008 Flavour physics of leptons and dipole moments *Eur. Phys. J. C* **57** 13–182 (*Preprint arXiv:0801.1826*)
- [60] Pospelov M and Ritz A 2005 Electric dipole moments as probes of new physics *Annals Phys.* **318** 119–169 (*Preprint arXiv:hep-ph/0504231*)
- [61] Roberts B L (Fermilab P989 Collaboration) 2011 The Fermilab muon (g-2) project *Nucl. Phys. Proc. Suppl.* **218** 237–241
- [62] Roberts B L (E821 Collaboration, E969 Collaboration) 2006 Muon (g-2): Past, present and future *Nucl. Phys. Proc. Suppl.* **155** 372–374 (*Preprint arXiv:hep-ex/0510056*)
- [63] Venanzoni G 2012 Latest on g-2 from experiment *J. Phys. Conf. Ser.* **349** 012008
- [64] Venanzoni G 2012 Latest on g-2 from experiment *Frascati Phys. Ser.* **54** 52–67 (*Preprint arXiv:1203.1501*)
- [65] E989 experiment at Fermilab URL <http://gm2.fnal.gov/>
- [66] Fukuyama T 2012 Searching for New Physics beyond the Standard Model in Electric Dipole Moment *Int. J. Mod. Phys. A* **27** 1230015 (*Preprint arXiv:1201.4252*)
- [67] Jung M and Pich A 2013 Electric Dipole Moments in Two-Higgs-Doublet Models (*Preprint arXiv:1308.6283*)

- [68] Drees M, Goldbole M and Roy P 2004 *Theory and Phenomenology of Sparticles* (World Scientific)
- [69] Petcov S, Profumo S, Takanishi Y and Yaguna C 2004 Charged lepton flavor violating decays: Leading logarithmic approximation versus full RG results *Nucl. Phys. B* **676** 453–480 (*Preprint arXiv: hep-ph/0306195*)
- [70] Nilles H P 1984 Supersymmetry, Supergravity and Particle Physics *Phys. Rept.* **110** 1–162
- [71] Haber H E and Kane G L 1985 The Search for Supersymmetry: Probing Physics Beyond the Standard Model *Phys. Rept.* **117** 75–263
- [72] Derendinger J P Lecture Notes on Globally Supersymmetric Theories in Four and Two Dimensions ETH Zürich URL <http://statistics.roma2.infn.it/~fucito/appunti/derendinger.pdf>
- [73] Wess J and Bagger J 1992 *Supersymmetry and Supergravity* 2nd ed Princeton Series in Physics (Princeton University Press)
- [74] Bajc B Lecture Notes on Introduction to Supersymmetry J. Stefan Institute Ljubljana URL <http://www-f1.ijs.si/~bajc/introsusy.pdf>
- [75] Herrero M 1998 The Standard model (*Preprint arXiv:hep-ph/9812242*)
- [76] Coleman S 1988 *Aspects of Symmetry: Selected Erice Lectures* (Cambridge University Press)
- [77] Witten E 1981 Dynamical Breaking of Supersymmetry *Nucl. Phys. B* **188** 513
- [78] Dimopoulos S and Georgi H 1981 Softly Broken Supersymmetry and SU(5) *Nucl. Phys. B* **193** 150
- [79] Sakai N 1981 Naturalness in Supersymmetric Guts *Z. Phys. C* **11** 153

- [80] Kaul R K 1982 Gauge Hierarchy in a Supersymmetric Model *Phys. Lett.* **B 109** 19
- [81] Arnowitt R, Chamseddine A H and Nath P 1984 *Applied N=1 Supergravity* (Singapore: World Scientific)
- [82] Aad G *et al.* (ATLAS Collaboration) 2012 Observation of a new particle in the search for the Standard Model Higgs boson with the ATLAS detector at the LHC *Phys. Lett.* **B 716** 1–29 (*Preprint arXiv:1207.7214*)
- [83] Chatrchyan S *et al.* (CMS Collaboration) 2012 Observation of a new boson at a mass of 125 GeV with the CMS experiment at the LHC *Phys. Lett.* **B 716** 30–61 (*Preprint arXiv:1207.7235*)
- [84] Chatrchyan S *et al.* (CMS Collaboration) 2013 Study of the Mass and Spin-Parity of the Higgs Boson Candidate Via Its Decays to Z Boson Pairs *Phys. Rev. Lett.* **110** 081803 (*Preprint arXiv:1212.6639*)
- [85] Minkowski P 1977 $\mu \rightarrow e\gamma$ at a Rate of One Out of 1-Billion Muon Decays? *Phys. Lett.* **B 67** 421
- [86] Gell-Mann M, Ramond P and Slansky R 1979 Complex Spinors and Unified Theories *Conf. Proc. C* **790927** 315–321 (*Preprint arXiv:1306.4669*)
- [87] Yanagida T 1979 *Proc. of the Workshop on the Unified Theory and the Baryon Number in the Universe* ed Sawada O and Sugamoto A (Tsukuba, Japan) unpublished
- [88] Glashow S 1979 Plenum *Quarks and Leptons* ed Levy M *et al.* (Cargese) p 707
- [89] Mohapatra R N and Senjanović G 1980 Neutrino Mass and Spontaneous Parity Violation *Phys. Rev. Lett.* **44** 912
- [90] Schechter J and Valle J 1980 Neutrino Masses in $SU(2) \times U(1)$ Theories *Phys. Rev. D* **22** 2227

- [91] Konetschny W and Kummer W 1977 Nonconservation of Total Lepton Number with Scalar Bosons *Phys. Lett.* **B 70** 433
- [92] Lazarides G, Shafi Q and Wetterich C 1981 Proton Lifetime and Fermion Masses in an SO(10) Model *Nucl. Phys.* **B 181** 287–300
- [93] Mohapatra R N and Senjanović G 1981 Neutrino Masses and Mixings in Gauge Models with Spontaneous Parity Violation *Phys. Rev.* **D 23** 165
- [94] Cheng T and Li L F 1980 Neutrino Masses, Mixings and Oscillations in $SU(2) \times U(1)$ Models of Electroweak Interactions *Phys. Rev.* **D 22** 2860
- [95] Schechter J and Valle J 1982 Neutrino Decay and Spontaneous Violation of Lepton Number *Phys. Rev.* **D 25** 774
- [96] Foot R, Lew H, He X and Joshi G C 1989 Seesaw neutrino masses induced by a triplet of leptons *Z. Phys.* **C 44** 441
- [97] Grimus W and Lavoura L 2000 The Seesaw mechanism at arbitrary order: Disentangling the small scale from the large scale *JHEP* **0011** 042 (*Preprint arXiv:hep-ph/0008179*)
- [98] Grimus W 2006 Neutrino Physics - Models for Neutrino Masses and Lepton Mixing *PoS P2GC* 001 (*Preprint arXiv:hep-ph/0612311*)
- [99] Wyler D and Wolfenstein L 1983 Massless Neutrinos in Left-Right Symmetric Models *Nucl. Phys.* **B 218** 205
- [100] Mohapatra R 1986 Mechanism for understanding small neutrino mass in superstring theories *Phys. Rev. Lett.* **56** 561–563
- [101] Mohapatra R and Valle J 1986 Neutrino Mass and Baryon Number Nonconservation in Superstring Models *Phys. Rev.* **D 34** 1642
- [102] Nandi S and Sarkar U 1986 A Solution to the Neutrino Mass Problem in Superstring E6 Theory *Phys. Rev. Lett.* **56** 564

- [103] Branco G, Grimus W and Lavoura L 1989 The seesaw mechanism in the presence of a conserved lepton number *Nucl. Phys.* **B** **312** 492
- [104] Pilaftsis A 1992 Radiatively induced neutrino masses and large Higgs neutrino couplings in the standard model with Majorana fields *Z. Phys.* **C** **55** 275–282 (*Preprint arXiv:hep-ph/9901206*)
- [105] Dev P B and Pilaftsis A 2012 Minimal Radiative Neutrino Mass Mechanism for Inverse Seesaw Models *Phys. Rev.* **D** **86** 113001 (*Preprint arXiv:1209.4051*)
- [106] Nardi E, Roulet E and Tommasini D 1994 Limits on neutrino mixing with new heavy particles *Phys. Lett.* **B** **327** 319–326 (*Preprint arXiv:hep-ph/9402224*)
- [107] Antusch S, Baumann J P and Fernandez-Martinez E 2009 Non-Standard Neutrino Interactions with Matter from Physics Beyond the Standard Model *Nucl. Phys.* **B** **810** 369–388 (*Preprint arXiv:0807.1003*)
- [108] Bergmann S and Kagan A 1999 Z - induced FCNCs and their effects on neutrino oscillations *Nucl. Phys.* **B** **538** 368–386 (*Preprint arXiv:hep-ph/9803305*)
- [109] del Aguila F, de Blas J and Perez-Victoria M 2008 Effects of new leptons in Electroweak Precision Data *Phys. Rev.* **D** **78** 013010 (*Preprint arXiv:0803.4008*)
- [110] Ilakovac A and Pilaftsis A 1995 Flavor violating charged lepton decays in seesaw-type models *Nucl. Phys.* **B** **437** 491 (*Preprint arXiv:hep-ph/9403398*)
- [111] Ilakovac A and Pilaftsis A 2009 Supersymmetric Lepton Flavour Violation in Low-Scale Seesaw Models *Phys. Rev.* **D** **80** 091902 (*Preprint arXiv:0904.2381*)

- [112] Ilakovac A and Pilaftsis A 2011 Charged LFV in a low-scale seesaw mSUGRA model *Nucl. Phys. Proc. Suppl.* **218** 26–31 (*Preprint arXiv*: 1012.2823)
- [113] Borzumati F and Masiero A 1986 Large Muon and electron Number Violations in Supergravity Theories *Phys. Rev. Lett.* **57** 961
- [114] Hisano J, Moroi T, Tobe K and Yamaguchi M 1996 Lepton flavor violation via right-handed neutrino Yukawa couplings in supersymmetric standard model *Phys. Rev. D* **53** 2442–2459 (*Preprint arXiv*: hep-ph/9510309)
- [115] Hisano J, Moroi T, Tobe K, Yamaguchi M and Yanagida T 1995 Lepton flavor violation in the supersymmetric standard model with seesaw induced neutrino masses *Phys. Lett. B* **357** 579–587 (*Preprint arXiv*: hep-ph/9501407)
- [116] Hisano J and Nomura D 1999 Solar and atmospheric neutrino oscillations and lepton flavor violation in supersymmetric models with the right-handed neutrinos *Phys. Rev. D* **59** 116005 (*Preprint arXiv*: hep-ph/9810479)
- [117] Carvalho D, Ellis J R, Gomez M and Lola S 2001 Charged lepton flavor violation in the CMSSM in view of the muon anomalous magnetic moment *Phys. Lett. B* **515** 323–332 (*Preprint arXiv*:hep-ph/0103256)
- [118] Hisano J, Nagai M, Paradisi P and Shimizu Y 2009 Waiting for $\mu \rightarrow e\gamma$ from the MEG experiment *JHEP* **0912** 030 (*Preprint arXiv*:0904.2080)
- [119] Ellis J R, Hisano J, Lola S and Raidal M 2002 CP violation in the minimal supersymmetric seesaw model *Nucl. Phys. B* **621** 208–234 (*Preprint arXiv*:hep-ph/0109125)
- [120] Arina C, Bazzocchi F, Fornengo N, Romao J and Valle J 2008 Minimal supergravity sneutrino dark matter and inverse seesaw neutrino masses *Phys. Rev. Lett.* **101** 161802 (*Preprint arXiv*:0806.3225)

- [121] Deppisch F and Pilaftsis A 2008 Thermal Right-Handed Sneutrino Dark Matter in the F(D)-Term Model of Hybrid Inflation *JHEP* **0810** 080 (*Preprint arXiv:0808.0490*)
- [122] Josse-Michaux F X and Molinaro E 2011 A Common Framework for Dark Matter, Leptogenesis and Neutrino Masses *Phys. Rev. D* **84** 125021 (*Preprint arXiv:1108.0482*)
- [123] An H, Dev P B, Cai Y and Mohapatra R 2012 Sneutrino Dark Matter in Gauged Inverse Seesaw Models for Neutrinos *Phys. Rev. Lett.* **108** 081806 (*Preprint arXiv:1110.1366*)
- [124] Dumont B, Belanger G, Fichet S, Kraml S and Schwetz T 2012 Mixed sneutrino dark matter in light of the 2011 XENON and LHC results *JCAP* **1209** 013 (*Preprint arXiv:1206.1521*)
- [125] Pilaftsis A 2005 Resonant tau-leptogenesis with observable lepton number violation *Phys. Rev. Lett.* **95** 081602 (*Preprint arXiv:hep-ph/0408103*)
- [126] Pilaftsis A and Underwood T E 2005 Electroweak-scale resonant leptogenesis *Phys. Rev. D* **72** 113001 (*Preprint arXiv:hep-ph/0506107*)
- [127] Deppisch F F and Pilaftsis A 2011 Lepton Flavour Violation and theta(13) in Minimal Resonant Leptogenesis *Phys. Rev. D* **83** 076007 (*Preprint arXiv:1012.1834*)
- [128] Pilaftsis A 1997 CP violation and baryogenesis due to heavy Majorana neutrinos *Phys. Rev. D* **56** 5431–5451 (*Preprint arXiv:hep-ph/9707235*)
- [129] Pilaftsis A and Underwood T E 2004 Resonant leptogenesis *Nucl. Phys. B* **692** 303–345 (*Preprint arXiv:hep-ph/0309342*)
- [130] Cohen T, Morrissey D E and Pierce A 2012 Electroweak Baryogenesis and Higgs Signatures *Phys. Rev. D* **86** 013009 (*Preprint arXiv:1203.2924*)

- [131] Carena M, Nardini G, Quiros M and Wagner C E 2013 MSSM Electroweak Baryogenesis and LHC Data *JHEP* **1302** 001 (*Preprint arXiv:1207.6330*)
- [132] Ferrara S and Remiddi E 1974 Absence of the Anomalous Magnetic Moment in a Supersymmetric Abelian Gauge Theory *Phys. Lett.* **B** **53** 347
- [133] Bernabéu J, Santamaria A, Vidal J, Mendez A and Valle J 1987 Lepton Flavor Nonconservation at High-Energies in a Superstring Inspired Standard Model *Phys. Lett.* **B** **187** 303
- [134] Körner J, Pilaftsis A and Schilcher K 1993 Leptonic flavor changing Z^0 decays in $SU(2) \times U(1)$ theories with right-handed neutrinos *Phys. Lett.* **B** **300** 381–386 (*Preprint arXiv:hep-ph/9301290*)
- [135] Bernabéu J, Korner J, Pilaftsis A and Schilcher K 1993 Universality breaking effects in leptonic Z decays *Phys. Rev. Lett.* **71** 2695–2698 (*Preprint arXiv:hep-ph/9307295*)
- [136] Deppisch F and Valle J 2005 Enhanced lepton flavor violation in the supersymmetric inverse seesaw model *Phys. Rev.* **D** **72** 036001 (*Preprint arXiv:hep-ph/0406040*)
- [137] Kersten J and Smirnov A Y 2007 Right-Handed Neutrinos at CERN LHC and the Mechanism of Neutrino Mass Generation *Phys. Rev.* **D** **76** 073005 (*Preprint arXiv:0705.3221*)
- [138] Pilaftsis A 2008 Electroweak Resonant Leptogenesis in the Singlet Majoron Model *Phys. Rev.* **D78** 013008 (*Preprint arXiv:0805.1677*)
- [139] Ilakovac A, Pilaftsis A and Popov L 2013 Charged Lepton Flavour Violation in Supersymmetric Low-Scale Seesaw Models *Phys. Rev.* **D** **87** 053014 (*Preprint arXiv:1212.5939*)
- [140] Cheng T and Li L F 1980 $\mu \rightarrow e\gamma$ in Theories With Dirac and Majorana Neutrino Mass Terms *Phys. Rev. Lett.* **45** 1908

- [141] Arganda E and Herrero M J 2006 Testing supersymmetry with lepton flavor violating τ and μ decays *Phys. Rev.* **D 73** 055003 (*Preprint arXiv:hep-ph/0510405*)
- [142] Chiang H, Oset E, Kosmas T, Faessler A and Vergados J 1993 Coherent and incoherent (μ, e) conversion in nuclei *Nucl. Phys.* **A 559** 526–542
- [143] Kitano R, Koike M and Okada Y 2002 Detailed calculation of lepton flavor violating muon electron conversion rate for various nuclei *Phys. Rev.* **D 66** 096002 (*Preprint arXiv:hep-ph/0203110*)
- [144] Ilakovac A 2000 Lepton flavor violation in the standard model extended by heavy singlet Dirac neutrinos *Phys. Rev.* **D 62** 036010 (*Preprint arXiv:hep-ph/9910213*)
- [145] Alonso R, Dhen M, Gavela M and Hambye T 2013 Muon conversion to electron in nuclei in type-I seesaw models *JHEP* **1301** 118 (*Preprint arXiv:1209.2679*)
- [146] Aad G *et al.* (ATLAS Collaboration) 2012 Hunt for new phenomena using large jet multiplicities and missing transverse momentum with ATLAS in 4.7 fb^{-1} of $\sqrt{s} = 7 \text{ TeV}$ proton-proton collisions *JHEP* **1207** 167 (*Preprint arXiv:1206.1760*)
- [147] Chatrchyan S *et al.* (CMS Collaboration) 2012 Search for new physics in the multijet and missing transverse momentum final state in proton-proton collisions at $\sqrt{s} = 7 \text{ TeV}$ *Phys. Rev. Lett.* **109** 171803 (*Preprint arXiv:1207.1898*)
- [148] Ellis J and Olive K A 2012 Revisiting the Higgs Mass and Dark Matter in the CMSSM *Eur. Phys. J. C* **72** 2005 (*Preprint arXiv:1202.3262*)
- [149] Carena M S, Haber H, Heinemeyer S, Hollik W, Wagner C *et al.* 2000 Reconciling the two loop diagrammatic and effective field theory computations of the mass of the lightest CP-even Higgs boson in the MSSM *Nucl. Phys.* **B 580** 29–57 (*Preprint arXiv:hep-ph/0001002*)

- [150] Lee J, Carena M, Ellis J, Pilaftsis A and Wagner C 2013 CPsuperH2.3: an Updated Tool for Phenomenology in the MSSM with Explicit CP Violation *Comput. Phys. Commun.* **184** 1220–1233 (*Preprint arXiv*: 1208.2212)
- [151] Lee J, Pilaftsis A, Carena M S, Choi S, Drees M *et al.* 2004 CPsuperH: A Computational tool for Higgs phenomenology in the minimal supersymmetric standard model with explicit CP violation *Comput. Phys. Commun.* **156** 283–317 (*Preprint arXiv*: hep-ph/0307377)
- [152] Heinemeyer S, Herrero M, Penaranda S and Rodriguez-Sanchez A 2011 Higgs Boson Masses in the MSSM with Heavy Majorana Neutrinos *JHEP* **1105** 063 (*Preprint arXiv*: 1007.5512)
- [153] Chankowski P H and Pokorski S 2002 Quantum corrections to neutrino masses and mixing angles *Int. J. Mod. Phys. A* **17** 575–614 (*Preprint arXiv*: hep-ph/0110249)
- [154] The Mu2e Project URL <http://mu2e.fnal.gov/>
- [155] The X-Project URL <http://projectx.fnal.gov>
- [156] Ritt S (MEG Collaboration) 2006 Status of the MEG experiment $\mu \rightarrow e\gamma$ *Nucl. Phys. Proc. Suppl.* **162** 279–282
- [157] Hirsch M, Staub F and Vicente A 2012 Enhancing $l_i \rightarrow 3l_j$ with the Z^0 -penguin *Phys. Rev. D* **85** 113013 (*Preprint arXiv*: 1202.1825)
- [158] Ilakovac A, Pilaftsis A and Popov L 2013 Lepton Dipole Moments in Supersymmetric Low-Scale Seesaw Models In press (*Preprint arXiv*: 1308.3633)
- [159] Branco G, Lavoura L and Silva J 1999 *CP violation* (Oxford University Press)
- [160] Farzan Y and Peskin M E 2004 The Contribution from neutrino Yukawa couplings to lepton electric dipole moments *Phys. Rev. D* **70** 095001 (*Preprint arXiv*: hep-ph/0405214)

- [161] Moroi T 1996 The Muon anomalous magnetic dipole moment in the minimal supersymmetric standard model *Phys. Rev.* **D 53** 6565–6575 (*Preprint arXiv:hep-ph/9512396*)
- [162] Carena M S, Giudice G and Wagner C 1997 Constraints on supersymmetric models from the muon anomalous magnetic moment *Phys. Lett.* **B 390** 234–242 (*Preprint arXiv:hep-ph/9610233*)
- [163] Stöckinger D 2007 The Muon Magnetic Moment and Supersymmetry *J. Phys.* **G 34** R45–R92 (*Preprint arXiv:hep-ph/0609168*)
- [164] Pilaftsis A 2002 Higgs mediated electric dipole moments in the MSSM: An application to baryogenesis and Higgs searches *Nucl. Phys.* **B 644** 263–289 (*Preprint arXiv:hep-ph/0207277*)
- [165] Glashow S L 2013 Particle Physics in The United States, A Personal View (*Preprint arXiv:1305.5482*)
- [166] Hahn T 2001 Generating Feynman diagrams and amplitudes with FeynArts 3 *Comput. Phys. Commun.* **140** 418–431 (*Preprint arXiv: hep-ph/0012260*)
- [167] Hahn T and Schappacher C 2002 The Implementation of the minimal supersymmetric standard model in FeynArts and FormCalc *Comput. Phys. Commun.* **143** 54–68 (*Preprint arXiv:hep-ph/0105349*)
- [168] Fritzsch T, Hahn T, Heinemeyer S, Rzehak H and Schappacher C 2013 The Implementation of the Renormalized Complex MSSM in FeynArts and FormCalc (*Preprint arXiv:1309.1692*)
- [169] Mertig R, Bohm M and Denner A 1991 FEYN CALC: Computer algebraic calculation of Feynman amplitudes *Comput.Phys.Commun.* **64** 345–359

Curriculum Vitæ

First name | Surname : Luka Popov

Address

Physics Department

Faculty of Science

University of Zagreb

Bijenička cesta 32, P.O.B. 331

HR-10002 Zagreb, Croatia

e-mail: lpopov@phy.hr | phone: +385 1 460 5605 | fax: +385 1 460 5606

Born February 19 1982 (Split Croatia)

Education

1989-1996 Elementary school (*Spinut* Split)

1996-2000 High school (*IV. Gimnazija* Split)

2000-2007 Faculty of Science, University of Zagreb

Nov 2007 **dipl. ing.**, Diploma thesis: *Neutral mesons mixings
in the MSSM*, advisor: Prof Amon Ilakovac

2009-2013 PhD student, University of Zagreb

Dec 2013 **PhD** thesis completed and submitted

Research interests

Physics beyond standard model; Supersymmetry; Lepton flavor violation

Position

Since 2008 research and teaching assistant at Faculty of Science, University of Zagreb.

Teaching assistant experience

- Classical electrodynamics (3th year courses)
- Relativistic quantum physics (4th year course)
- Theory of fields I (4th year course)
- Theory of fields II (5th year course)
- General physics (Faculty of Electrical Engineering, 1st year course)

List of publications

1. Ilakovac A and Popov L 2010 Two-step Lorentz Transformation of Force *Fizika A* **19** 3
2. Popov L 2013 Newtonian-Machian analysis of the neo-Tychonian model of planetary motions *Eur. J. Phys.* **34** 383 (*Preprint arXiv:1301.6045*)
3. Ilakovac A, Pilaftsis A and Popov L 2013 Charged Lepton Flavour Violation in Supersymmetric Low-Scale Seesaw Models *Phys. Rev. D* **87** 053014 (*Preprint arXiv:1212.5939*)
4. Ilakovac A, Pilaftsis A and Popov L 2013 Lepton Dipole Moments in Supersymmetric Low-Scale Seesaw Models (*Preprint arXiv:1308.3633*) In press

Conference proceedings

1. Popov L 2009 Einstein-Podolsky-Rosen (EPR) argument and consequences *Teorija relativnosti i filozofija. Povodom 100. obljetnice Einsteinove Specjalne teorije relativnosti* ed Petković, T (Zagreb: Hrvatsko filozofsko društvo)

Active participation in conferences

1. Ilakovac A, Pilaftsis A and Popov L 2012 Charged Lepton Flavour Violation in Supersymmetric Low-Scale Seesaw Models *LHC Days in Split* Poster